Pharmaceutical Compositions

TECHNICAL FIELD

[001] The present disclosure relates to crystal forms of pharmaceutical compounds, formulations including, methods of forming, and methods of using these crystal forms.

SUMMARY

[002] Described herein are new crystal forms of pharmaceutical compounds. In one embodiment, the pharmaceutical compounds are included in a pharmaceutical composition useful for treating a disease or condition. In one embodiment, the disease or condition is cancer.

[003] In some embodiments, pharmaceutical compositions are described including resiquimod in the form of a sulfate salt in crystal form A. The sulfate salt can be a monosulfate salt and/or an anhydrate. This crystal form can be prepared in an appropriate dosage from.

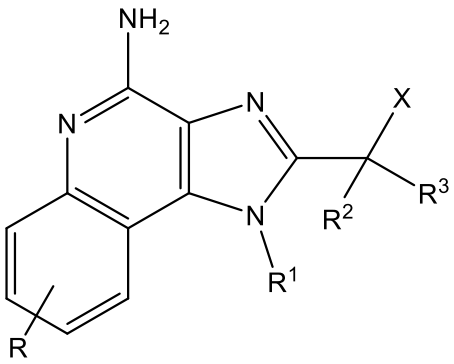
[003a] In one aspect, there is provided a dosage form comprising the composition described herein.

[004] In one embodiment, the sulfate salt in crystal form A is characterized by x-ray powder diffraction spectrum that comprises peaks at about 7 to about 8 degrees 2θ, about 13.5 to about 14.5 degrees 2θ, about 18 to about 19 degrees 2θ, and/or about 15 to about 16 degrees 2θ.

[004a] In another aspect, there is provided a composition comprising resiquimod in the form of a sulfate salt in crystal form A, wherein crystal form A is characterized by x-ray powder diffraction spectrum that comprises peaks at 7 to 8 degrees 2θ, 13.5 to 14.5 degrees 2θ, 19 to 20 degrees 2θ, and 19.5 to 20.5 degrees 2θ

[005] The sulfate salt in crystal form A can be stable at room temperature for at least about 2 days or at least about 1 week.

[006] Other embodiments describe pharmaceutical compositions comprising a crystal form of a compound of Formula I:

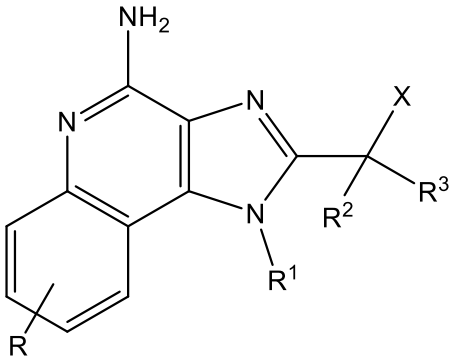


(I).

[007] Formula I can be a compound having a formula 4-amino-α-butyl-1-(2-methylpropyl)-1H-imidazo-[4,5-c]-quinoline-2-methanol hemihydrate, 4-amino-α,α-dimethyl-2-ethoxymethyl-1H-imidazo-[4,5-c]-quinoline-1-ethanol, 2-ethoxymethyl-1-(2-methylpropyl)-1H-imidazo-[4,5-c]-quinolin-4-amine, or 4-amino-1-phenylmethyl-1H-imidazo-[4,5-c]-quinoline-2-methanol. In one embodiment, Formula I is resiquimod.

[008] In some embodiments, the crystal form of a compound of Formula I can be in form A and/or be a sulfate salt. In one embodiment, a sulfate salt is a monosulfate salt and/or an anhydrate.

[009] Other embodiments provide methods of treating diseases or conditions. In one embodiment, methods of treating cancer are described. The methods can comprise: administering a pharmaceutical composition including a crystal form of a compound having a Formula I:



(I).

[009a] In another aspect, there is provided a use of a composition as described herein in the preparation of a medicament for the treatment of cancer in a subject in need thereof.

[009b] In yet another aspect, there is provided a use of a composition as described herein in the preparation of a medicament for the treatment of a tumor in a subject in need thereof.

BRIEF DESCRIPTION OF THE DRAWINGS

[0010] FIG. 1 illustrates XRPD patterns of mono-HCl salt crystal form Type A batches.

[0011] FIG. 2 illustrates a PLM image of mono-HCl salt crystal form Type A (807919-16-A).

[0012] FIG. 3 illustrates TGA/DSC curves of mono-HCl salt crystal form Type A (807919-16-A).

[0013] FIG. 4 illustrates an XRPD pattern of di-HCl salt crystal form Type A (807919-14-A).

[0014] FIG. 5 illustrates a PLM image of di-HCl salt crystal form Type A (807919-14-A).

[0015] FIG. 6 illustrates TGA/DSC curves of di-HCl salt crystal form Type A (807919-14-A).

[0016] FIG. 7 illustrates XRPD patterns of sulfate crystal form Type A batches.

[0017] FIG. 8 illustrates a PLM image of sulfate crystal form Type A (807919-11-A).

[0018] FIG. 9 illustrates TGA/DSC curves of sulfate crystal form Type A (807919-11-A).

[0019] FIG. 10 illustrates XRPD patterns of phosphate crystal form Type A batches.

[0020] FIG. 11 illustrates a PLM image of phosphate crystal form Type A (807919-11-C).

[0021] FIG. 12 illustrates TGA/DSC curves of phosphate crystal form Type A (807919-11-C).

[0022] FIG. 13 illustrates XRPD patterns of maleate crystal form Type A batches.

[0023] FIG. 14 illustrates a PLM image of maleate crystal form Type A (807919-11-B).

[0024] FIG. 15 illustrates TGA/DSC curves of maleate crystal form Type A (807919-11-B).

[0025] FIG. 16 illustrates XRPD patterns of malate crystal form Type A batches.

[0026] FIG. 17 illustrates a PLM image of malate crystal form Type A (807919-11-E).

[0027] FIG. 18 illustrates TGA/DSC curves of malate crystal form Type A (807919-11-E).

[0028] FIG. 19 illustrates XRPD patterns of adipate crystal form Type A batches.

[0029] FIG. 20 illustrates a PLM image of adipate crystal form Type A (807919-12-A).

[0030] FIG. 21 illustrates TGA/DSC curves of adipate crystal form Type A (807919-12-A).

[0031] FIG. 22 illustrates a DVS plot of sulfate crystal form Type A (807919-11-A).

[0032] FIG. 23 illustrates a XRPD overlay of sulfate crystal form Type A (807919-11-A) pre and post DVS test.

[0033] FIG. 24 illustrates a DVS plot of phosphate crystal form Type A (807919-11-C).

[0034] FIG. 25 illustrates a XRPD overlay of phosphate crystal form Type A (807919-11-C) pre and post DVS test.

[0035] FIG. 26 illustrates a DVS plot of maleate crystal form Type A (807919-11-B).

[0036] FIG. 27 illustrates a XRPD overlay of maleate crystal form Type A (807919-11-B) pre and post DVS test.

[0037] FIG. 28 illustrates a DVS plot of malate crystal form Type A (807919-11-E).

[0038] FIG. 29 illustrates a XRPD overlay of malate crystal form Type A (807919-11-E) pre and post DVS test.

[0039] FIG. 30 illustrates a DVS plot of adipate crystal form Type A (807919-12-A).

[0040] FIG. 31 illustrates a XRPD overlay of adipate crystal form Type A (807919-12-A) pre and post DVS test.

[0041] FIG. 32 illustrates a DVS plot of mono-HCl salt crystal form Type A (807919-16-A).

[0042] FIG. 33 illustrates a XRPD overlay of mono-HCl salt crystal form Type A (807919-16-A) pre and post DVS test.

[0043] FIG. 34 illustrates a DVS plot of di-HCl salt crystal form Type A (807919-14-A).

[0044] FIG. 35 illustrates a XRPD overlay of di-HCl salt crystal form Type A (807919-14-A) pre and post DVS test.

[0045] FIG. 36 illustrates kinetic solubility of seven crystal forms described herein and freebase crystal forms (short dashes: clear solutions were observed during the evaluation).

[0046] FIG. 37 illustrates a XRPD overlay of freebase crystal form Type A (807919-05-A) after suspended for 24 hrs.

[0047] FIG. 38 illustrates a XRPD overlay of adipate crystal form Type A (807919-12-A) after suspended for 24 hrs.

[0048] FIG. 39 illustrates a XRPD overlay of maleate crystal form Type A (807919-11-B) after suspended for 24 hrs.

[0049] FIG. 40 illustrates a XRPD overlay of freebase crystal form Type A (807919-05-A) pre and post stability test.

[0050] FIG. 41 illustrates a XRPD overlay of mono-HCl salt crystal form Type A (807919-16-A) pre and post stability test.

[0051] FIG. 42 illustrates a XRPD overlay of di-HCl salt crystal form Type A (807919-14-A) pre and post stability test.

[0052] FIG. 43 illustrates a XRPD overlay of sulfate crystal form Type A (807919-11-A) pre and post stability test.

[0053] FIG. 44 illustrates a XRPD overlay of phosphate crystal form Type A (807919-11-C) pre and post stability test.

[0054] FIG. 45 illustrates a XRPD overlay of maleate crystal form Type A (807919-11-B) pre and post stability test.

[0055] FIG. 46 illustrates a XRPD overlay of malate crystal form Type A (807919-11-E) pre and post stability test.

[0056] FIG. 47 illustrates a XRPD overlay of adipate crystal form Type A (807919-12-A) pre and post stability test.

[0057] FIG. 48 illustrates a XRPD pattern of sulfate crystal form Type B (807919-25-A13).

[0058] FIG. 49 illustrates TGA/DSC curves of sulfate crystal form Type B (807919-25-A13).

[0059] FIG. 50 illustrates a XRPD pattern of hemi-sulfate crystal form Type A (807919-34-A).

[0060] FIG. 51 illustrates TGA/DSC curves of hemi-sulfate crystal form Type A (807919-34-A).

[0061] FIG. 52 illustrates a XRPD overlay of slurry experiments at RT.

[0062] FIG. 53 illustrates a XRPD overlay of sulfate crystal form Type A (807919-21-A) before and after storage.

[0063] FIG. 54 illustrates a XRPD pattern of freebase crystal form Type A (807919-05-A).

[0064] FIG. 55 illustrates a PLM image of freebase crystal form Type A (807919-05-A).

[0065] FIG. 56 illustrates TGA/DSC curves of freebase crystal form Type A (807919-05-A).

[0066] FIG. 57 illustrates a DVS plot of freebase crystal form Type A (807919-05-A).

[0067] FIG. 58 illustrates a XRPD overlay of freebase crystal form Type A (807919-05-A) before and after DVS test.

[0068] FIG. 59 illustrates XRPD patterns of sulfate crystal form Type A batches.

[0069] FIG. 60 illustrates TGA/DSC curves of sulfate crystal form Type A (807919-21-A).

[0070] FIG. 61 illustrates XRPD patterns of HCl salt crystal forms.

[0071] FIG. 62 illustrates TGA/DSC curves of HCl salt crystal form Type B (807919-07-C2).

[0072] FIG. 63 illustrates a XRPD pattern of sulfate crystal form Type A (807919-07-A3).

[0073] FIG. 64 illustrates TGA/DSC curves of sulfate crystal form Type A (807919-07-A3).

[0074] FIG. 65 illustrates a XRPD pattern of phosphate crystal form Type A (807919-07-E5).

[0075] FIG. 66 illustrates TGA/DSC curves of phosphate crystal form Type A (807919-07-E5).

[0076] FIG. 67 illustrates a XRPD pattern of glycolate crystal form Type A (807919-07-B9).

[0077] FIG. 68 illustrates TGA/DSC curves of glycolate crystal form Type A (807919-07-B9).

[0078] FIG. 69 illustrates a XRPD pattern of maleate crystal form Type A (807919-07-D4).

[0079] FIG. 70 illustrates TGA/DSC curves of maleate crystal form Type A (807919-07-D4).

[0080] FIG. 71 illustrates a XRPD pattern of malate crystal form Type A (807919-07-B10).

[0081] FIG. 72 illustrates TGA/DSC curves of malate crystal form Type A (807919-07-B10).

[0082] FIG. 73 illustrates a XRPD pattern of adipate crystal form Type A (807919-07-B14).

[0083] FIG. 74 illustrates TGA/DSC curves of adipate crystal form Type A (807919-07-B14).

[0084] FIG. 75 illustrates a XRPD pattern of hippurate crystal form Type A (807919-07-B11).

[0085] FIG. 76 illustrates TGA/DSC curves of hippurate crystal form Type A (807919-07-B11).

[0086] FIG. 77 illustrates XRPD patterns of tartrate crystal form Type A (807919-07-A6).

[0087] FIG. 78 illustrates XRPD patterns of tartrate crystal form Type B (807919-07-E6).

[0088] FIG. 79 illustrates XRPD patterns of tartrate crystal Type C (807919-07-B6).

[0089] FIG. 80 illustrates TGA/DSC curves of tartrate crystal form Type A (807919-07-A6).

[0090] FIG. 81 illustrates TGA/DSC curves of tartrate crystal form Type B (807919-07-E6).

[0091] FIG. 82 illustrates TGA/DSC curves of tartrate crystal form Type C (807919-07-B6).

[0092] FIG. 83 illustrates XRPD patterns of fumarate crystal form Type A (807919-07-A7).

[0093] FIG. 84 illustrates XRPD patterns of fumarate crystal form Type B (807919-07-E7).

[0094] FIG. 85 illustrates XRPD patterns of fumarate crystal form Type C (807919-07-C7).

[0095] FIG. 86 illustrates TGA/DSC curves of fumarate crystal form Type A (807919-07-A7).

[0096] FIG. 87 illustrates TGA/DSC curves of fumarate crystal form Type B (807919-07-E7).

[0097] FIG. 88 illustrates TGA/DSC curves of fumarate crystal form Type C (807919-07-C7).

[0098] FIG. 89 illustrates XRPD patterns of citrate crystal form Type A (807919-07-A8).

[0099] FIG. 90 illustrates XRPD patterns of citrate crystal form Type B (807919-07-B8).

[00100] FIG. 91 illustrates TGA/DSC curves of citrate crystal form Type A (807919-07-A8).

[00101] FIG. 92 illustrates TGA/DSC curves of citrate crystal form Type B (807919-07-B8).

[00102] FIG. 93 illustrates XRPD patterns of lactate crystal form Type A (807919-07-C12).

[00103] FIG. 94 illustrates XRPD patterns of lactate crystal Type B (807919-07-A12).

[00104] FIG. 95 illustrates TGA/DSC curves of lactate crystal form Type A (807919-07-C12).

[00105] FIG. 96 illustrates TGA/DSC curves of lactate crystal form Type B (807919-07-A12).

[00106] FIG. 97 illustrates XRPD patterns of succinate crystal Type A (807919-07-C13).

[00107] FIG. 98 illustrates XRPD patterns of succinate crystal Type B (807919-07-E13).

[00108] FIG. 99 illustrates TGA/DSC curves of succinate crystal form Type A (807919-07-C13).

[00109] FIG. 100 illustrates TGA/DSC curves of succinate crystal form Type B (807919-07-E13).

[00110] FIG. 101 illustrates XRPD patterns of tosylate crystal Type A (807919-07-B15).

[00111] FIG. 102 illustrates XRPD patterns of tosylate crystal Type B (807919-07-D15).

[00112] FIG. 103 illustrates TGA/DSC curves of tosylate crystal form Type A (807919-07-B15).

[00113] FIG. 104 illustrates TGA/DSC curves of tosylate crystal form Type B (807919-07-D15).

[00114] FIG. 105 illustrates a XRPD pattern of mesylate crystal form Type A (807919-07-A16).

[00115] FIG. 106 illustrates TGA/DSC curves of mesylate crystal form Type A (807919-07-A16).

[00116] FIG. 107 illustrates XRPD patterns of oxalate crystal form Type A (807919-07-B17).

[00117] FIG. 108 illustrates XRPD patterns of oxalate crystal form Type B (807919-07-D17).

[00118] FIG. 109 illustrates TGA/DSC curves of oxalate crystal form Type A (807919-07-B17).

[00119] FIG. 110 illustrates TGA/DSC curves of oxalate crystal form Type B (807919-07-D17).

[00120] FIG. 111 illustrates XRPD patterns of gentisate crystal form Type A (807919-07-A18).

[00121] FIG. 112 illustrates XRPD patterns of gentisate crystal form Type B (807919-07-E18).

[00122] FIG. 113 illustrates TGA/DSC curves of gentisate crystal form Type A (807919-07-A18).

[00123] FIG. 114 illustrates TGA/DSC curves of gentisate crystal form Type B (807919-07-E18).

[00124] FIG. 115 illustrates XRPD patterns of benzoate crystal form Type A (807919-07-A19).

[00125] FIG. 116 illustrates XRPD patterns of benzoate crystal Type B (807919-07-E19).

[00126] FIG. 117 illustrates TGA/DSC curves of benzoate crystal form Type A (807919-07-A19).

[00127] FIG. 118 illustrates TGA/DSC curves of benzoate crystal form Type B (807919-07-E19).

[00128] FIG. 119 illustrates XRPD patterns of nitrate crystal form Type A (807919-07-D20).

[00129] FIG. 120 illustrates XRPD patterns of nitrate crystal form Type B (807919-07-B20).

[00130] FIG. 121 illustrates TGA/DSC curves of nitrate crystal form Type A (807919-07-D20).

[00131] FIG. 122 illustrates TGA/DSC curves of nitrate crystal form Type B (807919-07-B20).

[00132] FIG. 123 illustrates an inter-conversion of freebase crystal forms.

[00133] FIG. 124 illustrates a XRPD pattern of crystal form Type A (807920-05-A).

[00134] FIG. 125 illustrates TGA/DSC curves of crystal form Type A (807920-05-A).

[00135] FIG. 126 illustrates a XRPD pattern of crystal form Type C (807920-11-A11).

[00136] FIG. 127 illustrates a XRPD pattern of crystal form Type F (807920-09-A4).

[00137] FIG. 128 illustrates XRPD patterns of isomorphic Type B.

[00138] FIG. 129 illustrates TGA/DSC curves of a first batch of crystal form Type B (807920-07-A13).

[00139] FIG. 130 illustrates TGA/DSC curves of a second batch of crystal form Type B (807920-07-A13).

[00140] FIG. 131 illustrates TGA/DSC curves of a third batch of crystal form Type B (807920-07-A13).

[00141] FIG. 132 illustrates a XRPD pattern of crystal form Type D (807920-12-A9).

[00142] FIG. 133 illustrates TGA/DSC curves of crystal form Type D (807920-12-A9).

[00143] FIG. 134 illustrates a XRPD pattern of crystal form Type E (807920-16-A3).

[00144] FIG. 135 illustrates TGA/DSC curves of crystal form Type E (807920-16-A3).

[00145] FIG. 136 illustrates a XRPD pattern of crystal form Type G (807920-19-F).

[00146] FIG. 137 illustrates TGA/DSC curves of crystal form Type G (807920-19-F).

[00147] FIG. 138 illustrates a XRPD pattern of sample H (807920-22-A1).

[00148] FIG. 139 illustrates TGA/DSC curves of sample H (807920-22-A1).

[00149] FIG. 140 illustrates a DVS plot of crystal form Type A (807919-05-A).

[00150] FIG. 141 illustrates a XRPD overlay of crystal form Type A (807919-05-A) before and after DVS test.

[00151] FIG. 142 illustrates a XRPD overlay of crystal form Type A (807919-05-A) before and after stability test.

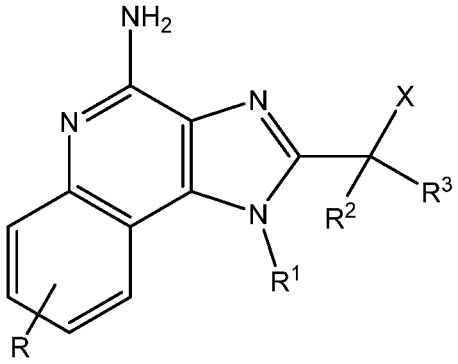
DETAILED DESCRIPTION

[00152] Described herein are new crystal forms of chemical compounds, formulations including these crystal forms, methods of forming these crystal forms, and methods of using these crystal forms. In some embodiments, these new crystal forms can be referred to as polymorphs or isomorphs. Pharmaceutical polymorphism can have a direct effect on delivery of a given pharmaceutical active agent, ingredient, or drug. Polymorphic purity of samples can be checked using techniques such as powder X-ray diffraction, IR/Raman spectroscopy, and utilizing the differences in their optical properties.

[00153] In general, active pharmaceutical ingredients (APIs) in pharmaceutical compositions can be prepared in a variety of different forms including prodrugs, amorphous forms, solvates, hydrates, co-crystals, salts, and the like. The discovery of novel API forms may provide an opportunity to improve the performance characteristics of a pharmaceutical composition. Additionally, discovery of drug forms expands the array of resources available for designing pharmaceutical dosage forms with targeted release profiles or other desired characteristics.

[00154] A specific characteristic that can be targeted includes the crystal form of an API. The alteration of the crystal form of a given API can result in modification of target molecule physical properties. For example, various polymorphs of a given API can exhibit different aqueous solubility, while the thermodynamically stable polymorph would exhibit a lower solubility than the meta-stable polymorph. In addition, pharmaceutical polymorphs can also differ in properties such as rate of dissolution, shelf life, bioavailability, morphology, vapor pressure, density, color, and compressibility. Accordingly, it may be desirable to enhance the properties of an API by forming molecular complexes such as a crystal, a co-crystal, a salt, a solvate or a hydrate with respect to aqueous solubility, rate of dissolution, bioavailability, C_{max}, T_{max}, physicochemical stability, down-stream processibility (e.g., flowability, compressibility, degree of brittleness, particle size manipulation), decrease in polymorphic form diversity, toxicity, taste, production costs, manufacturing methods, or a combination thereof.

[00155] New crystal forms of compounds and pharmaceutical compositions including the new crystal forms of these compounds are disclosed. The crystal forms can be of compounds having a structure of Formula I:



(I),

or a pharmaceutically acceptable salt thereof,

wherein R^1 is hydrogen; C_1-C_{10} straight chain or branched chain substituted or unsubstituted alkyl, wherein the substituent is C_3-C_6 cycloalkyl or C_3-C_6 cycloalkyl substituted by straight chain or branched chain C_1-C_4 alkyl; straight chain or branched chain C_2-C_{10} alkenyl; or substituted straight chain or branched chain C_2-C_{10} alkenyl, wherein the substituent is C_3-C_6 cycloalkyl or C_3-C_6 cycloalkyl substituted by straight chain or branched chain C_1-C_4 alkyl; C_1-C_6 hydroxyalkyl; alkoxyalkyl wherein the alkoxy moiety contains one to about four carbon atoms and the alkyl moiety contains one to about six carbon atoms; acyloxyalkyl wherein the acyloxy moiety is alkanoyloxy of two to about four carbon atoms or benzoyloxy, and the alkyl moiety contains one to about six carbon atoms; benzyl; (phenyl)ethyl; or phenyl; the benzyl, (phenyl)ethyl, or phenyl substituent being optionally substituted on the benzene ring by one or two moieties independently selected from C_1-C_4 alkyl, C_1-C_4 alkoxy, or halogen, with the proviso that if the benzene ring is substituted by two moieties, then the moieties together contain no more than six carbon atoms;

R^2 and R^3 are independently selected from hydrogen, C_1-C_4 alkyl, phenyl, or substituted phenyl, wherein the substituent is C_1-C_4 alkyl, C_1-C_4 alkoxy, or halogen;

X is C_1-C_4 alkoxy, alkoxyalkyl wherein the alkoxy moiety contains one to about four carbon atoms and the alkyl moiety contains one to about four carbon atoms, C_1-C_4 hydroxyalkyl, C_1-C_4 haloalkyl, alkylamido wherein the alkyl group contains one to about four carbon atoms, amino, substituted amino wherein the substituent is C_1-C_4 alkyl or C_1-C_4 hydroxyalkyl, azide, chloro, hydroxy, 1-morpholino, 1-pyrrolidino, or C_1-C_4 alkylthio; and

R is hydrogen, straight chain or branched chain C_1-C_4 alkoxy, halogen, or straight chain or branched chain C_1-C_4 alkyl.

[00156] In some embodiments, the crystal form of compounds having a structure of Formula I is a hydrochloric acid salt, a sulfate salt, a phosphate salt, a maleate salt, a malate

salt, an adipate salt, a glycolate salt, a hippurate salt, a tartrate salt, a fumarate salt, a citrate salt, a lactate salt, a succinate salt, a tosylate salt, mesylate salt, an oxalate salt, a gentisate salt, a benzoate salt, or a nitrate salt in crystalline form A, B, C, D, E, F or G.

[00157] In some embodiments, R^1 may contain two to about ten carbon atoms. In other embodiments, R^1 may contain two to about eight carbon atoms. In still other embodiments, R^1 is 2-methylpropyl or benzyl.

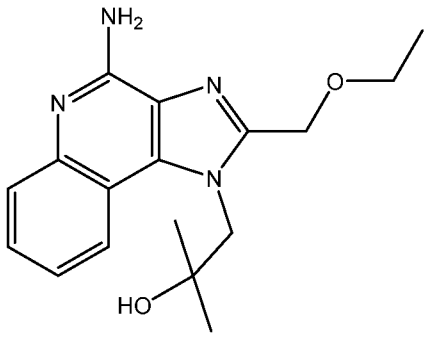
[00158] In some embodiments, X can be azido, hydroxy, ethoxy, methoxy, 1-morpholino, or methylthio. In some embodiments, X can be azido, hydroxy, ethoxy, methoxy, 1-morpholino, or methylthio when R^1 is 2-methylpropyl, 2-hydroxy-2-methylpropyl, or benzyl.

[00159] Other substituents in compounds of Formula I that contain an alkyl radical (e.g., R when R is alkoxy or alkyl, or X when X is alkylamido) can contain two carbon atoms or, in some embodiments, one carbon atom in each alkyl radical.

[00160] In some embodiments, R is hydrogen.

[00161] Compounds of Formula I can include 4-amino-α-butyl-1-(2-methylpropyl)-1H-imidazo-[4,5-c]-quinoline-2-methanol hemihydrate, 4-amino-α,α-dimethyl-2-ethoxymethyl-1H-imidazo-[4,5-c]-quinoline-1-ethanol, 2-ethoxymethyl-1-(2-methylpropyl)-1H-imidazo-[4,5-c]-quinolin-4-amine, and 4-amino-1-phenylmethyl-1H-imidazo-[4,5-c]-quinoline-2-methanol.

[00162] In one embodiment, a compound of Formula I can be resiquimod (1-[4-amino-2-(ethoxymethyl)imidazo-[4,5-c]-quinolin-1-yl]-2-methylpropan-2-ol). Resiquimod can have a structure



[00163] Halogen or halo groups in any of the compounds described herein can be F, Cl, Br, I, or At. In some embodiments, halogen or halo groups in any of the compounds described herein can be F, Cl, Br, or I.

[00164] These new crystal forms of Formula I compounds can be a HCl salt, a sulfate salt, a phosphate salt, a maleate salt, a malate salt, an adipate salt, a glycolate salt, a hippurate salt, a tartrate salt, a fumarate salt, a citrate salt, a lactate salt, a succinate salt, a tosylate

salt, mesylate salt, an oxalate salt, a gentisate salt, a benzoate salt, or a nitrate salt in crystalline form A, B, C, D, E, F or G.

[00165] One embodiment includes resiquimod in the form of a monosulfate salt in crystal form A. The crystal form A can be characterized by an x-ray powder diffraction spectrum that comprises peaks at about 7 to about 8 degrees 2θ, about 13.5 to about 14.5 degrees 2θ, about 19 to about 20 degrees 2θ, and/or about 19.5 to about 20.5 degrees 2θ.

[00166] Another embodiment includes resiquimod in the form of a sulfate salt in crystal form A. The crystal form A can be characterized by x-ray powder diffraction spectrum that comprises peaks at about 7 to about 8 degrees 2θ, about 9 to about 10 degrees 2θ, about 11 to about 12 degrees 2θ, about 14 to about 14.5 degrees 2θ, about 15 to about 16 degrees 2θ, about 17 to about 20 degrees 2θ, and/or about 24 to about 26 degrees 2θ. Resiquimod can also be formed as a sulfate salt in crystal form A characterized by x-ray powder diffraction spectrum that comprises peaks at about 7 to about 8 degrees 2θ, about 11.5 to about 12 degrees 2θ, about 14 to about 14.5 degrees 2θ, about 16 to about 16 degrees 2θ, about 17 to about 18.5 degrees 2θ, about 19.5 to about 20.5 degrees 2θ, and/or about 24 to about 25 degrees 2θ.

[00167] Resiquimod can be formed as a sulfate salt in crystal form B. Such a crystal form B can be characterized by x-ray powder diffraction spectrum that comprises peaks at about 7 to about 8 degrees 2θ, about 9 to about 10 degrees 2θ, and/or about 19 to about 20.5 degrees 2θ.

[00168] Resiquimod can also be formed as a hemi-sulfate salt in crystal form A. Such a crystal form can be characterized by x-ray powder diffraction spectrum that comprises peaks at about 6 to about 6.5 degrees 2θ, about 7 to about 8 degrees 2θ, about 8 to about 9 degrees 2θ, about 11 to about 12 degrees 2θ, about 12.5 to about 13 degrees 2θ, about 15 to about 15.5 degrees 2θ, about 16 to about 17 degrees 2θ, about 19 to about 19.5 degrees 2θ, about 21 to about 21.5 degrees 2θ, and/or about 23 to about 24 degrees 2θ.

[00169] Other compounds of resiquimod can be formed in an acetate/acetic acid co-crystal of the resiquimod freebase form. Such a crystal form can be characterized by x-ray powder diffraction spectrum that comprises peaks at about 6 to about 7 degrees 2θ, about 9 to about 10.5 degrees 2θ, about 11 to about 12 degrees 2θ, about 18 to about 19 degrees 2θ, about 19 to about 20 degrees 2θ, about 20.5 to about 21 degrees 2θ, about 22 to about 23 degrees 2θ, and/or about 25 to about 26 degrees 2θ.

[00170] Sulfate salts can also be provided in crystal form C, D, E, F, G, and H. Conversion of sulfate salt form C can be interconverted to form A by storage at ambient

temperature, for example, overnight. Conversion of sulfate salt form D can be interconverted to form A by heating, for example, to 100 °C. Conversion of sulfate salt form E can be interconverted to form A by heating, for example, to 120 °C. Conversion of sulfate salt form F can be interconverted to form A by storage at ambient temperature, for example, for two days. Conversion of sulfate salt form G can be interconverted to form A by heating, for example, to 80 °C. Because interconversion of each metastable forms and solvates converted to form A, in some embodiments, form A is the thermodynamically stable form at room temperature.

[00171] Resiquimod can be formed as an anhydrate (Type A) sulfate salt. Such a crystal form can be characterized by x-ray powder diffraction spectrum that comprises peaks at about 8.5 to about 9 degrees 2θ, about 12 to about 13 degrees 2θ, about 16 to about 17 degrees 2θ, about 17.5 to about 18 degrees 2θ, about 19 to about 20.5 degrees 2θ, about 21 to about 22 degrees 2θ, about 23 to about 24 degrees 2θ, and/or about 29 to about 30 degrees 2θ.

[00172] Resiquimod can be formed as a solvate (Type B) sulfate salt. Such a crystal form can be characterized by x-ray powder diffraction spectrum that comprises peaks at about 6 to about 6.5 degrees 2θ, about 12 to about 12.5 degrees 2θ, about 16 to about 16.5 degrees 2θ, about 21 to about 22.5 degrees 2θ, and/or about 24.5 to about 25 degrees 2θ.

[00173] Resiquimod can be formed as a sulfate salt Type C. Such a crystal form can be characterized by x-ray powder diffraction spectrum that comprises peaks at about 9 to about 10 degrees 2θ, about 12 to about 12.5 degrees 2θ, about 14 to about 15 degrees 2θ, about 18 to about 19 degrees 2θ, about 19 to about 21.5 degrees 2θ, and/or about 28 to about 29 degrees 2θ.

[00174] Resiquimod can be formed as a DMAc solvate (Type D) sulfate salt. Such a crystal form can be characterized by x-ray powder diffraction spectrum that comprises peaks at about 8 to about 9 degrees 2θ, about 11 to about 11.5 degrees 2θ, about 16.5 to about 17 degrees 2θ, about 17.5 to about 18 degrees 2θ, about 21 to about 21.5 degrees 2θ, about 22.5 to about 23 degrees 2θ, and/or about 23.5 to about 24.5 degrees 2θ.

[00175] Resiquimod can be formed as a NMP solvate (Type E) sulfate salt. Such a crystal form can be characterized by x-ray powder diffraction spectrum that comprises peaks at about 8 to about 9 degrees 2θ, about 9 to about 9.5 degrees 2θ, about 11 to about 11.5 degrees 2θ, about 12 to about 13 degrees 2θ, about 16.5 to about 18 degrees 2θ, about 21 to about 21.5 degrees 2θ, about 22.5 to about 23 degrees 2θ, and/or about 23.5 to about 24 degrees 2θ.

[00176] Resiquimod can be formed as a sulfate salt Type F. Such a crystal form can be characterized by x-ray powder diffraction spectrum that comprises peaks at about 8 to about 8.5 degrees 2θ, about 10 to about 11 degrees 2θ, about 12 to about 13 degrees 2θ, about 16 to about 17 degrees 2θ, about 17 to about 18 degrees 2θ, about 20.5 to about 21.5 degrees 2θ, about 24.5 to about 25 degrees 2θ, and/or about 28.5 to about 29 degrees 2θ.

[00177] Resiquimod can be formed as a anisole solvate (Type G) sulfate salt. Such a crystal form can be characterized by x-ray powder diffraction spectrum that comprises peaks at about 8.5 to about 9 degrees 2θ, about 9.5 to about 10 degrees 2θ, about 13 to about 14 degrees 2θ, about 19 to about 19.5 degrees 2θ, and/or about 27.5 to about 28.5 degrees 2θ.

[00178] Other Formula I compounds described herein can be formed in similar salt configurations.

[00179] Crystal forms of Formula I compounds can be in Type A, Type B, Type C, Type D, Type E, Type F, Type G, and/or Type H. In some embodiments, the forms can be described as Type A:anhydrate, Type B:solvate, Type C:mestable, Type D:dimethylacetamide (DMAc) solvate, Type E:N-methyl-2-pyrolidone (NMP) solvate, Type F:mestable, Type G:anisole solvate, and Type H:acetate/acetic acid co-crystal.

[00180] Still other compounds of Formula I described herein can be formed as a sulfate salt in crystal form B. Sulfate salt in crystal form B can be a dimethyl sulfoxide (DMSO) solvate. Still other compounds of Formula I described herein can be formed as a hemi-sulfate salt in crystal form A.

[00181] In some embodiments, form A can be stable at room temperature for at least about 1 day, at least about 2 days, at least about 3 days, at least about 1 week, at least about 2 weeks, at least about 1 month, at least about 6 months, or at least about 1 year.

[00182] Still other compounds of Formula I described herein can be formed as a HCl salts, sulfate salts, phosphate salts, maleate salts, malate salts, adipate salts or combinations thereof. In some embodiments, the salts can be formed in form or type A.

[00183] In one embodiment, compounds of Formula I described herein can be formed as a mono-HCl salt in crystal form A. In one embodiment, compounds of Formula I described herein can be formed as a di-HCl salt in crystal form A. Either form of HCl salt can be formed as an anhydrate.

[00184] One embodiment includes resiquimod in the form of a HCl salt in crystal form A. The crystal form A can be characterized by x-ray powder diffraction spectrum that comprises peaks at about 6 to about 7 degrees 2θ, about 9 to about 10 degrees 2θ, about 12 to about 13 degrees 2θ, about 14 to about 16 degrees 2θ, about 18 to about 23 degrees 2θ, about 23

to about 25 degrees 2θ, about 26 to about 27.5 degrees 2θ, and/or about 26 to about 27.5 degrees 2θ.

[00185] Another embodiment includes resiquimod in the form of a HCl salt in crystal form B. The crystal form B can be characterized by x-ray powder diffraction spectrum that comprises peaks at about 6 to about 8 degrees 2θ, about 19 to about 21 degrees 2θ, about 23 to about 24.5 degrees 2θ, about 26 to about 27 degrees 2θ, and/or about 28 to about 29 degrees 2θ.

[00186] Another embodiment includes resiquimod in the form of a mono-HCl salt in crystal form A. The crystal form A can be characterized by x-ray powder diffraction spectrum that comprises peaks at about 6 to about 7 degrees 2θ, about 9 to about 10 degrees 2θ, about 13 to about 14 degrees 2θ, about 17 to about 18 degrees 2θ, about 20 to about 21 degrees 2θ, about 27 to about 28 degrees 2θ, and/or about 34 to about 35 degrees 2θ.

[00187] Another embodiment includes resiquimod in the form of a di-HCl salt in crystal form A. The crystal form A can be characterized by x-ray powder diffraction spectrum that comprises peaks at about 7 to about 8 degrees 2θ, about 8 to about 9 degrees 2θ, about 14 to about 15 degrees 2θ, about 15 to about 16 degrees 2θ, about 19 to about 20 degrees 2θ, about 25 to about 26 degrees 2θ, and/or about 26.5 to about 27.5 degrees 2θ.

[00188] In one embodiment, compounds of Formula I described herein can be formed as an anhydrate phosphate salt in crystal form A.

[00189] Another embodiment includes resiquimod in the form of a phosphate salt in crystal form A. The crystal form A can be characterized by x-ray powder diffraction spectrum that comprises peaks at about 7 to about 8 degrees 2θ, about 10 to about 14.5 degrees 2θ, about 15 to about 16 degrees 2θ, about 20 to about 21 degrees 2θ, and/or about 25 to about 26 degrees 2θ. Other embodiments include resiquimod in the form of a phosphate salt in crystal form A characterized by x-ray powder diffraction spectrum that comprises peaks at about 7 to about 8.5 degrees 2θ, about 10 to about 15.5 degrees 2θ, about 16 to about 18.5 degrees 2θ, about 19 to about 21 degrees 2θ, about 22 to about 23 degrees 2θ, about 23 to about 27 degrees 2θ, and/or about 28 to about 29 degrees 2θ.

[00190] In one embodiment, compounds of Formula I described herein can be formed as an anhydrate maleate salt in crystal form A. In another embodiment, compounds of Formula I described herein can be formed as an anhydrate mono-maleate salt in crystal form A.

[00191] Another embodiment includes resiquimod in the form of a maleate salt in crystal form A. The crystal form A can be characterized by x-ray powder diffraction spectrum that comprises peaks at about 7 to about 8 degrees 2θ, about 9 to about 10 degrees 2θ, about

10 to about 11 degrees 2θ, about 15 to about 17 degrees 2θ, about 20 to about 21 degrees 2θ, about 21 to about 22 degrees 2θ, about 27 to about 28 degrees 2θ, and/or about 30 to about 31 degrees 2θ. Other embodiments include resiquimod in the form of a maleate salt in crystal form A characterized by x-ray powder diffraction spectrum that comprises peaks at about 7 to about 8 degrees 2θ, about 9 to about 10 degrees 2θ, about 10 to about 11 degrees 2θ, about 11 to about 12 degrees 2θ, about 15 to about 16.5 degrees 2θ, about 17 to about 19 degrees 2θ, about 20 to about 21 degrees 2θ, about 21 to about 22 degrees 2θ, about 24 to about 25 degrees 2θ, about 27 to about 28 degrees 2θ, and/or about 30 to about 31 degrees 2θ.

[00192] In one embodiment, compounds of Formula I described herein can be formed as a anhydrate malate salt in crystal form A.

[00193] Another embodiment includes resiquimod in the form of a malate salt in crystal form A. The crystal form A can be characterized by x-ray powder diffraction spectrum that comprises peaks at about 6 to about 7 degrees 2θ, about 8 to about 9 degrees 2θ, about 13 to about 14 degrees 2θ, about 17 to about 18 degrees 2θ, and/or about 24 to about 25.5 degrees 2θ. Other embodiments include resiquimod in the form of a malate salt in crystal form A characterized by x-ray powder diffraction spectrum that comprises peaks at about 6 to about 7 degrees 2θ, about 8 to about 9 degrees 2θ, about 17 to about 18 degrees 2θ, about 21.5 to about 23.5 degrees 2θ, and/or about 25 to about 26 degrees 2θ.

[00194] In one embodiment, compounds of Formula I described herein can be formed as an anhydrate adipate salt in crystal form A.

[00195] Another embodiment includes resiquimod in the form of an adipate salt in crystal form A. The crystal form A can be characterized by x-ray powder diffraction spectrum that comprises peaks at about 5.5 to about 6 degrees 2θ, about 11 to about 12 degrees 2θ, about 12 to about 13 degrees 2θ, about 13 to about 14 degrees 2θ, about 14 to about 15 degrees 2θ, about 18 to about 19 degrees 2θ, about 19 to about 20 degrees 2θ, about 21 to about 22 degrees 2θ, about 22 to about 23 degrees 2θ, and/or about 25 to about 28 degrees 2θ. Other embodiments include resiquimod in the form of an adipate salt in crystal form A characterized by x-ray powder diffraction spectrum that comprises peaks at about 5 to about 6.5 degrees 2θ, about 9 to about 11 degrees 2θ, about 12 to about 13.5 degrees 2θ, about 14 to about 15.5 degrees 2θ, about 17 to about 18 degrees 2θ, about 18 to about 19 degrees 2θ, about 19.5 to about 22 degrees 2θ, about 22 to about 25 degrees 2θ, and/or about 26 to about 27.5 degrees 2θ.

[00196] Formula I compounds can also be formed as glycolate salts. In one embodiment, compounds of Formula I described herein can be formed as a glycolate salt in crystal form A.

[00197] One embodiment includes resiquimod in the form of a glycolate salt in crystal form A. The crystal form A can be characterized by x-ray powder diffraction spectrum that comprises peaks at about 9 to about 10 degrees 2θ, about 11.5 to about 12.5 degrees 2θ, about 18 to about 19 degrees 2θ, about 19.5 to about 23 degrees 2θ, about 25 to about 26.5 degrees 2θ, and/or about 32 to about 33 degrees 2θ.

[00198] Formula I compounds can also be formed as hippurate salts. In one embodiment, compounds of Formula I described herein can be formed as a hippurate salt in crystal form A.

[00199] One embodiment includes resiquimod in the form of a hippurate salt in crystal form A. The crystal form A can be characterized by x-ray powder diffraction spectrum that comprises peaks at about 5.5 to about 6.5 degrees 2θ, about 9 to about 10 degrees 2θ, about 11.5 to about 12.5 degrees 2θ, about 18.5 to about 19.5 degrees 2θ, about 21 to about 22 degrees 2θ, and/or about 25 to about 26 degrees 2θ.

[00200] Formula I compounds can also be formed as tartrate salts. In another embodiment, compounds of Formula I described herein can be formed as a tartrate salt in crystal forms A, B, and/or C.

[00201] One embodiment includes resiquimod in the form of a tartrate salt in crystal form A. The crystal form A can be characterized by x-ray powder diffraction spectrum that comprises peaks at about 6 to about 7 degrees 2θ, about 9 to about 10 degrees 2θ, about 18 to about 19 degrees 2θ, about 20 to about 22 degrees 2θ, and/or about 25 to about 26 degrees 2θ.

[00202] One embodiment includes resiquimod in the form of a tartrate salt in crystal form B. The crystal form B can be characterized by x-ray powder diffraction spectrum that comprises peaks at about 8.5 to about 9 degrees 2θ, about 11 to about 12 degrees 2θ, about 13 to about 14 degrees 2θ, about 14 to about 15 degrees 2θ, about 16 to about 17 degrees 2θ, and/or about 23 to about 24.5 degrees 2θ.

[00203] One embodiment includes resiquimod in the form of a tartrate salt in crystal form C. The crystal form C can be characterized by x-ray powder diffraction spectrum that comprises peaks at about 7 to about 8 degrees 2θ, about 10 to about 11.5 degrees 2θ, and/or about 20 to about 21 degrees 2θ.

[00204] Formula I compounds can also be formed as fumarate salts. In another embodiment, compounds of Formula I described herein can be formed as a fumarate salt in crystal forms A, B, and/or C.

[00205] One embodiment includes resiquimod in the form of a fumarate salt in crystal form A. The crystal form A can be characterized by x-ray powder diffraction spectrum that

comprises peaks at about 6 to about 7 degrees 2θ, about 7 to about 8 degrees 2θ, about 9 to about 10.5 degrees 2θ, about 12 to about 14 degrees 2θ, about 18 to about 19 degrees 2θ, about 19 to about 20 degrees 2θ, about 23 to about 24.5 degrees 2θ, and/or about 25 to about 26 degrees 2θ.

[00206] One embodiment includes resiquimod in the form of a fumarate salt in crystal form B. The crystal form B can be characterized by x-ray powder diffraction spectrum that comprises peaks at about 9.5 to about 10.5 degrees 2θ, about 12 to about 13 degrees 2θ, about 15 to about 16 degrees 2θ, about 17 to about 18 degrees 2θ, about 19 to about 21 degrees 2θ, and/or about 25 to about 26 degrees 2θ.

[00207] One embodiment includes resiquimod in the form of a fumarate salt in crystal form C. The crystal form C can be characterized by x-ray powder diffraction spectrum that comprises peaks at about 6 to about 7 degrees 2θ, about 9 to about 10 degrees 2θ, about 11 to about 12 degrees 2θ, about 15 to about 16 degrees 2θ, about 21 to about 22 degrees 2θ, about 26 to about 27 degrees 2θ, and/or about 27.5 to about 28.5 degrees 2θ.

[00208] Formula I compounds can also be formed as citrate salts. In another embodiment, compounds of Formula I described herein can be formed as a citrate salt in crystal forms A and/or B.

[00209] One embodiment includes resiquimod in the form of a citrate salt in crystal form A. The crystal form A can be characterized by x-ray powder diffraction spectrum that comprises peaks at about 5 to about 6.5 degrees 2θ, about 11 to about 12 degrees 2θ, about 14.5 to about 15.5 degrees 2θ, about 17 to about 18.5 degrees 2θ, about 19 to about 20.5 degrees 2θ, about 21 to about 22 degrees 2θ, about 26 to about 27 degrees 2θ, and/or about 27.5 to about 28.5 degrees 2θ.

[00210] One embodiment includes resiquimod in the form of a citrate salt in crystal form B. The crystal form B can be characterized by x-ray powder diffraction spectrum that comprises peaks at about 5.5 to about 6.5 degrees 2θ, about 8 to about 9 degrees 2θ, about 9.5 to about 10.5 degrees 2θ, about 11 to about 12.5 degrees 2θ, about 18 to about 19.5 degrees 2θ, and/or about 21 to about 24.5 degrees 2θ.

[00211] Formula I compounds can also be formed as lactate salts. In another embodiment, compounds of Formula I described herein can be formed as a lactate salt in crystal forms A and/or B.

[00212] One embodiment includes resiquimod in the form of a lactate salt in crystal form A. The crystal form A can be characterized by x-ray powder diffraction spectrum that comprises peaks at about 5 to about 8 degrees 2θ, about 8 to about 9 degrees 2θ, about 10 to about

11 degrees 2θ, about 12.5 to about 13.5 degrees 2θ, about 18.5 to about 19.5 degrees 2θ, and/or about 22 to about 23 degrees 2θ.

[00213] One embodiment includes resiquimod in the form of a lactate salt in crystal form B. The crystal form B can be characterized by x-ray powder diffraction spectrum that comprises peaks at about 5 to about 6 degrees 2θ, about 6.5 to about 8 degrees 2θ, about 9 to about 10.5 degrees 2θ, and/or about 13.5 to about 14.5 degrees 2θ.

[00214] Formula I compounds can also be formed as succinate salts. In another embodiment, compounds of Formula I described herein can be formed as a succinate salt in crystal forms A and/or B.

[00215] One embodiment includes resiquimod in the form of a succinate salt in crystal form A. The crystal form A can be characterized by x-ray powder diffraction spectrum that comprises peaks at about 5 to about 8 degrees 2θ, about 9 to about 11.5 degrees 2θ, about 18 to about 19 degrees 2θ, about 23 to about 24 degrees 2θ, and/or about 24.5 to about 25.5 degrees 2θ.

[00216] One embodiment includes resiquimod in the form of a succinate salt in crystal form B. The crystal form B can be characterized by x-ray powder diffraction spectrum that comprises peaks at about 8 to about 9 degrees 2θ, about 10 to about 11 degrees 2θ, about 12 to about 13 degrees 2θ, about 14 to about 15 degrees 2θ, about 16 to about 17 degrees 2θ, about 17 to about 18 degrees 2θ, and/or about 23.5 to about 24.5 degrees 2θ.

[00217] Formula I compounds can also be formed as tosylate salts. In another embodiment, compounds of Formula I described herein can be formed as a tosylate salt in crystal forms A and/or B.

[00218] One embodiment includes resiquimod in the form of a tosylate salt in crystal form A. The crystal form A can be characterized by x-ray powder diffraction spectrum that comprises peaks at about 4 to about 5 degrees 2θ, about 9 to about 10 degrees 2θ, about 16 to about 17 degrees 2θ, about 19 to about 21 degrees 2θ, and/or about 24 to about 28 degrees 2θ.

[00219] One embodiment includes resiquimod in the form of a tosylate salt in crystal form B. The crystal form B can be characterized by x-ray powder diffraction spectrum that comprises peaks at about 5 to about 6 degrees 2θ, about 7 to about 9 degrees 2θ, about 9.5 to about 11.5 degrees 2θ, about 12 to about 14 degrees 2θ, about 15 to about 19 degrees 2θ, about 19 to about 20.5 degrees 2θ, and/or about 23 to about 24 degrees 2θ.

[00220] Formula I compounds can also be formed as mesylate salts. In one embodiment, compounds of Formula I described herein can be formed as a mesylate salt in crystal form A.

[00221] One embodiment includes resiquimod in the form of a mesylate salt in crystal form A. The crystal form A can be characterized by x-ray powder diffraction spectrum that comprises peaks at about 8 to about 9 degrees 2θ, about 12 to about 13 degrees 2θ, about 14 to about 15 degrees 2θ, about 16 to about 17 degrees 2θ, about 18 to about 19.5 degrees 2θ, about 21 to about 22 degrees 2θ, and/or about 25.5 to about 26.5 degrees 2θ.

[00222] Formula I compounds can also be formed as oxalate salts. In another embodiment, compounds of Formula I described herein can be formed as an oxalate salt in crystal forms A and/or B.

[00223] One embodiment includes resiquimod in the form of an oxalate salt in crystal form A. The crystal form A can be characterized by x-ray powder diffraction spectrum that comprises peaks at about 9 to about 10 degrees 2θ, about 14 to about 15 degrees 2θ, about 17 to about 18 degrees 2θ, about 18.5 to about 20 degrees 2θ, about 21 to about 22 degrees 2θ, about 23 to about 25.5 degrees 2θ, and/or about 30 to about 31 degrees 2θ.

[00224] One embodiment includes resiquimod in the form of an oxalate salt in crystal form B. The crystal form B can be characterized by x-ray powder diffraction spectrum that comprises peaks at about 5 to about 6 degrees 2θ, about 9.5 to about 10 degrees 2θ, about 10.5 to about 11.5 degrees 2θ, about 13 to about 13.5 degrees 2θ, about 14.5 to about 15.5 degrees 2θ, about 16.5 to about 18 degrees 2θ, about 22 to about 24.5 degrees 2θ, and/or about 27 to about 28 degrees 2θ.

[00225] Formula I compounds can also be formed as genisate salts. In another embodiment, compounds of Formula I described herein can be formed as a gentisate salt in crystal forms A and/or B.

[00226] One embodiment includes resiquimod in the form of a gentisate salt in crystal form A. The crystal form A can be characterized by x-ray powder diffraction spectrum that comprises peaks at about 6 to about 7.5 degrees 2θ, about 8 to about 9 degrees 2θ, about 10 to about 11 degrees 2θ, about 14 to about 15 degrees 2θ, about 16 to about 17 degrees 2θ, about 18 to about 19 degrees 2θ, about 20 to about 21.5 degrees 2θ, and/or about 22.5 to about 23.5 degrees 2θ.

[00227] One embodiment includes resiquimod in the form of a gentisate salt in crystal form B. The crystal form B can be characterized by x-ray powder diffraction spectrum that comprises peaks at about 6 to about 7 degrees 2θ, about 10 to about 10.5 degrees 2θ, about 12 to about 13 degrees 2θ, about 20 to about 21 degrees 2θ, about 24 to about 24.5 degrees 2θ, and/or about 26 to about 26.5 degrees 2θ.

[00228] Formula I compounds can also be formed as benzoate salts. In another embodiment, compounds of Formula I described herein can be formed as a benzoate salt in crystal forms A and/or B.

[00229] One embodiment includes resiquimod in the form of a benzoate salt in crystal form A. The crystal form A can be characterized by x-ray powder diffraction spectrum that comprises peaks at about 7 to about 9 degrees 2θ, about 10 to about 11.5 degrees 2θ, about 12 to about 12.5 degrees 2θ, about 14 to about 16.5 degrees 2θ, about 19 to about 22 degrees 2θ, about 23.5 to about 24.5 degrees 2θ, about 28.5 to about 29 degrees 2θ, and/or about 29 to about 30 degrees 2θ.

[00230] One embodiment includes resiquimod in the form of a benzoate salt in crystal form B. The crystal form B can be characterized by x-ray powder diffraction spectrum that comprises peaks at about 7 to about 8.5 degrees 2θ, about 12 to about 14 degrees 2θ, about 18 to about 19 degrees 2θ, about 19.5 to about 20.5 degrees 2θ, about 21 to about 23 degrees 2θ, about 24 to about 25 degrees 2θ, and/or about 26 to about 27 degrees 2θ.

[00231] Formula I compounds can also be formed as nitrate salts. In another embodiment, compounds of Formula I described herein can be formed as a nitrate salt in crystal forms A and/or B.

[00232] One embodiment includes resiquimod in the form of a nitrate salt in crystal form A. The crystal form A can be characterized by x-ray powder diffraction spectrum that comprises peaks at about 9 to about 9.5 degrees 2θ, about 10 to about 10.5 degrees 2θ, about 11.5 to about 12.5 degrees 2θ, about 14 to about 15 degrees 2θ, about 16 to about 17.5 degrees 2θ, about 20 to about 22.5 degrees 2θ, about 25 to about 26 degrees 2θ, and/or about 28.5 to about 29.5 degrees 2θ.

[00233] One embodiment includes resiquimod in the form of a nitrate salt in crystal form B. The crystal form B can be characterized by x-ray powder diffraction spectrum that comprises peaks at about 9 to about 10 degrees 2θ, about 12.5 to about 13 degrees 2θ, about 14 to about 16 degrees 2θ, about 19.5 to about 21 degrees 2θ, about 25 to about 26 degrees 2θ, and/or about 26 to about 27 degrees 2θ.

[00234] In some embodiments, a monosulfate salt in crystal form A can convert to a hemi-sulfate at water activity of 0.8. Further, a monosulfate salt in crystal form A can demonstrate good physicochemical stability at 80 °C for 24 hours or more.

[00235] In some embodiments, crystal forms of compounds described herein have an XRPD pattern of Fig. 1, Fig. 4, Fig. 7, Fig. 10, Fig. 13, Fig. 16, Fig. 19, Fig. 48, Fig. 50, Fig. 54, Fig. 59, Fig. 61, Fig. 63, Fig. 65, Fig. 67, Fig. 69, Fig. 71, Fig. 73, Fig. 75, Fig. 77, Fig. 78,

Fig. 79, Fig. 83, Fig. 84, Fig. 85, Fig. 89, Fig. 90, Fig. 93, Fig. 94, Fig. 97, Fig. 98, Fig. 101, Fig. 102, Fig. 105, Fig. 107, Fig. 108, Fig. 111, Fig. 112, Fig. 115, Fig. 116, Fig. 119, Fig. 120, Fig. 124, Fig. 126, Fig. 127, Fig. 128, Fig. 132, Fig. 134, Fig. 136, or Fig. 138.

[00236] In some embodiments, crystal forms of Formula I compounds may be slightly hygroscopic. In other embodiments, crystal forms of Formula I compounds may be non-hygroscopic. These crystal forms may also exhibit no form change after a Dynamic Vapor Sorption (DVS) test.

[00237] In other embodiments, when compared to a freebase form of a Formula I compound, crystal forms show improved or comparable solubility in water and bio-relevant media at room temperature.

[00238] Further, the crystal forms can have physical and chemical stability when compared to a Formula I compound freebase. In some embodiments, no form change and/or purity decrease may be exhibited when compared to freebase form, at 25 ºC/60%RH and 40 ºC/75%RH. In some embodiments, this absence of form change and/or purity decrease may remain for at least about 1 week, at least about 2 weeks, at least about 1 month, at least about 6 months, or at least about 1 year.

[00239] Another aspect provides improved aqueous solubility of Formula I compound crystal forms compared with the parent compound or a freebase form thereof. Another aspect provides improved aqueous solubility of resiquimod crystal forms compared with the parent compound or a freebase form thereof.

[00240] Another aspect provides modified oral bioavailability values of Formula I compound crystal forms compared with the orally delivered parent compound or a freebase form thereof. Another aspect provides modified oral bioavailability values of resiquimod crystal forms compared with the orally delivered parent compound or a freebase form thereof.

[00241] The techniques and approaches set forth in the present disclosure can further be used by the person of ordinary skill in the art to prepare variants thereof; the variants are considered to be part of the present disclosure.

[00242] The presently described crystal forms of Formula I compounds can be used to treat a disease or condition. In some embodiments, the disease or condition is a cancer. Cancers can include breast cancer, head and neck cancer, ovarian cancer, uterine cancer, skin cancer, brain cancer, bladder cancer, thyroid cancer, liver cancer, pancreatic cancer, lung cancer, ocular cancer, throat cancer, esophageal cancer, stomach cancer, intestinal cancer, rectal cancer, testicular cancer, ovarian cancer, vaginal cancer, bone cancer, blood cancer, prostate cancer, and the like.

[00243] The presently described crystal forms of Formula I compounds can be used to treat a tumor in a subject in need thereof. In some embodiments, the tumor is a carcinoma, a sarcoma, a blastomas, or a combination thereof.

[00244] A carcinoma can include, without limitation, an adrenal gland tumor, a bone tumor, a brain tumor, a breast tumor, a bronchi tumor, a colon tumor, a gallbladder tumor, a kidney tumor, a larynx tumor, a liver tumor, a lung tumor, a neural tumor, a pancreatic tumor, a prostate tumor, a parathyroid tumor, a skin tumor, a stomach tumor, and a thyroid tumor. In other aspects of this embodiment, a carcinoma includes, without limitation, an adenocarcinoma, an adenosquamous carcinoma, an anaplastic carcinoma, a large cell carcinoma, a small cell carcinoma, and a squamous cell carcinoma. In other aspects of this embodiment, a carcinoma includes, without limitation, a small cell carcinoma, a combined small cell carcinoma, a verrucous carcinoma, a squamous cell carcinoma, a basal cell carcinoma, a transitional cell carcinoma, an inverted papilloma, a linitis plastica, a familial adenomatous polyposis, an insulinoma, a glucagonoma, a gastrinoma, a VIPoma, a somatostatinoma, a cholangiocarcinoma, a Klatskin tumor, a hepatocellular adenoma, a hepatocellular carcinoma, a renal cell carcinoma, a endometrioid tumor, a renal oncocytoma, a prolactinoma, a multiple endocrine neoplasia, an adrenocortical adenoma, an adrenocortical carcinoma, a Hurthle cell, a neuroendocrine tumor, an adenoid cystic carcinoma, an oncocytoma, a clear cell adenocarcinoma, an apudoma, a cylindroma, a papillary hidradenoma, a hidrocystoma, a syringoma, a syringocystadenoma papilliferum, a cystadenoma, a cystadenocarcinoma, signet ring cell carcinoma, a mucinous cystadenoma, a mucinous cystadenocarcinoma, a mucoepidermoid carcinoma, an ovarian serous cystadenoma, a pancreatic serous cystadenoma, a serous cystadenocarcinoma, a papillary serous cystadenocarcinoma, a mammary ductal carcinoma, a pancreatic ductal carcinoma, a comedocarcinoma, a Paget's disease of the breast, an extramammary Paget's disease, a lobular carcinoma in situ, an invasive lobular carcinoma, a medullary carcinoma of the breast, a medullary thyroid cancer, an acinic cell carcinoma, a Warthin's tumor, or a thymoma.

[00245] Sarcomas can include, without limitation, a soft tissue sarcoma, a connective tissue sarcoma, a lipomatous sarcoma, a myomatous sarcoma, a complex mixed and stromal sarcoma, and a mesothelial. In aspects of this embodiment, a non-hematologic sarcoma includes, without limitation, an adenomatoid tumor, an adenomyoma, an aggressive infantile fibromatosis, an alveolar rhabdomyosarcoma, an angiolipoleiomyoma, an angiomyolipoma, an angioleiomyoma, an angiomyxoma, an angiosarcoma, an aponeurotic fibroma, an Askin's tumor, an atypical fibroxanthoma, a benign lipoblastomatosis, a Brenner tumor, a carcinosarcoma, a chondroid lipoma, a chondrosarcoma, a clear-cell sarcoma, a clear-cell sarcoma of the kidney, a collagenous

fibroma, a cystosarcoma phyllodes, a dermatofibrosarcoma, a dermatofibrosarcoma protuberans (DFSP), a desmoplastic fibroma, a desmoplastic small round cell tumor, a diffuse infantile fibromatosis, an Ewing's/PNET sarcoma, a familial myxovascular fibroma, a fibroadenoma, a fibroma of tendon sheath, a fibromatosis colli, a fibrous histiocytoma, a fibrosarcoma, a gastrointestinal stromal tumor (GIST), a genital leiomyoma, a hemangioendothelioma, a hepatoblastoma, a hibernoma, a histiocytoma, an infantile digital fibromatosis, an intradermal spindle cell lipoma, a juvenile hyaline fibromatosis, a Kaposi's sarcoma, a leiomyosarcoma, a liposarcoma, a mesoblastic nephroma, a mesothelioma, a mixed Müllerian tumor, a multiple cutaneous leiomyoma, a multiple cutaneous and uterine leiomyomatosis syndrome, a myelolipoma, a myosarcoma, a myxoid liposarcoma, a myxosarcoma, a neural fibrolipoma, a neurofibrosarcoma, an oral submucous fibrosis, an ossifying fibromyxoid tumor, an osteosarcoma, a pancreatoblastoma, a phyllodes tumor, a plantar fibromatosis, a pleomorphic adenoma, a pleomorphic fibroma, a pleomorphic lipoma, a rhabdomyosarcoma, a sarcoma botryoides, a schwannoma sarcoma, a solitary cutaneous leiomyoma, a solitary fibrous tumor, a spindle cell lipoma, a stromal tumor of undetermined malignant potential (STUMP), a synovial sarcoma, a vascular sarcoma, or a Wilms' tumor.

[00246] Blastomas can include, without limitation, a chondroblastoma, a hepatoblastoma, a medulloblastoma, a nephroblastoma, a neuroblastoma, a pancreatoblastoma, a pleuropulmonary blastoma, a retinoblastoma, or a lioblastoma multiforme.

[00247] Resiquimod and related Formula I compounds described herein can be agonists of TLR7/TLR8. Studies have found that many solid tumors, such as breast cancer, head and neck cancer, or ovarian cancer, have pDC's invasion and factors secreted by tumor cells that inhibit DC maturation. These immature DC cells did not play a role in promoting anti-tumor immunity. By contrast, DCs within the tumor microenvironment promote tumor growth by inhibiting antitumor immunity and by promoting angiogenesis. There is evidence that Toll-like receptor 7 agonist imiquimod, and Toll-like receptor 9 agonist CpG drugs can stimulate pDC within the tumor microenvironment to inhibit tumor development.

[00248] Natural killer (NK) cells are a type of cytotoxic lymphocyte that constitutes a major component of the immune system. NK cells are a subset of peripheral blood lymphocytes defined by the expression of CD56 or CD 16 and the absence of the T cell receptor (CD3). They recognize and kill transformed cell lines without priming in an MHC-unrestricted fashion. NK cells play a major role in the rejection of tumors and cells infected by viruses. The process by which an NK cell recognizes a target cell and delivers a sufficient signal to trigger target lysis is determined by an array of inhibitory and activating receptors on the cell surface. NK discrimination of self from altered self involves inhibitory receptor recognition of MHC-I molecules and non-MHC ligands like CD48 and Clr-1b. NK recognition

of infected or damaged cells (altered self) is coordinated through stress induced ligands (e.g., MICA, MICB, Rae1, H60, Mult1) or virally encoded ligands (e.g., m157, hemagluttinin) recognized by various activating receptors, including NKG2D, Ly49H and NKp46/Ncr1.

[00249] NK cells represent the predominant lymphoid cell in the peripheral blood for many months after allogeneic or autologous stem cell transplant and they have a primary role in immunity to pathogens during this period.

[00250] Human NK cells mediate the lysis of tumor cells and virus-infected cells via natural cytotoxicity and antibody-dependent cellular cytotoxicity (ADCC).

[00251] Human NK cells are controlled by positive and negative cytolytic signals. Negative (inhibitory) signals are transduced by C-lectin domain containing receptors CD94/NKG2A and by some Killer Immunoglobulin-like Receptors (KIRs). The regulation of NK lysis by inhibitory signals is known as the "missing self" hypothesis in which specific HLA-class I alleles expressed on the target cell surface ligate inhibitory receptors on NK cells. The down-regulation of HLA molecules on tumor cells and some virally infected cells (e.g. CMV) lowers this inhibition below a target threshold and the target cells may become susceptible to NK cell- mediated lysis if the target cells also carry NK-priming and activating molecules. TLR7, TLR8 or TLR9 agonists can activate both mDC and pDCs to produce type I IFNs and express costimulatory molecules such as GITR-ligand, which subsequently activate NK cells to produce IFN-g and potently promote NK cell killing function.

[00252] Inhibitory receptors fall into two groups, those of the Ig-superfamily called Killer Immunoglobulin-like Receptors (KIRs) and those of the lectin family, the NKG2, which form dimers with CD94 at the cell surface. KIRs have a 2- or 3-domain extracellular structure and bind to HLA-A, -B or -C. The NKG2/CD94 complexes ligate HLA-E.

[00253] Inhibitory KIRs have up to 4 intracellular domains which contain ITIMs and the best characterized are KIR2DL1, KIR2DL2 and KIR2DL3 which are known to bind HLA-C molecules. KIR2DL2 and KIR2DL3 bind the group 1 HLA-C alleles while KIR2DL1 binds to group 2 alleles. Certain leukemia/lymphoma cells express both group 1 and 2 HLA-C alleles and are known to be resistant to NK-mediated cell lysis.

[00254] With regards to positive activating signals, ADCC is thought to be mediated via CD 16, and a number of triggering receptors responsible for natural cytotoxicity have been identified, including CD2, CD38, CD69, NKRP-I, CD40, B7-2, NK-TR, NKp46, NKp30 and NKp44. In addition, several KIR molecules with short intracytoplasmic tails are also stimulatory. These KIRs (KIR2DS1, KIR2DS2 and KIR2DS4) are known to bind to HLA-C; their extracellular domains being identical to their related inhibitory KIRs. The activatory

KIRs lack the ITIMs and instead associate with DAP 12 leading to NK cell activation. The mechanism of control of expression of inhibitory versus activatory KIRs remains unknown.

[00255] Several reports have described the expression of TLRs in mouse or human cancer or cancer cell lines. For example, TLR1 to TLR6 are expressed by colon, lung, prostate, and melanoma mouse tumor cell lines, TLR3 is expressed in human breast cancer cells, hepatocarcinoma and gastric carcinoma cells express TLR2 and TLR4, and TLR9 and TLR4 are expressed by human lung cancer cells. TLR7 and TLR8 are found in tumor cells of human lung cancer.

[00256] TLR are a family of proteins that sense a microbial product and/or initiates an adaptive immune response. TLRs activate a dendritic cell (DC). TLRs are conserved membrane spanning molecules containing an ectodomain of leucine-rich repeats, a transmembrane domain and an intracellular TIR (Toll/interleukin receptor) domain. TLRs recognize distinct structures in microbes, often referred to as “PAMPs” (pathogen associated molecular patterns). Ligand binding to TLRs invokes a cascade of intra-cellular signaling pathways that induce the production of factors involved in inflammation and immunity.

[00257] TLR7 and TLR8 are phylogenetically and structurally related. TLR7 is selectively expressed by human pDCs and B cells. TLR8 is predominantly expressed mDCs, monocytes, macrophages and myeloid suppressor cells. TLR7-specific agonists activate plasmacytoid DCs (pDCs) to produce large amounts of type 1 IFNs and expressing high levels of costimulatory molecules that promote activation of T cells, NK cells, B cells and mDCs. TLR8-specific agonists activate myeloid DCs, monocytes, macrophages or myeloid-derived suppressor cells to produce large amounts of type 1 IFN, IL-12 and IL-23, and express high levels of MHC class I, MHC class II and costimulatory molecules that promote the activation of antigen specific CD4 and CD8+ T cells.

[00258] Pharmaceutical compositions including the crystal forms of the herein described compounds can be administered to an animal, such as a mammal. In some embodiments, the mammal can be a human, a cat, a dog, a horse, a pig, a cow, a whale, or the like.

[00259] Pharmaceutical compositions may be prepared by combining a therapeutically effective amount of at least one crystal form of a herein described compound with conventional acceptable pharmaceutical excipients, and by preparation of unit dosage forms suitable for therapeutic use. As used herein, the term “pharmaceutical composition” and refers to a therapeutically effective concentration of an active compound, such as, *e.g.*, any of the crystal forms of herein described compounds. Preferably, the pharmaceutical composition does not produce an adverse, allergic, or other untoward or unwanted reaction when administered. A pharmaceutical composition disclosed herein can be useful for

medical and veterinary applications. A pharmaceutical composition may be administered alone, or in combination with other supplementary active compounds, agents, drugs or hormones. The pharmaceutical compositions may be manufactured using any of a variety of processes, including, without limitation, conventional mixing, dissolving, granulating, dragee-making, levigating, emulsifying, encapsulating, entrapping, and lyophilizing. The pharmaceutical composition can take any of a variety of forms including, without limitation, a sterile solution, suspension, emulsion, lyophilizate, tablet, pill, pellet, capsule, powder, syrup, elixir, or any other dosage form suitable for administration.

[00260] A pharmaceutical composition can be a liquid formulation, semi-solid formulation, or a solid formulation. A formulation disclosed herein can be produced in a manner to form one phase, such as, *e.g.*, an oil or a solid. Alternatively, a formulation disclosed herein can be produced in a manner to form two phase, such as, *e.g.*, an emulsion. A pharmaceutical composition disclosed herein intended for such administration may be prepared according to any method known to the art for the manufacture of pharmaceutical compositions.

[00261] Liquid formulations suitable for injection or topical (e.g., ocular) delivery may comprise physiologically acceptable sterile aqueous or non-aqueous solutions, dispersions, suspensions or emulsions and sterile powders for reconstitution into sterile injectable solutions or dispersions. Examples of suitable aqueous and non-aqueous carriers, diluents, solvents or vehicles include water, ethanol, polyols (propylene glycol, polyethyleneglycol (PEG), glycerol, and the like), suitable mixtures thereof, vegetable oils (such as olive oil) and injectable organic esters such as ethyl oleate. Proper fluidity can be maintained, for example, by the use of a coating such as lecithin, by the maintenance of the required particle size in the case of dispersions and by the use of surfactants.

[00262] Semi-solid formulations suitable for topical administration include, without limitation, ointments, creams, salves, and gels. In such solid formulations, the active compound may be admixed with at least one inert customary excipient (or carrier) such as, a lipid and/or polyethylene glycol.

[00263] Solid formulations suitable for oral administration include capsules, tablets, pills, powders and granules. In such solid formulations, the active compound may be admixed with at least one inert customary excipient (or carrier) such as sodium citrate or dicalcium phosphate or (a) fillers or extenders, as for example, starches, lactose, sucrose, glucose, mannitol and silicic acid, (b) binders, as for example, carboxymethylcellulose, alignates, gelatin, polyvinylpyrrolidone, sucrose and acacia, (c) humectants, as for example, glycerol, (d) disintegrating agents, as for example, agar-agar, calcium carbonate, potato or tapioca starch, alginic acid, certain complex silicates and sodium carbonate, (e) solution retarders,

as for example, paraffin, (f) absorption accelerators, as for example, quaternary ammonium compounds, (g) wetting agents, as for example, cetyl alcohol and glycerol monostearate, (h) adsorbents, as for example, kaolin and bentonite, and (i) lubricants, as for example, talc, calcium stearate, magnesium stearate, solid polyethylene glycols, sodium lauryl sulfate or mixtures thereof. In the case of capsules, tablets and pills, the dosage forms may also comprise buffering agents.

[00264] In liquid and semi-solid formulations, a concentration of crystal forms of the herein described compounds may be between about 50 mg/mL to about 1,000 mg/mL. In aspects of this embodiment, a therapeutically effective amount of a crystal form of the herein described compounds may be from, *e.g.*, about 50 mg/mL to about 100 mg/mL, about 50 mg/mL to about 200 mg/mL, about 50 mg/mL to about 300 mg/mL, about 50 mg/mL to about 400 mg/mL, about 50 mg/mL to about 500 mg/mL, about 50 mg/mL to about 600 mg/mL, about 50 mg/mL to about 700 mg/mL, about 50 mg/mL to about 800 mg/mL, about 50 mg/mL to about 900 mg/mL, about 50 mg/mL to about 1,000 mg/mL, about 100 mg/mL to about 200 mg/mL, about 100 mg/mL to about 300 mg/mL, about 100 mg/mL to about 400 mg/mL, about 100 mg/mL to about 500 mg/mL, about 100 mg/mL to about 600 mg/mL, about 100 mg/mL to about 700 mg/mL, about 100 mg/mL to about 800 mg/mL, about 100 mg/mL to about 900 mg/mL, about 100 mg/mL to about 1,000 mg/mL, about 200 mg/mL to about 300 mg/mL, about 200 mg/mL to about 400 mg/mL, about 200 mg/mL to about 500 mg/mL, about 200 mg/mL to about 600 mg/mL, about 200 mg/mL to about 700 mg/mL, about 200 mg/mL to about 800 mg/mL, about 200 mg/mL to about 900 mg/mL, about 200 mg/mL to about 1,000 mg/mL, about 300 mg/mL to about 400 mg/mL, about 300 mg/mL to about 500 mg/mL, about 300 mg/mL to about 600 mg/mL, about 300 mg/mL to about 700 mg/mL, about 300 mg/mL to about 800 mg/mL, about 300 mg/mL to about 900 mg/mL, about 300 mg/mL to about 1,000 mg/mL, about 400 mg/mL to about 500 mg/mL, about 400 mg/mL to about 600 mg/mL, about 400 mg/mL to about 700 mg/mL, about 400 mg/mL to about 800 mg/mL, about 400 mg/mL to about 900 mg/mL, about 400 mg/mL to about 1,000 mg/mL, about 500 mg/mL to about 600 mg/mL, about 500 mg/mL to about 700 mg/mL, about 500 mg/mL to about 800 mg/mL, about 500 mg/mL to about 900 mg/mL, about 500 mg/mL to about 1,000 mg/mL, about 600 mg/mL to about 700 mg/mL, about 600 mg/mL to about 800 mg/mL, about 600 mg/mL to about 900 mg/mL, or about 600 mg/mL to about 1,000 mg/mL.

[00265] In semi-solid and solid formulations, an amount of a crystal form of the herein described compounds may be between about 0. 01% to about 45% by weight. In aspects of this embodiment, an amount of a crystal form of the herein described compounds may be from, *e.g.*, about 0.1% to about 45% by weight, about 0.1% to about 40% by weight, about

0.1% to about 35% by weight, about 0.1% to about 30% by weight, about 0.1% to about 25% by weight, about 0.1% to about 20% by weight, about 0.1% to about 15% by weight, about 0.1% to about 10% by weight, about 0.1% to about 5% by weight, about 1% to about 45% by weight, about 1% to about 40% by weight, about 1% to about 35% by weight, about 1% to about 30% by weight, about 1% to about 25% by weight, about 1% to about 20% by weight, about 1% to about 15% by weight, about 1% to about 10% by weight, about 1% to about 5% by weight, about 5% to about 45% by weight, about 5% to about 40% by weight, about 5% to about 35% by weight, about 5% to about 30% by weight, about 5% to about 25% by weight, about 5% to about 20% by weight, about 5% to about 15% by weight, about 5% to about 10% by weight, about 10% to about 45% by weight, about 10% to about 40% by weight, about 10% to about 35% by weight, about 10% to about 30% by weight, about 10% to about 25% by weight, about 10% to about 20% by weight, about 10% to about 15% by weight, about 15% to about 45% by weight, about 15% to about 40% by weight, about 15% to about 35% by weight, about 15% to about 30% by weight, about 15% to about 25% by weight, about 15% to about 20% by weight, about 20% to about 45% by weight, about 20% to about 40% by weight, about 20% to about 35% by weight, about 20% to about 30% by weight, about 20% to about 25% by weight, about 25% to about 45% by weight, about 25% to about 40% by weight, about 25% to about 35% by weight, or about 25% to about 30% by weight.

[00266] A pharmaceutical composition disclosed herein can optionally include a pharmaceutically acceptable carrier that facilitates processing of an active compound into pharmaceutically acceptable compositions. Such a carrier generally is mixed with an active compound or permitted to dilute or enclose the active compound and can be a solid, semi-solid, or liquid agent. Any of a variety of pharmaceutically acceptable carriers can be used including, without limitation, aqueous media such as, *e.g.*, water, saline, glycine, hyaluronic acid and the like; solid carriers such as, *e.g.*, starch, magnesium stearate, mannitol, sodium saccharin, talcum, cellulose, glucose, sucrose, lactose, trehalose, magnesium carbonate, and the like; solvents; dispersion media; coatings; antibacterial and antifungal agents; isotonic and absorption delaying agents; or any other inactive ingredient.

[00267] A pharmaceutical composition disclosed herein can optionally include, without limitation, other pharmaceutically acceptable components (or pharmaceutical components), including, without limitation, buffers, preservatives, tonicity adjusters, salts, antioxidants, osmolality adjusting agents, physiological substances, pharmacological substances, bulking agents, emulsifying agents, wetting agents, sweetening or flavoring agents, and the like. Various buffers and means for adjusting pH can be used to prepare a pharmaceutical composition disclosed herein, provided that the resulting preparation is pharmaceutically acceptable. Such buffers include, without limitation, acetate buffers, borate buffers, citrate

buffers, phosphate buffers, neutral buffered saline, and phosphate buffered saline. It is understood that acids or bases can be used to adjust the pH of a composition as needed. Pharmaceutically acceptable antioxidants include, without limitation, sodium metabisulfite, sodium thiosulfate, acetylcysteine, butylated hydroxyanisole, and butylated hydroxytoluene. Useful preservatives include, without limitation, benzalkonium chloride, chlorobutanol, thimerosal, phenylmercuric acetate, phenylmercuric nitrate, a stabilized oxy chloro composition, such as, *e.g.*, sodium chlorite and chelants, such as, *e.g.*, DTPA or DTPA-bisamide, calcium DTPA, and CaNaDTPA-bisamide. Tonicity adjustors useful in a pharmaceutical composition include, without limitation, salts such as, *e.g.*, sodium chloride, potassium chloride, mannitol or glycerin and other pharmaceutically acceptable tonicity adjustor.

[00268] Method of treating a disease or condition, such as a cancer, include administering a Formula I new crystal form such as in a pharmaceutical form. Administration can be once daily, twice daily, three times daily four times daily or more. In other embodiments, administration can be one every other day, once every three days, every four day, every five days, every six days, one a week, once every other week, once every three weeks, once a month, once every other month, every six months, once a year, or the like.

Examples

Example 1

1. Summary

[00269] Salt screening for resiquimod freebase was conducted to identify salt candidates with suitable physicochemical properties. Additionally, polymorph screening was carried out to identify leading crystal forms of the salt candidate.

[00270] Initial salt screening was performed under 100 conditions using 19 acids (two molar ratios of HCl) and five solvent systems. A total of 32 crystalline hits were isolated and characterized by X-ray powder diffraction (XRPD), thermogravimetric analysis (TGA), differential scanning calorimetry (DSC), with the stoichiometry determined using proton nuclear magnetic resonance (^{1}H NMR) or HPLC/IC. Considering the safety class of acids used, number of polymorphs observed, and physicochemical properties, seven crystalline salts namely mono-HCl salt, di-HCl salt, sulfate, phosphate, maleate, malate, and adipate were selected as leading salts for further evaluation.

[00271] All the seven salt leads were re-prepared to hundreds of milligrams (except di-HCl salt was provided) and further evaluated on hygroscopicity, kinetic solubility, and solid-state stability. As results show, 1) all salt leads were slightly hygroscopic with no form change

after DVS test except HCl salts, 2) compared with freebase Type A, all salt leads show improved or comparable solubility in water and bio-relevant media (SGF, FaSSIF, and FeSSIF) at room temperature (RT, 20 ± 3 ºC) except maleate, 3) no form change and decrease of HPLC purity were detected for salt leads and freebase Type A under 25 ºC/60%RH and 40 ºC/75%RH for one week except di-HCl salt, suggesting good physical and chemical stability.

[00272] Based on the characterization and evaluation results, sulfate was selected as a salt candidate and re-prepared on 6-g scale for polymorphism investigation. Using sulfate Type A as starting material, a polymorph screening was performed under 100 conditions. A total of three crystal forms were obtained, including one anhydrate (Type A), one DMSO solvate (Type B), and one hemi-sulfate. Thus, sulfate Type A was selected as the leading form of mono-sulfate. Disproportionation risk and thermo-stability were investigated on sulfate Type A, and the result shows, 1) sulfate Type A converted to hemi-sulfate at water activity of 0.8, indicating the disproportionation risk at high relative humidity, 2) sulfate Type A shows good physicochemical stability at 80 ºC for 24 hours.

2. Salt Screening

2.1 Experiment Summary

[00273] According to the pKa value of 7.2 determined on Sirius T3 and approximate solubility of freebase (807919-05-A) at RT, nineteen salt formers and five solvent systems were used for the screening. Freebase was dispersed in selected solvent with a glass vial and corresponding salt former was added with a molar charge ratio of 1:1 (for HCl/freebase, two ratios of both 1:1 and 2:1 were used). The mixtures of freebase and acid were stirred at RT for 2.5 days. Clear solutions obtained were slurried at 5 ºC overnight to induce precipitation. If the samples were still clear, they would be subjected to evaporation to dryness at RT, in order to maximize the chance of identifying as many crystalline hits as possible. Resulted solids were isolated and analyzed by XRPD.

[00274] As summarized in Table 2-1, a total of 32 crystalline hits were obtained and characterized by TGA and DSC, with the stoichiometry determined by ^{1}H NMR or HPLC/IC. The characterization data were summarized in Table 2-2, and detailed information was provided in Section 5.4.

Table 2-1 Summary of salt screening experiments

Solvent / Former	Acetone A	EtOH B	EtOAc C	THF D	MeOH/H_2O (v/v, 9:1) E

Former \ Solvent		Acetone A	EtOH B	EtOAc C	THF D	MeOH/H_2O (v/v, 9:1) E
0	blank	freebase Type A	freebase Type A*	freebase Type A	freebase Type A*	freebase Type A*
1	HCl (1:1)	HCl salt Type A	HCl salt Type A+FB Type A*	HCl salt Type A	HCl salt Type A	HCl salt Type A+FB Type A*
2	HCl (2:1)	HCl salt Type A	HCl salt Type A	HCl salt Type B	HCl salt Type A	HCl salt Type A*
3	H_2SO_4	sulfate Type A	gel*	sulfate Type A	sulfate Type A	sulfate Type A*
4	maleic acid	maleate Type A	maleate Type A	maleate Type A	maleate Type A	maleate Type A
5	H_3PO_4	phosphate Type A	phosphate Type A	phosphate Type A	phosphate Type A	phosphate Type A
6	L-tartaric acid	tartrate Type A	tartrate Type C	tartrate Type A	tartrate Type A	tartrate Type B
7	fumaric acid	fumarate Type A	fumarate Type A	fumarate Type C	fumarate Type A	fumarate Type B
8	citric acid	citrate Type A	citrate Type B	citrate Type A	citrate Type A	gel*
9	glycolic acid	glycolate Type A	glycolate Type A	glycolate Type A	glycolate Type A	glycolate Type A
10	L-malic acid	malate Type A	malate Type A	malate Type A	malate Type A	malate Type A
11	hippuric acid	hippurate Type A	hippurate Type A	hippurate Type A	hippurate Type A	hippurate Type A
12	L-lactic acid	lactate Type B	lactate Type A*	lactate Type A	lactate Type A**	lactate Type A*
13	succinic acid	succinate Type A	succinate Type A	succinate Type A	succinate Type A	succinate Type B
14	adipic acid	adipate Type A	adipate Type A	adipate Type A	adipate Type A	adipate Type A
15	p-toluenesulfonic acid	tosylate Type A	tosylate Type A	tosylate Type A	tosylate Type B	tosylate Type A*
16	methanesulfonic acid	mesylate Type A	mesylate Type A*	mesylate Type A	mesylate Type A	mesylate Type A+FB Type A*
17	oxalic acid	oxalate Type A	oxalate Type A	oxalate Type A	oxalate Type B	oxalate Type A*
18	gentisic acid	gentisate Type A	gentisate Type A	gentisate Type B	gentisate Type A	gentisate Type B
19	benzoic acid	benzoate Type A	benzoate Type A	benzoate Type A	benzoate Type A	benzoate Type B
20	HNO_3	nitrate Type A	nitrate Type B	nitrate Type A	nitrate Type A	nitrate Type B+FB Type A*

**: Solids were generated via slurry at 5 ºC overnight. FB: freebase.

*: Samples were obtained via evaporation to dryness at RT.

Blank experiments were set up to detect any possible change of freebase.

Table 2-2 Characterization summary of crystalline hits

Hit		Acid		Sample ID	Weight Loss (TGA, %)	Endotherm (DSC, °C, peak)	Molar ratio (acid/base)
		Safety Class	Mw				
HCl Salt	Type A	I	36.46	807919-07-D1	3.5	250.0, 266.6	1.00
	Type B			807919-07-C2	10.8	103.5, 110.2, 181.1, 249.8, 266.0	1.73
Sulfate	Type A	I	98.08	807919-07-A3	0.4	213.1	0.98
Phosphate	Type A	I	98.00	807919-07-E5	0.5	260.3	0.92
Glycolate	Type A	I	76.05	807919-07-B9	0.9	206.8	1.04
Maleate	Type A	I	116.08	807919-07-D4	1.4	226.7	0.98
Malate	Type A	I	134.09	807919-07-B10	0.8	195.0	1.04
Adipate	Type A	I	146.14	807919-07-B14	1.0	218.9	0.52
Hippurate	Type A	I	179.17	807919-07-B11	2.8	214.8	1.00
Tartrate	Type A	I	150.09	807919-07-A6	2.1	168.1	1.02
	Type B			807919-07-E6	3.2	144.9, 245.8	0.52
	Type C			807919-07-B6	2.1	72.2, 245.0	0.52
Fumarate	Type A	I	116.08	807919-07-A7	0.8	229.9, 238.0, 252.9	0.81
	Type B			807919-07-E7	4.2	109.6, 226.8, 237.9, 255.9	0.61
	Type C			807919-07-C7	0.4	156.3, 237.8, 248.8	1.03
Citrate	Type A	I	192.13	807919-07-A8	0.3	165.4	1.02
	Type B			807919-07-B8	2.3	197.7	0.53
Lactate	Type A	I	90.08	807919-07-C12	4.9	85.4, 159.5, 169.4	1.07
	Type B			807919-07-A12	0.6	142.9, 160.2	0.96
Succinate	Type A	I	118.09	807919-07-C13	2.0	175.8	1.00
	Type B			807919-07-E13	4.6	103.5, 188.4, 209.6	0.52
Tosylate	Type A	II	172.21	807919-07-B15	1.3	202.5	0.89

Hit		Acid		Sample ID	Weight Loss (TGA, %)	Endotherm (DSC, °C, peak)	Molar ratio (acid/base)
		Safety Class	Mw				
	Type B			807919-07-D15	5.3	61.1, 185.4, 189.9, 201.9	0.92
Mesylate	Type A	II	96.10	807919-07-A16	1.5	207.6	0.93
Oxalate	Type A	II	90.04	807919-07-B17	0.7	228.7	0.92
	Type B			807919-07-D17	1.8	190.5, 218.2	1.02
Gentisate	Type A	II	154.12	807919-07-A18	4.9	211.5	0.99
	Type B			807919-07-E18	1.7	210.7	1.00
Benzoate	Type A	II	122.12	807919-07-A19	0.6	200.1	0.98
	Type B			807919-07-E19	4.0	102.5, 200.4	0.99
Nitrate	Type A	III	63.02	807919-07-D20	1.6	214.5	1.04
	Type B			807919-07-B20	0.6	219.9	1.04

Samples were dried at 50 ºC overnight before characterization.

2.2 Re-preparation and Characterization of Salt Leads

[00275] Based on the characterization results, seven salt leads were selected and re-prepared to hundreds of milligrams (except di-HCl salt Type A). The selection criteria include but not limited to: 1) low safety concern of acid (safety class I), 2) sharp x-ray powder diffraction (XRPD) peaks without apparent amorphous halo, 3) negligible weight loss in thermogravimetric analysis (TGA), and 4) neat thermal event with a sharp melting in differential scanning calorimetry (DSC). Preparation procedures for salt leads as well as other salts described herein are described in Table 2-3.

Table 2-3 Preparation procedures of salts

Crystal Form	Preparation Procedures
Mono-HCl salt Type A (807919-16-A) Method 1	1. Weigh 200 mg of freebase (807919-05-A) into 5 mL tetrahydrofuran (THF) and stir at 50 ºC to dissolve the sample. 2. Add 59 µL HCl (charge ratio of 1:1) to the freebase solution, and then stir magnetically with a speed of 750 rpm at room temperature (RT). 3. Add ~2 mg seed (807919-07-D1) into the system. Subsequently, stir the suspension at RT for 5.5 hrs. 4. Characterize the wet sample by XRPD and the crystal form conforms to mono-HCl salt Type A. 5. Centrifuge and dry the wet cake at 50 ºC for 2 hrs followed by drying under

Crystal Form	Preparation Procedures
	vacuum at RT for 1 hr. 6. Collect the solids, 205.4 mg with a yield of 92.0%.
Mono-HCl salt Type A (807919-16-A) Method 2	1. Weigh 328.5 mg freebase Type A to 10.5 mL THF to get a clear solution. 2. Pipette 0.5 mL freebase solution to a 1.5-mL glass vial. 3. Pipette 4.0 µL HCl to the freebase solution and stir at RT for 2.5 days. 4. Isolate the solids by centrifuging and then dry at 50 ºC overnight.
HCl Salt Type B (807919-07-C2)	1. Weigh 14.8 mg freebase Type A to 0.5 mL EtOAc. 2. Add 8.0 µL HCl to the freebase suspension and stir at RT for 2.5 days. 3. Isolate the solids by centrifuging and then dry at 50 ºC overnight.
Sulfate Type A (807919-11-A) Method 1	1. Weigh 65 mg of sulfuric acid into a 20-mL glass vial with 5 mL of THF. 2. Weigh 200 mg of freebase (807919-05-A, charge ratio of 1:1) to the acid solution, and stir magnetically with a speed of 750 rpm at RT. 3. Add ~2 mg seed (807919-07-A3) into the system and still stir at RT overnight. 4. Characterize the wet sample by XRPD and the crystal form conforms to sulfate Type A. 5. Cool the suspension to 5 ºC at a rate of 0.1 ºC/min, and age at 5 ºC overnight. 6. Centrifuge and dry the wet cake at 50 ºC for 2 hrs followed by drying under vacuum at RT overnight. 7. Collect the solids, 247.1 mg with a yield of 94.2%.
Sulfate Type A (807919-11-A) Method 2	1. Weigh 330.3 mg freebase Type A to 21 mL acetone to get a clear solution. 2. Pipette 1.0 mL freebase solution to a 1.5 mL glass vial. 3. Pipette 2.7 µL sulfuric acid to the freebase solution and stir at RT for 2.5 days. 4. Isolate the solids by centrifuging and then dry at 50 ºC overnight.

Crystal Form	Preparation Procedures
Sulfate Type B (807919-25-A13)	1. Weigh 9.9 mg sulfate Type A to a 3-mL glass vial. 2. Add 2 mL DMSO to a 20-mL glass vial. 3. Seal the 3-mL vial into the 20-mL vial and keep the system at RT for 7 days. 4. Isolate the solids for analysis.
Hemi-sulfate Type A (807919-34-A) Method 1	1. Weigh 14.9 mg sulfate Type A to a 1.5-mL glass vial. 2. Add 0.5 mL acetone/H_2O (604:396, v/v) and stir at RT for 5 days. 3. Isolate the solids by centrifuging.
Hemi-sulfate Type A (807919-34-A) Method 2	1. Weigh 60.7 mg freebase Type A to 0.3 mL acetone/H_2O (604:396, v/v). 2. Pipette 5.5 μL sulfuric acid to freebase suspension. 3. Add ~1 mg seed and stir at RT overnight. 4. Isolate the solids by vacuum filter.
Phosphate Type A (807919-11-C) Method 1	1. Weigh 200 mg of freebase (807919-05-A) into 5 mL THF and stir at 50 ºC to dissolve the sample. 2. Add 45 μL phosphoric acid (charge ratio of 1:1) to the freebase solution, and then stir magnetically with a speed of 750 rpm at RT. 3. Add ~2 mg seed (807919-07-E5) into the system and still stir at RT overnight. 4. Characterize the wet sample by XRPD and the crystal form conforms to phosphate Type A. 5. Cool the suspension to 5 ºC at a rate of 0.1 ºC/min, and age at 5 ºC overnight. 6. Centrifuge and dry the wet cake at 50 ºC for 2 hrs followed by drying under vacuum at RT overnight. 7. Collect the solids, 234.0 mg with a yield of 89.2%.
Phosphate Type A (807919-11-C) Method 2	1. Weigh 330.7 mg freebase Type A to 10.5 mL MeOH/H_2O (9:1, v/v) to get a clear solution. 2. Pipette 0.5 mL freebase solution to a 1.5 mL glass vial. 3. Pipette 3.2 μL phosphoric acid to the freebase solution and stir at RT for 2.5 days. 4. Isolate the solids by centrifuging and then dry at 50 ºC overnight.
Maleate Type A (807919-11-B) Method 1	1. Weigh 200 mg of freebase (807919-05-A) into 5 mL THF and stir at 50 ºC to dissolve the sample. 2. Add 82 mg maleic acid (charge ratio of 1:1) to the freebase solution, and then stir magnetically with a speed of 750 rpm at RT.

Crystal Form	Preparation Procedures
	3. Add ~2 mg seed (807919-07-D4) into the system and still stir at RT overnight. 4. Characterize the wet sample by XRPD and the crystal form conforms to maleate Type A. 5. Cool the suspension to 5 ºC at a rate of 0.1 ºC/min, and age at 5 ºC overnight. 6. Centrifuge and dry the wet cake at 50 ºC for 2 hrs followed by drying under vacuum at RT overnight. 7. Collect the solids, 266.5 mg with a yield of 97.3%.
Maleate Type A (807919-11-B) Method 2	1. Weigh 328.5 mg freebase Type A to 10.5 mL THF to get a clear solution. 2. Add 5.9 mg maleic acid to a 1.5-mL glass vial. 3. Pipette 0.5 mL freebase solution to the vial and stir at RT for 2.5 days. 4. Isolate the solids by centrifuging and then dry at 50 ºC overnight.
Malate Type A (807919-11-E) Method 1	1. Weigh 200 mg of freebase (807919-05-A) into 5 mL ethanol (EtOH) and stir at 50 ºC to dissolve the sample. 2. Add 91 mg L-malic acid (charge ratio of 1:1) to the freebase solution, and then stir magnetically with a speed of 750 rpm at RT. 3. Add additional 5.0 mL EtOH and ~2 mg seed (807919-07-B10) into the system. Subsequently, stir the suspension at RT overnight. 4. Characterize the wet sample by XRPD and the crystal form conforms to malate Type A. 5. Cool the suspension to 5 ºC at a rate of 0.1 ºC/min, and age at 5 ºC overnight. 6. Centrifuge and dry the wet cake at 50 ºC for 4 hrs followed by drying under vacuum at RT overnight. 7. Collect the solids, 238.4 mg with a yield of 83.6%.
Malate Type A (807919-11-E) Method 2	1. Weigh 329.5 mg freebase Type A to 16.5 mL EtOH to get a clear solution. 2. Add 6.8 mg L-malic acid to a 1.5-mL glass vial. 3. Pipette 0.8 mL freebase solution to the vial and stir at RT for 2.5 days. 4. Isolate the solids by centrifuging and then dry at 50 ºC overnight.
Adipate Type A (807919-12-A) Method 1	1. Weigh 150 mg of freebase (807919-05-A) into 5 mL EtOH and stir at 50 ºC to dissolve the sample. 2. Add 45 mg adipic acid (charge ratio of 1:2, acid/base) to the freebase solution, and then stir magnetically with a speed of 750 rpm at RT. 3. Add ~2 mg seed (807919-07-B14) into the system. Subsequently, stir the suspension at RT overnight. 4. Characterize the wet sample by XRPD and the crystal form conforms to adipate Type A.

Crystal Form	Preparation Procedures
	5. Centrifuge and dry the wet cake under vacuum at RT overnight. 6. Collect the solids, 159.7 mg with a yield of 86.8%.
Adipate Type A (807919-12-A) Method 2	1. Weigh 329.5 mg freebase Type A to 16.5 mL EtOH to get a clear solution. 2. Add 7.1 mg adipic acid to a 1.5-mL glass vial. 3. Pipette 0.8 mL freebase solution to the vial and stir at RT for 2.5 days. 4. Isolate the solids by centrifuging and then dry at 50 ºC overnight.
Tartrate Type A (807919-07-A6)	1. Weigh 330.3 mg freebase Type A to 21 mL acetone to get a clear solution. 2. Add 7.5 mg L-tartaric acid to a 1.5-mL glass vial. 3. Pipette 1.0 mL freebase solution to the vial and stir at RT for 2.5 days. 4. Isolate the solids by centrifuging and then dry at 50 ºC overnight.
Tartrate Type B (807919-07-E6)	1. Weigh 330.7 mg freebase Type A to 10.5 mL MeOH/H_2O (9:1, v/v) to get a clear solution. 2. Add 7.5 mg L-tartaric acid to a 1.5-mL glass vial. 3. Pipette 0.5 mL freebase solution to the vial and stir at RT for 2.5 days. 4. Isolate the solids by centrifuging and then dry at 50 ºC overnight.
Tartrate Type C (807919-07-B6)	1. Weigh 329.5 mg freebase Type A to 16.5 mL EtOH to get a clear solution. 2. Add 7.6 mg L-tartaric acid to a 1.5-mL glass vial. 3. Pipette 0.8 mL freebase solution to the vial and stir at RT for 2.5 days. 4. Isolate the solids by centrifuging and then dry at 50 ºC overnight.
Fumarate Type A (807919-07-A7)	1. Weigh 330.3 mg freebase Type A to 21 mL acetone to get a clear solution. 2. Add 5.5 mg fumaric acid to a 1.5-mL glass vial. 3. Pipette 1.0 mL freebase solution to the vial and stir at RT for 2.5 days. 4. Isolate the solids by centrifuging and then dry at 50 ºC overnight.
Fumarate Type B (807919-07-E7)	1. Weigh 330.7 mg freebase Type A to 10.5 mL MeOH/H_2O (9:1, v/v) to get a clear solution. 2. Add 5.8 mg fumaric acid to a 1.5-mL glass vial. 3. Pipette 0.5 mL freebase solution to the vial and stir at RT for 2.5 days. 4. Isolate the solids by centrifuging and then dry at 50 ºC overnight.
Fumarate Type C (807919-07-C7)	1. Weigh 15.2 mg freebase Type A to 0.5 mL EtOAc. 2. Weigh 5.9 mg fumaric acid to the freebase suspension and stir at RT for 2.5 days. 3. Isolate the solids by centrifuging and then dry at 50 ºC overnight.

Crystal Form	Preparation Procedures
Citrate Type A (807919-07-A8)	1. Weigh 330.3 mg freebase Type A to 21 mL acetone to get a clear solution. 2. Add 9.3 mg citric acid to a 1.5-mL glass vial. 3. Pipette 1.0 mL freebase solution to the vial and stir at RT for 2.5 days. 4. Isolate the solids by centrifuging and then dry at 50 ºC overnight.
Citrate Type B (807919-07-B8)	1. Weigh 329.5 mg freebase Type A to 16.5 mL EtOH to get a clear solution. 2. Add 9.6 mg citric acid to a 1.5-mL glass vial. 3. Pipette 0.8 mL freebase solution to the vial and stir at RT for 2.5 days. 4. Isolate the solids by centrifuging and then dry at 50 ºC overnight.
Glycolate Type A (807919-07-B9)	1. Weigh 329.5 mg freebase Type A to 16.5 mL EtOH to get a clear solution. 2. Add 4.0 mg glycolic acid to a 1.5-mL glass vial. 3. Pipette 0.8 mL freebase solution to the vial and stir at RT for 2.5 days. 4. Isolate the solids by centrifuging and then dry at 50 ºC overnight.
Hippurate Type A (807919-07-B11)	1. Weigh 329.5 mg freebase Type A to 16.5 mL EtOH to get a clear solution. 2. Add 8.4 mg hippuric acid to a 1.5-mL glass vial. 3. Pipette 0.8 mL freebase solution to the vial and stir at RT for 2.5 days. 4. Isolate the solids by centrifuging and then dry at 50 ºC overnight.
Lactate Type A (807919-07-C12)	1. Weigh 14.8 mg freebase Type A to 0.5 mL EtOAc. 2. Weigh 5.1 mg L-lactic acid to the freebase suspension and stir at RT for 2.5 days. 3. Isolate the solids by centrifuging and then dry at 50 ºC overnight.
Lactate Type B (807919-07-A12)	1. Weigh 330.3 mg freebase Type A to 21 mL acetone to get a clear solution. 2. Add 5.2 mg L-lactic acid to a 1.5-mL glass vial. 3. Pipette 1.0 mL freebase solution to the vial and stir at RT for 2.5 days. 4. Isolate the solids by centrifuging and then dry at 50 ºC overnight.
Succinate Type A (807919-07-C13)	1. Weigh 15.5 mg freebase Type A to 0.5 mL EtOAc. 2. Weigh 5.6 mg succinic acid to the freebase suspension and stir at RT for 2.5 days. 3. Isolate the solids by centrifuging and then dry at 50 ºC overnight.
Succinate Type B (807919-07-E13)	1. Weigh 330.7 mg freebase Type A to 10.5 mL MeOH/H_2O (9:1, v/v) to get a clear solution. 2. Add 5.6 mg succinic acid to a 1.5-mL glass vial.

Crystal Form	Preparation Procedures
	3. Pipette 0.5 mL freebase solution to the vial and stir at RT for 2.5 days. 4. Isolate the solids by centrifuging and then dry at 50 ºC overnight.
Tosylate Type A (807919-07-B15)	1. Weigh 329.5 mg freebase Type A to 16.5 mL EtOH to get a clear solution. 2. Add 9.6 mg p-toluenesulfonic acid to a 1.5-mL glass vial. 3. Pipette 0.8 mL freebase solution to the vial and stir at RT for 2.5 days. 4. Isolate the solids by centrifuging and then dry at 50 ºC overnight.
Tosylate Type B (807919-07-D15)	1. Weigh 328.5 mg freebase Type A to 10.5 mL THF to get a clear solution. 2. Add 9.4 mg p-toluenesulfonic acid to a 1.5-mL glass vial. 3. Pipette 0.5 mL freebase solution to the vial and stir at RT for 2.5 days. 4. Isolate the solids by centrifuging and then dry at 50 ºC overnight.
Mesylate Type A (807919-07-A16)	1. Weigh 330.3 mg freebase Type A to 21 mL acetone to get a clear solution. 2. Add 4.6 mg methanesulfonic acid to a 1.5-mL glass vial. 3. Pipette 1.0 mL freebase solution to the vial and stir at RT for 2.5 days. 4. Isolate the solids by centrifuging and then dry at 50 ºC overnight.
Oxalate Type A (807919-07-B17)	1. Weigh 329.5 mg freebase Type A to 16.5 mL EtOH to get a clear solution. 2. Add 6.1 mg oxalic acid to a 1.5-mL glass vial. 3. Pipette 0.8 mL freebase solution to the vial and stir at RT for 2.5 days. 4. Isolate the solids by centrifuging and then dry at 50 ºC overnight.
Oxalate Type B (807919-07-D17)	1. Weigh 328.5 mg freebase Type A to 10.5 mL THF to get a clear solution. 2. Add 6.2 mg oxalic acid to a 1.5-mL glass vial. 3. Pipette 0.5 mL freebase solution to the vial and stir at RT for 2.5 days. 4. Isolate the solids by centrifuging and then dry at 50 ºC overnight.
Gentisate Type A (807919-07-A18)	1. Weigh 330.3 mg freebase Type A to 21 mL acetone to get a clear solution. 2. Add 7.3 mg gentisic acid to a 1.5-mL glass vial. 3. Pipette 1.0 mL freebase solution to the vial and stir at RT for 2.5 days. 4. Isolate the solids by centrifuging and then dry at 50 ºC overnight.
Gentisate Type B (807919-07-E18)	1. Weigh 330.7 mg freebase Type A to 10.5 mL MeOH/H_2O (9:1, v/v) to get a clear solution. 2. Add 7.6 mg gensitic acid to a 1.5-mL glass vial. 3. Pipette 0.5 mL freebase solution to the vial and stir at RT for 2.5 days. 4. Isolate the solids by centrifuging and then dry at 50 ºC overnight.

Crystal Form	Preparation Procedures
Benzoate Type A (807919-07-A19)	1. Weigh 330.3 mg freebase Type A to 21 mL acetone to get a clear solution. 2. Add 6.1 mg benzoic acid to a 1.5-mL glass vial. 3. Pipette 1.0 mL freebase solution to the vial and stir at RT for 2.5 days. 4. Isolate the solids by centrifuging and then dry at 50 ºC overnight.
Benzoate Type B (807919-07-E19)	1. Weigh 330.7 mg freebase Type A to 10.5 mL MeOH/H_2O (9:1, v/v) to get a clear solution. 2. Add 6.0 mg benzoic acid to a 1.5-mL glass vial. 3. Pipette 0.5 mL freebase solution to the vial and stir at RT for 2.5 days. 4. Isolate the solids by centrifuging and then dry at 50 ºC overnight.
Nitrate Type A (807919-07-D20)	1. Weigh 328.5 mg freebase Type A to 10.5 mL THF to get a clear solution. 2. Pipette 0.5 mL freebase solution to a 1.5-mL vial. 3. Pipette 3.0 µL nitric acid to the vial and stir at RT for 2.5 days. 4. Isolate the solids by centrifuging and then dry at 50 ºC overnight.
Nitrate Type B (807919-07-B20)	1. Weigh 329.5 mg freebase Type A to 16.5 mL EtOH to get a clear solution. 2. Pipette 0.8 mL freebase solution to a 1.5-mL vial. 3. Pipette 3.0 µL nitric acid to the vial and stir at RT for 2.5 days. 4. Isolate the solids by centrifuging and then dry at 50 ºC overnight.
Acetate/acetic acid co-crystal (807920-22-A1)	1. Weigh 15.0 mg freebase Type A to 0.3 mL ethyl lactate. 2. Weigh 1.1 mg acetic acid to 1.5 mL n-heptane. 3. Pipette the acid solution to the freebase suspension and stir at RT overnight. 4. Isolate the solids and then dry at ambient conditions overnight.

2.2.1 Mono-HCl Salt Type A

[00276] Mono-HCl salt Type A was successfully re-prepared as evidenced by XRPD results in FIG. 1. XRPD data for mono-HCl salt Type A provide (peak shift within ±0.2°) primary peaks at 20.5, 6.9, and 27.3; secondary peaks at 9.8, 13.7, and 34.3; and tertiary peaks at 17.4, 21.3, and 24.8.

[00277] PLM image displayed in FIG. 2 illustrated aggregation of small particles (< 10 µm). As per TGA and DSC data in FIG. 3, sample (807919-16-A) shows a weight loss of 1.1% up to 130 ºC and two endothermic peaks at 250.4 ºC and 266.2 ºC (peak temperature) before decomposition, indicating an anhydrate for mono-HCl salt Type A. A purity of 99.5 area%

was detected by high performance liquid chromatography (HPLC) in Table 2-4. Also, the stoichiometric ratio was determined as 1.01 (acid/base) by HPLC/IC for the re-prepared sample.

Table 2-4 HPLC purity profile of mono-HCl salt Type A (807919-16-A)

#	RRT	Area%	#	RRT	Area%
1	0.75	0.04	3	1.00	**99.54**
2	0.83	0.38	4	1.43	0.04

2.2.2 Di-HCl Salt Type A

[00278] Di-HCl salt Type A was characterized by XRPD, TGA, DSC, polarized light microscope (PLM) and HPLC/IC. The XRPD pattern was shown in FIG. 4 and PLM image was displayed in FIG. 5. XRPD data for di-HCl salt Type A provide (peak shift within ±0.2°) primary peaks at 7.1, 8.2, and 19.6; secondary peaks at 15.4, 16.4, and 25.6; and tertiary peaks at 7.3, 14.9, and 27.0.

[00279] TGA and DSC results shown in FIG. 6, a weight loss of 1.2% up to 100 ºC and four endothermic peaks at 99.5 ºC, 191.7 ºC, 250.7 ºC and 261.9 ºC (peak temperature) before decomposition. Also, a purity of 99.5 area% was detected by HPLC in Table 2-5 and the stoichiometry was calculated as 2.15 (acid/base) by HPLC/IC.

Table 2-5 HPLC purity profile of di-HCl salt Type A (807919-14-A)

#	RRT	Area%	#	RRT	Area%
1	0.75	0.04	3	1.00	**99.53**
2	0.83	0.39	4	1.43	0.04

2.2.3 Sulfate Type A

[00280] XRPD patterns comparison in FIG. 7 shows that the re-produced sample (807919-11-A) conformed to sulfate Type A. XRPD data for sulfate Type A provide (peak shift within ±0.2°) primary peaks at 7.6, 11.7, and 18.2; secondary peaks at 15.5, 17.6, and 24.4; and tertiary peaks at 9.6, 13.4, and 23.5.

[00281] Small particles (< 10 μm) and aggregates were illustrated in FIG. 8. TGA and DSC results were displayed in FIG. 9. A weight loss of 0.9% was observed up to 130 ºC in TGA and the DSC curve shows a sharp melting peak at 214.4 ºC (onset temperature) before decomposition. A purity of 99.2 area% was detected by HPLC in Table 2-6. Also, the stoichiometric ratio was determined as 1.03 (acid/base) for the re-prepared batch. Combined

with ^{1}H NMR and TGA/DSC results, sulfate Type A was identified as an anhydrate of mono-sulfate.

Table 2-6 HPLC purity profile of sulfate Type A (807919-11-A)

#	RRT	Area%	#	RRT	Area%
1	0.75	0.05	3	1.00	**99.19**
2	0.83	0.68	4	1.43	0.09

2.2.4 Phosphate Type A

[00282] Phosphate Type A was successfully re-prepared as evidenced by XRPD results in FIG. 10. XRPD data for phosphate Type A provide (peak shift within ±0.2°) primary peaks at 7.7, 15.3, and 20.6; secondary peaks at 12.4, 18.5, and 25.2; and tertiary peaks at 14.3, 16.7, and 17.7.

[00283] PLM image displayed in FIG. 11 illustrated aggregation of small particles (< 10 μm). As per TGA and DSC data in FIG. 12, phosphate Type A (807919-11-C) shows a weight loss of 1.2% up to 130 ºC and an endothermic peak at 241.0 ºC (onset temperature) before decomposition. A purity of 99.4 area% was detected by HPLC in Table 2-7. Also, the stoichiometry of re-prepared sample was determined as 1.07 (acid/base) by HPLC/IC.

Table 2-7 HPLC purity profile of phosphate Type A (807919-11-C)

#	RRT	Area%	#	RRT	Area%
1	0.83	0.55	3	1.43	0.09
2	1.00	**99.36**	--	--	--

2.2.5 Maleate Type A

[00284] Maleate Type A (807919-07-D4) was generated via reactive crystallization (molar ratio of 1:1) in THF at RT. XRPD results in FIG. 13 shows maleate Type A was successfully re-prepared. XRPD data for maleate Type A provide (peak shift within ±0.2°) primary peaks at 7.5, 10.3, and 24.7; secondary peaks at 9.3, 16.5, and 18.0; and tertiary peaks at 15.7, 20.7, and 21.4.

[00285] Small particles (< 10 μm) and aggregates were illustrated in FIG. 14. TGA and DSC data shows a weight loss of 1.3% up to 130 ºC, and a possible melting endotherm at 224.1 ºC (onset temperature) before decomposition was observed in DSC (FIG. 15). A purity of 99.2 area% was detected by HPLC in Table 2-8. ^{1}H NMR results indicate a stoichiometry of 0.96 (acid/base) for the re-prepared maleate Type A (807919-11-B). Combined with ^{1}H NMR and TGA/DSC results, maleate Type A was identified to be an anhydrate of mono-

maleate

Table 2-8 HPLC purity profile of maleate Type A (807919-11-B)

#	RRT	Area%	#	RRT	Area%
1	0.75	0.10	3	1.00	**99.19**
2	0.83	0.63	4	1.43	0.09

2.2.6 Malate Type A

[00286] Malate Type A was successfully re-prepared as evidenced by XRPD results in FIG. 16. XRPD data for malate Type A provide (peak shift within ±0.2°) primary peaks at 6.5, 8.5, and 23.2; secondary peaks at 12.0, 13.0, and 17.1; and tertiary peaks at 8.8, 20.5, and 25.3.

[00287] PLM image displayed in FIG. 17 illustrated aggregation of irregular particles. As per TGA and DSC data in FIG. 18, malate Type A (807919-11-E) shows a weight loss of 1.0% up to 130 ºC and a sharp endothermic peak at 192.9 ºC (onset temperature) before decomposition. A purity of 99.9 area % was detected by HPLC in Table 2-9. Further, the stoichiometry of re-prepared sample was determined as 1.02 (acid/base) by ^{1}H NMR.

Table 2-9 HPLC purity profile of malate Type A (807919-11-E)

#	RRT	Area%	#	RRT	Area%
1	0.75	0.55	3	1.43	0.07
2	1.00	**99.88**	--	--	--

2.2.7 Adipate Type A

[00288] XRPD patterns comparison in FIG. 19 shows that the re-produced sample (807919-12-A) conformed to adipate Type A. XRPD data for adipate Type A provide (peak shift within ±0.2°) primary peaks at 5.9, 12.5, and 21.3; secondary peaks at 13.9, 18.8, and 26.7; and tertiary peaks at 14.4, 19.7, and 22.6.

[00289] Small particles (< 10 μm) and severe aggregates were illustrated in FIG. 20. TGA and DSC results were displayed in FIG. 21. A weight loss of 0.9% was observed up to 130 ºC in TGA and the DSC curve shows a sharp melting peak at 218.0 ºC (onset temperature) before decomposition. A purity of 99.9 area% was detected by HPLC in Table 2-10. Further, the stoichiometric ratio was determined as 0.52 (acid/base) for the re-prepared batch, suggesting the formation of hemi-adipate.

Table 2-10 HPLC purity profile of adipate Type A (807919-12-A)

#	RRT	Area%	#	RRT	Area%
1	0.83	0.06	2	1.00	**99.94**

2.3 Evaluation of Salt Leads

[00290] Further evaluation study of hygroscopicity, kinetic solubility, and solid-state stability was conducted to better understand the physicochemical properties of seven leads. As results shows: 1) All salt leads are slightly hygroscopic with no form change after DVS evaluation except mono-HCl salt Type A and di-HCl salt Type A, 2) Compared with freebase Type A, all salt leads displayed improved or comparable solubility in water and bio-relevant media except maleate Type A, 3) As evidenced by no substantial change in crystal form or HPLC purity, all salt leads shows good physical and chemical stability except di-HCl salt Type A.

2.3.1 Hygroscopicity

[00291] DVS isotherm plot was collected at 25 ºC to investigate the solid form stability as a function of humidity. For the six anhydrous salts (mono-HCl salt Type A, sulfate Type A, phosphate Type A, maleate Type A, malate Type A, and adipate Type A), solids were pre-dried at 0% RH to remove the unbounded solvent or water before started. For the possible hydrate/solvate di-HCl salt Type A, solids were equilibrated at ambient humidity (~30%RH) before testing.

[00292] As evidenced by the water uptake of 0.2~1.1% up to 80%RH, five salt forms (sulfate Type A, phosphate Type A, maleate Type A, malate Type A, and adipate Type A) were slightly hygroscopic. No solid form change was observed for all the five leads after DVS evaluation (FIG. 22-31).

[00293] DVS plots displayed in FIG. 32 and FIG. 34 illustrate that both HCl salt forms were hygroscopic. For mono-HCl salt Type A (807919-16-A), a water uptake of 2.9% was observed up to 80%RH and no form change was detected after DVS test (FIG. 33). For di-HCl salt Type A (807919-14-A), a water uptake of 12.2% was detected up to 80%RH and one plateau was observed at ~20%RH, suggesting the possible existence of a hydrate. In addition, di-HCl salt Type A converted to a new form which contains diffraction peaks of mono-HCl salt Type A after DVS evaluation (FIG. 35), indicating the disproportionation risk of di-HCl salt Type A at high relative humidity.

2.3.2 Kinetic Solubility

[00294] Kinetic solubility of seven salt leads was measured in water and three bio-relevant media (SGF, FeSSIF, and FeSSIF) at RT, using freebase Type A (807919-05-A) as control. All solubility samples (initial solid loading of ~5 mg/mL) were kept rolling on a rolling

incubator at a speed of 25 rpm, and sampled at 1, 2, 4 and 24 hours, respectively. After being centrifuged and separated using 0.45 μm Nylon filter, filtrates were collected for HPLC and pH test, and wet cakes for XRPD characterization. If clear solutions were obtained after 24 hours, accurate concentration and purity were measured for the solutions.

[00295] The results were summarized in Table 2-11, and the kinetic solubility profiles are displayed in FIGs. 36A-D. Compared with freebase Type A, mono-HCl salt Type A, di-HCl salt Type A, sulfate Type A, phosphate Type A, malate Type A, and adipate Type A shows improved or comparable solubility in water and bio-relevant buffers. Also, remaining solids after suspended 24 hours shows no form change (FIG. 37-38). Meanwhile, decreased solubility was observed in SGF, FaSSIF, and FeSSIF after the formation of mono-maleate (maleate Type A) while no form change was detected after kinetic solubility evaluation (FIG. 39). In addition, no degradation was observed for clear solutions after 24 hours as evidenced by the HPLC results in Table 2-12.

Table 2-11 Summary of kinetic solubility results at RT

Kinetic Solubility in Water												
Solid Form	1 hr			2 hrs			4 hrs			24 hrs		
	S	pH	FC	S	pH	FC	S	pH	FC	S	pH	FC
Mono-HCl salt Type A	C	N/A	N/A	C	N/A	N/A	C	N/A	N/A	4.5*	4.7	N/A
Di-HCl salt Type A	C	N/A	N/A	C	N/A	N/A	C	N/A	N/A	3.8*	2.0	N/A
Sulfate Type A	C	N/A	N/A	C	N/A	N/A	C	N/A	N/A	4.1*	2.2	N/A
Phosphate Type A	C	N/A	N/A	C	N/A	N/A	C	N/A	N/A	3.9*	4.2	N/A
Malate Type A	C	N/A	N/A	C	N/A	N/A	C	N/A	N/A	3.7*	4.3	N/A
Maleate Type A	0.93	4.2	No	0.98	4.3	No	1.1	4.2	No	0.97	5.2	No
Adipate Type A	2.8	5.9	No	2.7	5.8	No	2.8	5.9	No	2.7	6.0	No
Freebase Type A	0.5	8.4	No	0.5	8.6	No	0.5	8.1	No	0.5	8.1	No

Kinetic Solubility in SGF

Solid Form	1 hr			2 hrs			4 hrs			24 hrs		
	S	pH	FC	S	pH	FC	S	pH	FC	S	pH	FC
Mono-HCl salt Type A	C	N/A	N/A	C	N/A	N/A	C	N/A	N/A	4.7*	1.8	N/A
Di-HCl salt Type A	C	N/A	N/A	C	N/A	N/A	C	N/A	N/A	3.9*	1.6	N/A
Sulfate Type A	C	N/A	N/A	C	N/A	N/A	C	N/A	N/A	3.9*	1.8	N/A
Phosphate Type A	C	N/A	N/A	C	N/A	N/A	C	N/A	N/A	4.0*	2.2	N/A
Malate Type A	C	N/A	N/A	C	N/A	N/A	C	N/A	N/A	4.3*	2.4	N/A
Maleate Type A	1.4	2.0	No	1.5	2.0	No	1.6	2.1	No	1.5	1.9	No
Adipate Type A	4.7	3.4	N/A*	C	N/A	N/A	C	N/A	N/A	4.7*	3.4	N/A
Freebase Type A	2.7	3.6	N/A*	3.5	5.0	N/A*	5.0	5.0	N/A	5.0	4.9	N/A

Kinetic Solubility in FaSSIF

Solid Form	1 hr			2 hrs			4 hrs			24 hrs		
	S	pH	FC	S	pH	FC	S	pH	FC	S	pH	FC
Mono-HCl salt Type A	C	N/A	N/A	C	N/A	N/A	C	N/A	N/A	4.5*	6.3	N/A
Di-HCl salt Type A	C	N/A	N/A	C	N/A	N/A	C	N/A	N/A	3.9*	3.5	N/A
Sulfate Type A	C	N/A	N/A	C	N/A	N/A	C	N/A	N/A	4.0*	3.2	N/A
Phosphate Type A	C	N/A	N/A	C	N/A	N/A	C	N/A	N/A	4.3*	6.4	N/A
Malate Type A	C	N/A	N/A	C	N/A	N/A	C	N/A	N/A	3.7*	5.5	N/A
Maleate Type A	2.2	6.1	No	2.3	6.3	No	2.4	6.1	No	2.3	6.1	No
Adipate Type A	4.3	6.4	No	4.5	6.2	N/A*	4.6	6.4	N/A*	4.5*	6.4	N/A
Freebase Type A	2.7	7.0	No	2.8	7.0	No	2.8	7.1	No	2.9	7.0	No

Kinetic Solubility in FeSSIF												
Solid Form	1 hr			2 hrs			4 hrs			24 hrs		
	S	pH	FC	S	pH	FC	S	pH	FC	S	pH	FC
Mono-HCl salt Type A	C	N/A	N/A	C	N/A	N/A	C	N/A	N/A	4.6*	5.0	N/A
Di-HCl salt Type A	C	N/A	N/A	C	N/A	N/A	C	N/A	N/A	3.9*	4.9	N/A
Sulfate Type A	C	N/A	N/A	C	N/A	N/A	C	N/A	N/A	4.2*	4.8	N/A
Phosphate Type A	C	N/A	N/A	C	N/A	N/A	C	N/A	N/A	3.8*	5.0	N/A
Malate Type A	C	N/A	N/A	C	N/A	N/A	C	N/A	N/A	3.5*	4.8	N/A
Maleate Type A	1.5	4.9	No	1.6	5.0	No	1.7	5.0	No	1.6	5.2	No
Adipate Type A	C	N/A	N/A	C	N/A	N/A	C	N/A	N/A	4.2*	5.0	N/A
Freebase Type A	4.9	N/A	N/A	4.9	N/A	N/A	4.9	N/A	N/A	4.9*	5.4	N/A

S: Solubility, pH: Final pH of supernatant, FC: Solid form change.

C: Clear, N/A: No data was available, N/A*: Limited solid for analysis.

*: The concentration and pH data of clear solutions were collected.

Table 2-12 HPLC purity results of clear samples after kinetic solubility test

Crystal Form (Batch No.)	Condition	HPLC Purity	
		Area%	% of Initial
Mono-HCl salt Type A (807919-16-A)	Initial	99.54	--
	Water	99.56	100.0
	SGF	99.55	100.0
	FaSSIF	99.61	100.1
	FeSSIF	99.56	100.0
Di-HCl salt Type A (807919-14-A)	Initial	99.56	--
	Water	99.51	99.9
	SGF	99.56	100.0
	FaSSIF	99.57	100.0

Crystal Form (Batch No.)	Condition	HPLC Purity	
		Area%	% of Initial
	FeSSIF	99.57	100.0
Sulfate Type A (807919-11-A)	Initial	99.32	--
	Water	99.31	100.0
	SGF	99.30	100.0
	FaSSIF	99.36	100.0
	FeSSIF	99.31	100.0
Phosphate Type A (807919-11-C)	Initial	99.31	--
	Water	99.34	100.0
	SGF	99.33	100.0
	FaSSIF	99.34	100.0
	FeSSIF	99.30	100.0
Malate Type A (807919-11-E)	Initial	99.81	--
	Water	99.80	100.0
	SGF	99.73	99.9
	FaSSIF	99.78	100.0
	FeSSIF	99.86	100.1
Adipate Type A (807919-12-A)	Initial	99.90	--
	SGF	99.87	100.0
	FeSSIF	99.94	100.0
Freebase Type A (807919-05-A)	Initial	99.32	--
	FeSSIF	99.25	99.9

2.3.3 Physical and Chemical Stability

[00296] Physicochemical stability of seven salt leads was evaluated under 25 ºC/60%RH and 40 ºC/75%RH for one week, using freebase Type A (807919-05-A) as control. Stability samples were characterized by XRPD and HPLC, with the results summarized in Table 2-13. The XRPD patterns were shown from FIG. 40-47, indicating no form change for investigated forms except di-HCl salt Type A. Also, no substantial purity change was observed for seven leads and freebase Type A. All the data indicated good physical and chemical stability for mono-HCl salt Type A, sulfate Type A, phosphate Type A, maleate Type A, malate Type A, adipate Type A, and freebase Type A under tested conditions at least one week.

Table 2-13 Stability evaluation summary of salt leads and freebase Type A

Crystal Form (Batch No.)	HPLC Purity (Initial, area%)	Condition	HPLC Purity		Form change
			Area%	% of Initial	
Freebase Type A (807919-05-A)	99.32	25 °C/60%RH	99.15	99.8	No
		40 °C/75%RH	99.28	100.0	No
Mono-HCl salt Type A (807919-16-A)	99.54	25 °C/60%RH	99.46	99.9	No
		40 °C/75%RH	99.47	99.9	No
Di-HCl salt Type A (807919-14-A)	99.56	25 °C/60%RH	99.62	100.1	Yes
		40 °C/75%RH	99.70	100.1	Yes
Sulfate Type A (807919-11-A)	99.32	25 °C/60%RH	99.33	100.0	No
		40 °C/75%RH	99.37	100.1	No
Phosphate Type A (807919-11-C)	99.31	25 °C/60%RH	99.31	100.0	No
		40 °C/75%RH	99.37	100.1	No
Maleate Type A (807919-11-B)	99.32	25 °C/60%RH	99.32	100.0	No
		40 °C/75%RH	99.36	100.0	No
Malate Type A (807919-11-E)	99.81	25 °C/60%RH	99.83	100.0	No
		40 °C/75%RH	99.77	100.0	No
Adipate Type A (807919-12-A)	99.90	25 °C/60%RH	99.88	100.0	No
		40 °C/75%RH	99.89	100.0	No

2.4 Conclusions

[00297] A total of 32 crystalline hits were generated via salt screening. Based on the characterization results, seven salt leads, namely mono-HCl salt Type A, di-HCl salt Type A, sulfate Type A, phosphate Type A, maleate Type A, malate Type A, and adipate Type A, were selected to re-prepared for further evaluation including hygroscopicity, kinetic solubility, and solid-state stability. Considering the results summarized in Table 2-14 and Table 2-15, sulfate was recommended as a salt candidate for further polymorphism investigation.

Table 2-14 Characterization summary of salt leads and freebase Type A (I/II)

Crystal Form	Mono-HCl salt Type A	Di-HCl salt Type A	Sulfate Type A	Phosphate Type A
Batch No.	807919-16-A	807919-14-A	807919-11-A	807919-11-C
Speculated Form	Anhydrate	Hydrate/Solvate	Anhydrate	Anhydrate
Safety Class*	I	I	I	I
Stoichiometry	1.01	2.15	1.03	1.07

Crystal Form	Mono-HCl salt Type A	Di-HCl salt Type A	Sulfate Type A	Phosphate Type A
(acid/base)				
Crystallinity	High	High	High	High
Weight Loss (%)	1.1	1.2	0.9	1.2
Endotherm (onset, ºC)	246.7, 264.8	(99.5, 191.7, 250.7, 261.9)**	214.4	(250.9, 254.2)**
HPLC Purity (area%)	99.54	99.53	99.19	99.36
Morphology	Small particles (<10 μm) and aggregation			
Water Uptake at 25 ºC/80% RH	2.9	12.2	0.4	1.1
Form Change Post DVS Test	No	Yes	No	No
Kinetic Solubility at RT (mg/mL)	>3.8 (water/bio-relevant media)			
One-week Solid-state Stability	Good physiochemical stability under 25 ºC/60%RH and 40 ºC/75%RH at least one week for all salt forms except di-HCl salt Type A exhibited form change			

*: Safety class of acid used, according to *Handbook of Pharmaceutical Salts: Properties, Selection and Uses*, Wiley-VCH: Zurich, 2002.

**: peak temperature

Table 2-15 Characterization summary of salt leads and freebase Type A (II/II)

Crystal Form	Maleate Type A	Malate Type A	Adipate Type A	Freebase Type A
Batch No.	807919-11-B	807919-11-E	807919-12-A	807919-05-A
Speculated Form	Anhydrate	Anhydrate	Anhydrate	Anhydrate
Safety Class*	I	I	I	--
Stoichiometry (acid/base)	0.96	1.02	0.52	--
Crystallinity	High	High	High	High
Weight Loss (%)	1.3	1.0	0.9	0.3
Endotherm (onset, ºC)	224.1	192.9	218.0	193.3
HPLC Purity (area%)	99.19	99.88	99.94	99.09
Morphology	Small particles (<10 μm) and aggregation	Irregular particles and aggregation	Small particles (<10 μm) and aggregation	

Crystal Form	Maleate Type A	Malate Type A	Adipate Type A	Freebase Type A
Water Uptake at 25 ºC/80% RH	0.4	0.2	0.7	0.1
Form Change Post DVS Test	No	No	No	No
Kinetic Solubility at RT (mg/mL)	~1.0 (water) ~1.5 (bio-relevant media)	>3.5 (water/bio-relevant media)	~2.7 (water) >4.2 (bio-relevant media)	~0.5 (water) ~2.9 (FaSSIF) >4.9 (SGF/FeSSIF)
One-week Solid-state Stability	Good physiochemical stability under 25 ºC/60%RH and 40 ºC/75%RH			

*: Safety class of acid used, according to *Handbook of Pharmaceutical Salts: Properties, Selection and Uses*, Wiley-VCH: Zurich, 2002.

3 Polymorphism Investigation on Sulfate

3.1 Polymorph Screening Summary

[00298] Using re-prepared sulfate Type A (807919-21-A) as starting material, polymorph screening experiments were conducted under 100 conditions with different crystallization or solid transition methods. The detailed procedures can be found in Section 5.5.

[00299] As results summarized in Table 3-1 and Table 3-2, three crystal forms were obtained, with starting sulfate Type A as an anhydrate, sulfate Type B as a DMSO solvate, and hemi-sulfate Type A as a hydrate.

Table 3-1 Summary of polymorph screening experiments

Method	No. of Experiments	Crystal Form
Anti-solvent Addition	18	Sulfate Type A
Solid Vapor Diffusion	13	Sulfate Type A, B
Solution Vapor Diffusion	10	Sulfate Type A
Slow Evaporation	8	Sulfate Type A, hemi-sulfate Type A
Polymer-induced Crystallization	6	Sulfate Type A
Slurry at RT/50 ºC	38	Sulfate Type A, hemi-sulfate Type A
Slow Cooling	7	Sulfate Type A, B
Total	100	Sulfate Type A/B, hemi-sulfate Type A

Table 3-2 Characterization summary of sulfate forms

Crystal Form (Sample ID)	Crystallization Condition	Wt Loss	Endotherm (onset, ºC)	Stoichiometry (acid/base)	HPLC purity	Comment

		(%)			(area%)	
Sulfate Type A (807919-21-A)	Reactive crystallization in THF	2.0	209.6	1.1	99.4	Anhydrate
Sulfate Type B (807919-25-A13)	Solid vapor diffusion in DMSO	11.7	111.2, 202.2	N/A	N/A	DMSO solvate
Hemi-sulfate Type A (807919-34-A)	Reactive crystallization acetone/H_2O (a_w=0.8)	5.9	105.3*, 217.0	0.5	99.6	Hydrate

*: peak temperature

3.1.1 Sulfate Type B

[00300] Sulfate Type B sample (807919-25-A13) was obtained via solid vapor diffusion in DMSO at RT, with the XRPD pattern displayed in FIG. 48. XRPD data for sulfate Type B provide (peak shift within ±0.2°) primary peaks at 7.0, 9.6, and 20.0; secondary peaks at 18.2, 19.6, and 25.2; and tertiary peaks at 14.0, 24.6, and 28.3.

[00301] TGA and DSC results were shown in FIG. 49. A weight loss of 11.7% was observed up to 130 ºC and DSC shows two endothermic peaks at 111.2 ºC and 202.2 ºC (onset temperature) before decomposition, with the first due to desolvation and second attributed to melting. Sulfate Type B converts to anhydrate sulfate Type A after being heated to 120 ºC. Also, DMSO content of 11.3% was detected by ^{1}H NMR, which was consistent with weight loss in TGA. Considering all the characterization data, sulfate Type B was calculated as a DMSO solvate.

3.1.2 Hemi-sulfate Type A

[00302] Hemi-sulfate Type A was obtained in acetone/H_2O (a_w=0.8) system. Hemi-sulfate Type A sample (807919-34-A) was generated via reactive crystallization in acetone/H_2O (a_w=0.8) at RT, with a molar charge ratio of 0.5:1 (acid/base). The XRPD pattern was shown in FIG. 50 and TGA/DSC data were displayed in FIG. 51. XRPD data for hemi-sulfate Type A provide (peak shift within ±0.2°) primary peaks at 8.5, 11.4, and 12.7; secondary peaks at 6.3, 16.6, and 19.2; and tertiary peaks at 7.6, 15.3, and 23.4.

[00303] A weight loss of 5.9% was observed up to 80 ºC in TGA and DSC result shows two endothermic peaks at 105.3 ºC and 219.2 ºC (peak temperature) before decomposition, with the first due to dehydration and the second attributed to melting. A purity of 99.6 area% was detected via HPLC (Table 3-3). ^{1}H NMR results shows limited acetone detected.

Combined with the stoichiometry of 0.50 (acid/base) detected by HPLC/IC, sample (807919-34-A) was speculated as a hydrate of hemi-sulfate.

Table 3-3 HPLC purity profile of hemi-sulfate Type A (807919-34-A)

#	RRT	Area%	#	RRT	Area%
1	0.75	0.05	3	1.00	**99.62**
2	0.83	0.33	--	--	--

3.2 Stability Research for Sulfate Type A

3.2.1 Disproportionation Risk Study

[00304] A series of slurry experiments were performed at various water activities (0~0.8) to evaluate the disproportionation risk. For details, about 15 mg sulfate Type A sample were weighed to 0.5 mL acetone/H_2O systems with a_w range from 0 to 0.8. After the suspensions stirred at RT for 5 days, the remaining solids were characterized by XRPD. As results shown in Table 3-4 and FIG. 52, no form change was observed when a_w lower than 0.6 while hemi-sulfate Type A was generated at a_w=0.8, suggesting the disproportionation risk of sulfate Type A at high relative humidity.

Table 3-4 Summary of slurry experiments results at RT

Experiment ID	Starting Form	Acetone/H_2O (v:v)	a_w^*	Final Form
807919-29-A17	Sulfate Type A	1000:0	0	Sulfate Type A
807919-29-A18		984:16	0.211	Sulfate Type A
807919-29-A19		948:52	0.406	Sulfate Type A
807919-29-A20		857:143	0.600	Sulfate Type A
807919-29-A21		604:396	0.801	Hemi-sulfate Type A

*: calculated value

3.2.2 Thermo-stability Study

[00305] To understand the thermo-stability under elevated temperature, sulfate Type A sample (807919-21-A) was stored at 80 ºC for 24 hours and then tested by XRPD and HPLC. As displayed in Table 3-5 and FIG. 53, no solid form change or HPLC impurity increase was observed, suggesting good physical and chemical stability under the tested condition.

Table 3-5 HPLC purity profile of sulfate Type A (807919-21-A) before and after storage

RRT	Area (%)	
	Initial	80 °C/24 hrs
0.75	0.11	0.07

0.83	0.64	0.63
1.00	99.14	99.21
1.42	0.11	0.09

3.3 Conclusions

[00306] A total of three crystal forms were obtained via polymorph screening, including two mono-sulfate (anhydrate Type A/DMSO solvate Type B) and hemi-sulfate Type A.

[00307] In addition, the disproportionation risk and thermo-stability were evaluated for sulfate Type A. As results show: 1) sulfate Type A converted to hemi-sulfate Type A at a_w=0.8, suggesting the disproportionation risk at high relative humidity, 2) sulfate Type A shows no substantial change in crystal form or HPLC purity, indicating the good thermo-stability after storage at 80 ºC for 24 hours. Based on the polymorph screening and evaluation results, sulfate Type A was speculated as the thermodynamically stable form at RT of mono-sulfate.

4. Conclusions

[00308] Salt screening for resiquimod freebase was performed under 100 conditions and a total of 32 crystalline hits were isolated. Based on the characterization results, seven salt leads of mono-HCl salt, di-HCl salt, sulfate, phosphate, maleate, malate, and adipate were selected as leading salts for further evaluation including hygroscopicity, kinetic solubility, and solid-state stability. As evidenced by the results, sulfate with good physicochemical properties was recommended as salt candidate. Using sulfate Type A as starting material, a polymorph screening was performed under 100 conditions and three crystalline forms were observed, including one anhydrate (Type A), one DMSO solvate (Type B), and one hemi-sulfate, suggesting sulfate Type A as a leading form of mono-sulfate. In addition, sulfate Type A shows good physicochemical properties under 80 ºC for 24 hours but could convert to hemi-sulfate at high relative humidity.

5.1 Characterization of Starting Materials

5.1.1 Starting Freebase of Salt Screening

[00309] The starting freebase (sample resiquimod, with a CP ID of 807919-05-A) was characterized by XRPD, PLM, TGA, DSC, HPLC, and DVS.

[00310] XRPD result in FIG. 54 shows the sample (807919-05-A) was crystalline and defined as freebase Type A. PLM image displayed in FIG. 55 illustrated aggregation of small particles (< 10 μm). As per TGA and DSC results shown in FIG. 56, a weight loss of 0.3% was observed up to 150 ºC in TGA and the DSC curve show a single endothermic peak at 193.3 ºC (onset temperature). A purity of 99.1 area% was detected via HPLC (Table 5-1).

DVS plot in FIG. 57 shows a water uptake of 0.1% up to 80%RH, suggesting freebase Type A was non-hygroscopic. Also, no form change was observed after DVS evaluation in FIG. 58.

[00311] The received freebase Type A (807919-05-A) was used as the starting material for salt screening. Solubility of Type A was estimated in nine solvents at RT. Approximately 2 mg of solids were weighed into each 3-mL glass vial, to which each of the solvents in Table 5-2 was added in increments of 100 µL until the solids dissolved completely or the total volume reached 1 mL. Solubility ranges of the starting material summarized in Table 5-2 were used to guide the solvent selection for salt screening.

Table 5-1 HPLC purity profile of freebase Type A (807919-05-A)

#	RRT	Area%	#	RRT	Area%
1	0.75	0.05	4	1.00	**99.09**
2	0.83	0.72	5	1.44	0.10
3	0.87	0.05	--	--	--

Table 5-2 Solubility estimation of freebase Type A (807919-05-A) at RT

Solvent	Solubility (mg/mL)	Solvent	Solubility (mg/mL)
MeOH	S>42.0	DCM	2.1<S<7.0
EtOH	22.0<S<44.0	EtOAc	2.0<S<6.7
THF	20.0<S<40.0	n-heptane	S<2.1
Acetone	7.3<S<22.0	H_2O	S<2.0
ACN	2.2<S<7.3	--	--

5.1.2 Starting Sulfate of Polymorph Screening

[00312] XRPD comparison in FIG. 59 indicated sulfate Type A (807919-21-A) was successfully re-prepared on 6-g scale. Detailed procedures were provided in Table 5-3. As per TGA and DSC results shown in FIG. 60, a weight loss of 2.0% was observed up to 100 ºC and DSC data show a sharp melting peak at 209.6 ºC (onset temperature). Also, a purity of 99.4 area% was detected via HPLC in Table 5-4 and the stoichiometry was determined as 1.11 (acid/base) by HPLC/IC.

[00313] The re-prepared sulfate Type A (807919-21-A) was used as the starting material of polymorph screening. The solubility data in Table 5-5 were collected adopting the same procedures as Section 5.1.1 and used to guide the solvent selection in polymorph screening design.

Table 5-3 Preparation procedures of sulfate Type A (807919-21-A)

Preparation Procedures
1. Weigh 4 g freebase (807919-05-A) into a 200-mL glass vial and dissolve the solids with 80 mL THF at 50 ºC.
2. Measure 1.3 g of sulfuric acid (charge ratio of 1:1, acid/base) and dilute with 20 mL THF.
3. Add the acid solution to the freebase solution drop by drop with stirring magnetically at a speed of 1500 rpm.
4. Add ~ 50 mg seed (807919-11-A) into the system and continue to stir at RT overnight.
5. Sampling for XRPD and DSC analysis, and both results conform to the reference.
6. Mix the 4-g batch with the 1-g batch (807919-20-A) prepared previously and stir for 1 hr.
7. Vacuum filter and dry the wet cake at 50 ºC for 2 hrs followed by vacuum drying at RT overnight.
8. Collect 6.4 g solids for analysis (approximate yield of 96.8%).

Table 5-4 HPLC purity profile of sulfate Type A (807919-21-A)

#	RRT	Area%	#	RRT	Area%
1	0.84	0.58	3	1.40	0.06
2	1.00	**99.36**	--	--	--

Table 5-5 Solubility estimation of sulfate Type A (807919-21-A) at RT

Solvent	Solubility (mg/mL)	Solvent	Solubility (mg/mL)
MeOH	20.0<S<40.0	2-MeTHF	S<2.2
EtOH	7.0<S<21.0	1,4-dioxane	S<2.1
IPA	S<2.2	Anisole	S<2.2
IBA	S<2.1	ACN	S<2.2
Acetone	S<2.0	$CHCl_3$	S<2.0
MEK	S<2.0	n-heptane	S<2.1
MIBK	S<2.1	toluene	S<2.0
EtOAc	S<2.2	DMAc	S>40.0
IPAc	S<2.0	DMSO	S>44.0
Ethyl lactate	S<2.2	NMP	S>44.0
MTBE	S<2.3	H_2O	S>44.0
THF	S<2.3	DCM	S<2.3

5.2 Abbreviations for Solvents Used

[00314] The abbreviations for solvents used are listed in Table 5-6.

Table 5-6 Abbreviations of solvents

Abbreviation	Solvent	Abbreviation	Solvent
MeOH	Methanol	THF	Tetrahydrofuran
EtOH	Ethanol	2-MeTHF	2-Methyltetrahydrofuran
IPA	Isopropyl alcohol	DCM	Dichloromethane
IBA	Isobutyl alcohol	$CHCl_3$	Trichloromethane
MEK	2-Butanone	ACN	Acetonitrile
MIBK	4-Methyl-2-pentanone	DMSO	Dimethylsulfoxide
EtOAc	Ethyl acetate	DMAc	N,N-Dimethylacetamide
IPAc	Isopropyl acetate	NMP	1-Methyl-2-pyrrolidone
MTBE	Methyl tert-butyl ether	--	--

5.3 Instruments and Methods

5.3.1 XRPD

[00315] For XRPD analysis, a PANalytical Empyrean X-ray powder diffractometer was used. The parameters used are listed in Table 5-7.

Table 5-7 Parameters for XRPD test

Parameter	Value
X-Ray wavelength	Cu, kα, Kα1 (Å): 1.540598, Kα2 (Å): 1.544426 Kα2/Kα1 intensity ratio: 0.50
X-Ray tube setting	45 kV, 40 mA
Divergence slit	Automatic
Scan mode	Continuous
Scan range (º2TH)	3º - 40º
Step size (º2TH)	0.013
Scan speed (º/min)	About 10

5.3.2 TGA/DSC

[00316] TGA data were collected using a TA Q500/Q5000 TGA from TA Instruments. DSC was performed using a TA Q200/Q2000 DSC from TA Instruments. Detailed parameters used are listed in Table 5-8.

Table 5-8 Parameters for TGA and DSC test

Parameters	TGA	DSC
Method	Ramp	Ramp
Sample pan	Platinum, open	Aluminum, crimped
Temperature	RT – desired temperature	
Heating rate	10 ºC/min	
Purge gas	N_2	

5.3.3 HPLC

[00317] Agilent 1100 HPLC was utilized to analyze purity and solubility, with detailed method listed in Table 5-9 and Table 5-10.

Table 5-9 HPLC method for purity test

HPLC	Agilent 1100 with DAD Detector	
Column	Alltima C18, 150×4.6 mm, 5μm	
Mobile phase	A: 0.1% TFA in H_2O	
	B: 0.1% TFA in Acetonitrile	
Gradient table	Time (min)	%B
	0.0	10
	10.0	40
	18.0	90
	20.0	90
	20.1	10
	23.0	10
Run time	23.0 min	
Post time	0.0 min	
Flow rate	1.0 mL/min	
Injection volume	5 μL	
Detector wavelength	UV at 228 nm, reference 500 nm	
Column temperature	40 ºC	
Sampler temperature	RT	
Diluent	Acetonitrile:H_2O=1:1	

Table 5-10 HPLC method for solubility test

HPLC	Agilent 1100 with DAD Detector
Column	Waters Xbridge C18, 150×4.6 mm, 5μm
Mobile phase	A: 0.1% TFA in H_2O
	B: 0.1% TFA in Acetonitrile

HPLC	Agilent 1100 with DAD Detector	
Gradient table	Time (min)	%B
	0.0	10
	5.0	90
	7.0	90
	7.1	10
	10.0	10
Run time	10.0 min	
Post time	0.0 min	
Flow rate	1.0 mL/min	
Injection volume	10 μL	
Detector wavelength	UV at 228 nm, reference 500 nm	
Column temperature	40 ºC	
Sampler temperature	RT	
Diluent	Acetonitrile:H_2O=1:1	

5.3.4 IC

[00318] IC method for counter-ion content measurement was listed in Table 5-11 below.

Table 5-11 IC method for counter-ion content measurement

Parameters	Settings
Column	IonPac AS18 Analytical Column (4 × 250 mm)
Mobile Phase	25 mM NaOH
Injection volume	25 μL
Flow rate	1.0 mL/min
Cell temperature	35 ºC
Column temperature	35 ºC
Current	80 mA
Run Time	8 mins (Cl^-), 28 mins (PO_4^{3-}), 12 mins (SO_4^{2-}/NO_3^-) 14 mins ($C_2O_4^{2-}$)

5.3.5 PLM

[00319] Polarized light microscopic picture was captured on Axio Lab. A1 upright microscope at room temperature.

5.3.6 DVS

[00320] DVS was measured via a SMS (Surface Measurement Systems) DVS Intrinsic. The relative humidity at 25 ºC were calibrated against deliquescence point of LiCl, $Mg(NO_3)_2$ and KCl. Actual parameters for DVS test were listed in Table 5-12.

Table 5-12 Parameters for DVS test

Parameters	DVS
Temperature	25 ºC
Sample size	10 ~ 20 mg
Gas and flow rate	N_2, 200 mL/min
dm/dt	0.002%/min
Min. dm/dt stability duration	10 min
Max. equilibrium time	180 min
RH range	0%RH to 95%RH
RH step size	10%RH from 0%RH to 90%RH 5%RH from 90%RH to 95%RH

5.3.7 ^{1}H NMR

[00321] ^{1}H NMR spectrum was collected on Bruker 400M NMR Spectrometer using DMSO-d6 as solvent.

5.3.8 pKa

[00322] pKa was determined on Sirius T3 TM according to the manufacturer's instructions and the parameters for pKa test was listed in Table 5-13.

Table 5-13 Parameters for pKa test

pH electrode	Ag/AgCl, double junction reference
Stirrer	Overhead, variable speed, computer controlled
Temperature probe	Thermocouple, Temperature measured with every datapoint
Temperature control	Peltier, Range: 12 ºC to 70 ºC
Turbidity detection	Turbidity sensor
Precision dispensers	Water, Acid, Base
MultiTip dispenser	Multi-tip capillary bundle
Electrode storage/calibration	Home position for electrode storage and pH7 buffer positions for calibration
Washes	Two static washes and flowing water wash station

Purge gas	Two internal flow meters, nitrogen supply requied
CoSolvents	Methanol, DMSO and MDM
System standardisation	Sirius Four-Plus™ procedure
pH-range	2.0-12.0
Assay volume	0.5 to 3.5 mls

5.4 Characterization of Crystalline Hits from Salt Screening

5.4.1 HCl Salt Type B

A total of two HCl salt crystal forms were obtained from screening. HCl salt Type A (807919-07-D1) was obtained via solution crystallization (molar charge of 1:1) in THF and Type B (807919-07-C2) was generated via reactive crystallization (molar ratio of 2:1, acid/base) in EtOAc at RT. The XRPD patterns were displayed in FIG. 69. XRPD data for HCl salt Type B show (peak shift within ±0.2°) primary peaks at 7.4, 24.3, and 26.2; secondary peaks at 6.7, 15.4, and 20.3; and tertiary peaks at 12.7, 19.1, and 28.5.

[00323] For HCl salt Type B, TGA and DSC data (FIG. 62) show a two-step weight loss of 10.8% up to 150 ºC and multiple endotherms before decomposition and five endotherms at 103.5 ºC, 110.2 ºC, 181.1 ºC, 249.8 ºC and 266.0 ºC (peak temperature) before decomposition. The stoichiometry of 1.73 (acid/base) was determined by HPLC/IC and a purity of 99.2 area% was detected by HPLC in Table 5-15.

Table 5-14 HPLC purity profile of HCl salt Type A (807919-07-D1)

#	RRT	Area%	#	RRT	Area%
1	0.79	0.09	2	1.00	**99.91**

Table 5-15 HPLC purity profile of HCl salt Type B (807919-07-C2)

#	RRT	Area%	#	RRT	Area%
1	0.79	0.71	3	1.48	0.09
2	1.00	**99.21**	--	--	--

5.4.2 Sulfate

[00324] One sulfate crystal form was generated via screening. Sulfate Type A (807919-07-A3) was produced via solution crystallization in acetone (molar ratio of 1:1) at RT and its XRPD pattern was shown in FIG. 63. As per TGA and DSC data shown in FIG. 64, a weight loss of 0.4% was viewed up to 130 ºC and the DSC curve shows an endothermic peak at 210.1 ºC (onset temperature). A purity of 99.3 area% was detected by HPLC in Table 5-16

and the stoichiometry of sulfate Type A (807919-07-A3) was determined as 0.98 (acid/base) by HPLC/IC.

Table 5-16 HPLC purity profile of sulfate Type A (807919-07-A3)

#	RRT	Area%	#	RRT	Area%
1	0.79	0.64	3	1.48	0.08
2	1.00	**99.28**	--	--	--

5.4.3 Phosphate

[00325] One phosphate crystal form was obtained from screening. Phosphate Type A (807919-07-E5) was obtained via solution crystallization (molar ratio of 1:1) in MeOH/H_2O (9:1, v/v) at RT, and its XRPD pattern was shown in FIG. 65. TGA and DSC curves (FIG. 66) show a weight loss of 0.5% up to 150 ºC and an endotherm at 254.5 ºC (onset temperature) possibly due to melting along with decomposition. Also, a purity of 99.9 area% was detected by HPLC in Table 5-17 and the stoichiometry was determined as 0.92 (acid/base) for phosphate Type A (807919-07-E5) via HPLC/IC.

Table 5-17 HPLC purity profile of phosphate Type A (807919-07-E5)

#	RRT	Area%	#	RRT	Area%
1	0.79	0.08	2	1.00	**99.92**

5.4.4 Glycolate

[00326] One glycolate crystal form was obtained via screening. Glycolate Type A (807919-07-B9) was generated via reactive crystallization (molar ratio of 1:1) in EtOH at RT. The XRPD pattern was displayed in FIG. 67. XRPD data for glycolate Type A provide (peak shift within ±0.2°) primary peaks at 9.3, 11.8, and 22.5; secondary peaks at 14.4, 19.7, and 25.6; and tertiary peaks at 13.1, 18.0, and 21.5.

[00327] As per TGA and DSC data in FIG. 68, a weight loss of 0.9% was observed up to 130 ºC and the DSC result shows a sharp endothermic peak at 206.0 ºC (onset temperature) before decomposition. Also, a purity of 99.7 area% was detected by HPLC in Table 5-18 and the stoichiometry of glycolate Type A (807919-07-B9) was determined as 1.04 (acid/base) by ^{1}H NMR.

Table 5-18 HPLC purity profile of glycolate Type A (807919-07-B9)

#	RRT	Area%	#	RRT	Area%
1	0.79	0.18	3	1.48	0.08
2	1.00	**99.74**	--	--	--

5.4.5 Maleate

[00328] One maleate crystal form was obtained via screening. Maleate Type A (807919-07-D4) was generated via reactive crystallization (molar ratio of 1:1) in THF at RT. The XRPD pattern was displayed in FIG. 69.

[00329] TGA and DSC results in FIG. 70 show a weight loss of 1.4% up to 150 ºC and an endothermic peak at 223.8 ºC (onset temperature) possibly due to melting. Also, a purity of 99.3 area% was detected by HPLC in Table 5-19 and the stoichiometric ratio was speculated as 0.98 (acid/base) by ^{1}H NMR.

Table 5-19 HPLC purity profile of maleate Type A (807919-07-D4)

#	RRT	Area%	#	RRT	Area%
1	0.79	0.67	3	1.48	0.09
2	1.00	**99.25**	--	--	--

5.4.6 Malate

[00330] One malate crystal form was obtained via screening. Malate Type A (807919-07-B10) was generated via reactive crystallization (charge molar ratio of 1:1) in EtOH at RT. The XRPD pattern was displayed in FIG. 71.

[00331] As per TGA and DSC data in FIG. 72, a weight loss of 0.8% was viewed up to 130 ºC and DSC result shows a sharp endotherm at 193.3 ºC (onset temperature), possibly due to melting. Also, a purity of 99.9 area% was detected by HPLC in Table 5-20 and the stoichiometric ratio was determined as 1.04 (acid/freebase) by ^{1}H NMR.

Table 5-20 HPLC purity profile of malate Type A (807919-07-B10)

#	RRT	Area%	#	RRT	Area%
1	0.79	0.07	3	1.48	0.07
2	1.00	**99.87**	--	--	--

5.4.7 Adipate

One adipate crystal form was obtained from screening. Adipate Type A (807919-07-B14) was produced via reactive crystallization (molar ratio of 1:1) in EtOH at RT. XRPD pattern and TGA/DSC curves were shown in FIG. 73 and FIG. 74 respectively.

[00332] A weight loss of 1.0% was observed up to 130 ºC in TGA and DSC result shows an endothermic peak at 217.7 ºC (onset temperature) possibly due to melting. Also, a purity of 100.0 area% was detected by HPLC in Table 5-21 and the stoichiometry of adipate Type A (807919-07-B14) was speculated as 0.52 (acid/base) by ^{1}H NMR.

Table 5-21 HPLC purity profile of adipate Type A (807919-07-B14)

#	RRT	Area%	#	RRT	Area%
1	0.79	0.05	2	1.00	**99.95**

5.4.8 Hippurate

[00333] One hippurate crystal form was obtained via screening. Hippurate Type A (807919-07-B11) was generated via reactive crystallization (molar ratio of 1:1) in EtOH at RT. XRPD pattern was displayed in FIG. 75. XRPD data for hippurate Type A provide (peak shift within ±0.2°) primary peaks at 5.9, 9.5, and 12.1; secondary peaks at 18.9, 21.2, and 25.2; and tertiary peaks at 10.8, 23.3, and 29.2.

[00334] TGA and DSC results in FIG. 76 show a weight loss of 2.8% before 130 ºC and an endothermic peak at 213.9 ºC (onset temperature) before decomposition. Also, a purity of 99.6 area% was detected by HPLC in Table 5-22. The stoichiometric ratio was determined as 1.00 (acid/base) by ^{1}H NMR.

Table 5-22 HPLC purity profile of hippurate Type A (807919-07-B11)

#	RRT	Area%	#	RRT	Area%
1	0.79	0.05	3	1.48	0.08
2	1.00	**99.61**	--	--	--

5.4.9 Tartrate

[00335] A total of three tartrate crystal forms were obtained via screening. Tartrate Type A (807919-07-A6), Type B (807919-07-E6), and Type C (807919-07-B6) were generated via reactive crystallization in acetone, MeOH/H_2O (9:1, v/v), and EtOH at RT respectively, with a molar charge ratio of 1:1. The XRPD pattern for tartrate Type A is displayed in FIG. 77. XRPD data for tartrate Type A provide (peak shift within ±0.2°) primary peaks at 6.3, 18.2, and 20.9; secondary peaks at 9.1, 19.4, and 25.9; and tertiary peaks at 16.3, 23.1, and 23.6.

[00336] The XRPD pattern for Tartrate Type B is displayed in FIG. 78. XRPD data for tartrate Type B provide (peak shift within ±0.2°) primary peaks at 8.9, 14.5, and 23.5; secondary peaks at 11.3, 16.9, and 24.2; and tertiary peaks at 9.9, 13.4, and 15.4.

[00337] The XRPD pattern for Tartrate Type C is displayed in FIG. 79. XRPD data for tartrate Type C provide (peak shift within ±0.2°) primary peaks at 7.2, 10.2, and 11.1; secondary peaks at 9.3, 13.8, and 18.9; and tertiary peaks at 8.7, 20.4, and 23.5.

[00338] For Type A, a weight loss of 2.1% was observed up to 130 ºC and DSC data (FIG. 80) shows an endothermic peak at 161.4 ºC (onset temperature) before decomposition. For Type B, TGA and DSC results in FIG. 81 show a weight loss of 3.2% up to 130 ºC and two endothermic peaks at 144.9 ºC and 245.8 ºC (peak temperature) before decomposition. For Type C, a weight loss of 2.1% was viewed up to 150 ºC in TGA and DSC result (FIG. 82) shows an endotherm at 72.2 ºC (peak temperature) before melting at 240.9 ºC (onset temperature) before decomposition.

[00339] Also, the stoichiometric ratio was determined as 1.02 (acid/base) for Type A, 0.52 (acid/base) for Type B and C by ^{1}H NMR.

5.4.10 Fumarate

[00340] A total of three fumarate crystal forms were obtained via screening. Fumarate Type A (807919-07-A7), Type B (807919-07-E7), and Type C (807919-07-C7) were generated via reactive crystallization (molar ratio of 1:1) in acetone, MeOH/H_2O (9:1, v/v), and EtOAc at RT respectively. The XRPD pattern for fumarate Type A is shown in FIG. 83. XRPD data for fumarate Type A provide (peak shift within ±0.2°) primary peaks at 6.4, 9.9, and 18.4; secondary peaks at 7.9, 23.7, and 26.0; and tertiary peaks at 7.2, 13.3, and 25.2.

[00341] The XRPD patterns for fumarate Type B are shown in FIG. 84. XRPD data for fumarate Type B provide (peak shift within ±0.2°) primary peaks at 10.0, 12.4, and 17.2; secondary peaks at 15.3, 19.1, and 20.3; and tertiary peaks at 17.2, 22.6, and 24.9.

[00342] The XRPD patterns for fumarate Type C are shown in FIG. 85. XRPD data for fumarate Type C provide (peak shift within ±0.2°) primary peaks at 6.7, 9.1, and 26.6; secondary peaks at 11.2, 15.4, and 20.1; and tertiary peaks at 13.7, 19.4, and 21.1.

[00343] For Type A, TGA and DSC data shows a weight loss of 0.8% up to 150 ºC and three endothermic peaks at 229.9 ºC, 238.0 ºC and 252.9 ºC (peak temperature) before decomposition (FIG. 86). For Type B, TGA and DSC data shows a weight loss of 4.2% up to 100 ºC and four endothermic peaks at 109.6 ºC, 226.8 ºC, 237.9 ºC and 255.9 ºC (peak temperature) before decomposition (FIG. 87). For Type C, TGA and DSC data show a

weight loss of 0.4% up to 100 ºC and four endothermic peaks at 156.3 ºC, 237.8 ºC and 248.8 ºC (peak temperature) before decomposition (FIG. 88).

[00344] Also, the stoichiometry was determined as 0.81, 0.61, and 1.03 (acid/base) for Type A ~ C by ^{1}H NMR

5.4.11 Citrate

[00345] Two citrate crystal forms were obtained via screening. Citrate Type A (807919-07-A8) and Type B (807919-07-B8) were produced via reactive crystallization (molar ratio of 1:1) in acetone and EtOH at RT. The XRPD pattern for citrate Type A is shown in FIG. 89. XRPD data for citrate Type A provide (peak shift within ±0.2°) primary peaks at 6.3, 11.5, and 21.3; secondary peaks at 14.9, 17.6, and 19.6; and tertiary peaks at 5.7, 10.0, and 26.3.

[00346] The XRPD patterns for citrate Type B are shown in FIG. 90. XRPD data for citrate Type B provide (peak shift within ±0.2°) primary peaks at 6.0, 10.0, and 18.2; secondary peaks at 8.2, 12.1, and 21.5; and tertiary peaks at 11.0, 13.4, and 19.2.

[00347] For Type A, a weight loss of 0.3% was viewed up to 100 ºC and DSC result (FIG. 91) shows a sharp endothermic peak at 163.1 ºC (onset temperature) before decomposition. For Type B, TGA and DSC data in FIG. 92 shows a weight loss of 2.3% before 100 ºC and a sharp endothermic peak at 195.3 ºC (onset temperature) before decomposition.

[00348] Also, the stoichiometric ratio was determined as 1.02 and 0.53 (acid/base) for Type A and B by ^{1}H NMR in FIG. 108 and FIG. 109, respectively.

5.4.12 Lactate

[00349] Two lactate crystal forms were obtained via screening. Lactate Type A (807919-07-C12) and Type B (807919-07-A12) were generated via reactive crystallization (molar ratio of 1:1) in EtOAc and acetone at RT. The XRPD pattern for lactate Type A is displayed in FIG. 93. XRPD data for lactate Type A provide (peak shift within ±0.2°) primary peaks at 5.6, 7.5, and 9.0; secondary peaks at 6.7, 10.1, and 22.3; and tertiary peaks at 8.4, 13.2, and 19.2.

[00350] The XRPD patterns for lactate Type B are shown in FIG. 94. XRPD data for lactate Type B provide (peak shift within ±0.2°) primary peaks at 5.8, 7.6, and 9.4; secondary peaks at 6.8, 11.6, and 14.0; and tertiary peaks at 8.5, 18.8, and 25.6.

[00351] For Type A, a weight loss of 4.9% was observed up to 100 ºC in TGA and DSC result in FIG. 95 show endothermic peaks at 85.4 ºC, 159.5 ºC and 169.4 ºC (peak temperature) before decomposition. For Type B, TGA and DSC result in FIG. 96 shows a weight loss of 0.6% up to 100 ºC and two endothermic peaks at 142.9 ºC and 160.2 ºC (peak temperature) before decomposition.

[00352] Also, the stoichiometric ratio was determined as 1.07 and 0.96 (acid/base) for lactate Type A and B by ^{1}H NMR

5.4.13 Succinate

[00353] Two succinate crystal forms were obtained via screening. Succinate Type A (807919-07-C13) and Type B (807919-07-E13) were generated via reactive crystallization (molar ratio of 1:1) in EtOAc and MeOH/H_2O (9:1, v/v) at RT. The XRPD pattern for succinate Type A is displayed in FIG. 97. XRPD data for succinate Type A provide (peak shift within ±0.2°) primary peaks at 6.4, 7.1, and 9.9; secondary peaks at 11.3, 18.4, and 23.1; and tertiary peaks at 5.0, 20.1, and 24.9.

[00354] The XRPD pattern for succinate Type B is shown in FIG. 98. XRPD data for succinate Type B provide (peak shift within ±0.2°) primary peaks at 10.5, 17.5, and 23.9; secondary peaks at 8.7, 12.2, and 14.1; and tertiary peaks at 16.6, 19.7, and 22.3.

[00355] For Type A, TGA and DSC results in FIG. 99 show a weight loss of 2.0% up to 130 ºC and a sharp endothermic peak at 174.4 ºC (onset temperature) before decomposition. For Type B, data (FIG. 100) show a weight loss of 4.6% up to 100 ºC and three endothermic peaks at 103.5 ºC, 188.4 ºC and 209.6 ºC (peak temperature) before decomposition. Also, the stoichiometric ratio was determined as 1.00 and 0.52 (acid/base) by ^{1}H NMR.

5.4.14 Tosylate

[00356] Two tosylate crystal forms were obtained via screening. Tosylate Type A (807919-07-B15) and Type B (807919-07-D15) were generated via reactive crystallization (molar ratio of 1:1) in EtOH and THF at RT. The XRPD pattern for tosylate Type A is displayed in FIG. 101. XRPD data for tosylate Type A provide (peak shift within ±0.2°) primary peaks at 4.8, 9.3, and 19.2; secondary peaks at 14.9, 16.3, and 19.7; and tertiary peaks at 20.7, 24.6, and 27.9.

[00357] The XRPD pattern for tosylate Type B is shown in FIG. 102. XRPD data for tosylate Type B provide (peak shift within ±0.2°) primary peaks at 7.7, 8.6, and 10.0; secondary peaks at 13.5, 15.5, and 19.9; and tertiary peaks at 17.4, 23.3, and 27.8.

[00358] For Type A, TGA and DSC results in FIG. 103 show a weight loss of 1.3% up to 130 ºC and a sharp endothermic peak at 201.5 ºC (onset temperature) before decomposition. For Type B, data (FIG. 104) show a weight loss of 5.3% up to 150 ºC and four endothermic peaks at 61.1 ºC, 185.4 ºC, 189.9 ºC and 201.9 ºC (peak temperature) before decomposition. Also, the stoichiometric ratio was determined as 0.89 and 0.92 (acid/base) for Type A and B by ^{1}H NMR.

5.4.15 Mesylate

[00359] One mesylate crystal form was obtained via screening. Mesylate Type A (807919-07-A16) was generated via reactive crystallization (molar ratio of 1:1) in acetone at RT. The XRPD pattern was displayed in FIG. 105. XRPD data for mesylate Type A provide (peak shift within ±0.2°) primary peaks at 8.6, 12.7, and 25.8; secondary peaks at 14.2, 18.6, and 19.5; and tertiary peaks at 16.4, 17.4, and 21.3.

[00360] As per TGA and DSC data in FIG. 106, it shows a weight loss of 1.5% up to 130 ºC and a sharp endothermic peak at 206.6 ºC (onset temperature) before decomposition. Also, the stoichiometric ratio was determined as 0.93 (acid/base) by ^{1}H NMR.

5.4.16 Oxalate

[00361] Two oxalate crystal forms were obtained via screening. Oxalate Type A (807919-07-B17) and Type B (807919-07-D17) were produced via reactive crystallization (molar ratio of 1:1) in EtOH and THF at RT respectively. The XRPD pattern for oxalate Type A is displayed in FIG. 107. XRPD data for oxalate Type A provide (peak shift within ±0.2°) primary peaks at 9.2, 19.1, and 23.4; secondary peaks at 14.5, 17.7, and 25.0; and tertiary peaks at 11.5, 22.6, and 30.2.

[00362] The XRPD pattern for oxalate Type B is shown in FIG. 108. XRPD data for oxalate Type B provide (peak shift within ±0.2°) primary peaks at 5.4, 18.0, and 23.1; secondary peaks at 9.9, 10.9, and 27.8; and tertiary peaks at 13.0, 16.9, and 24.2.

[00363] For Type A, TGA and DSC data (FIG. 109) show a weight loss of 0.7% up to 130 ºC and a sharp endothermic peak at 227.3 ºC (onset temperature) before decomposition. For Type B, TGA and DSC results (FIG. 110) show a weight loss of 1.8% up to 130 ºC and two endothermic peaks at 190.5 ºC and 218.2 ºC (peak temperature) before decomposition.Also, the stoichiometric ratio was speculated as 0.92 and 1.02 (acid/base) for Type A and B by HPLC/IC.

5.4.17 Gentisate

[00364] A total of two gentisate crystal forms were obtained via screening. Gentisate Type A (807919-07-A18) and Type B (807919-07-E18) were generated via reactive crystallization (molar ratio of 1:1) in acetone and MeOH/H_2O (9:1, v/v) at RT respectively. The XRPD pattern for genistate Type A is displayed in FIG. 111. XRPD data for gentisate Type A provide (peak shift within ±0.2°) primary peaks at 6.7, 10.0, and 22.9; secondary peaks at 7.1, 8.4, and 16.4; and tertiary peaks at 14.4, 18.4, and 20.5.

[00365] The XRPD pattern for gentisate Type B is shown in FIG. 112. XRPD data for gentisate Type B provide (peak shift within ±0.2°) primary peaks at 6.3, 10.1, and 24.2; secondary peaks at 12.7, 20.6, and 26.2; and tertiary peaks at 11.1, 14.8, and 15.8.

[00366] For Type A, TGA and DSC data (FIG. 113) show a weight loss of 4.9% up to 150 ºC and an endothermic peak at 210.4 ºC (onset temperature) and an exothermic peak at 145.5 ºC (peak temperature) before decomposition. For Type B, TGA and DSC results in FIG. 114 show a weight loss of 1.7% up to 150 ºC and an endothermic peak at 208.2 ºC (onset temperature) and an exothermic peak at 148.5 ºC (peak temperature) before decomposition. Also, the stoichiometric ratio was determined as 0.99 and 1.00 (acid/base) for Type A and B by ^{1}H NMR.

5.4.18 Benzoate

[00367] A total of two benzoate crystal forms were obtained from screening. Benzoate Type A (807919-07-A19) and Type B (807919-07-E19) were produced via reactive crystallization (molar ratio of 1:1) in acetone and MeOH/H_2O (9:1, v/v) at RT. The XRPD pattern for benzoate Type A is shown in FIG. 115. XRPD data for benzoate Type A provide (peak shift within ±0.2°) primary peaks at 7.9, 20.8, and 21.5; secondary peaks at 12.0, 15.6, and 23.9; and tertiary peaks at 8.7, 19.9, and 29.4.

[00368] The XRPD pattern for benzoate Type B is shown in FIG. 116. XRPD data for benzoate Type B provide (peak shift within ±0.2°) primary peaks at 7.7, 12.5, and 18.8; secondary peaks at 13.5, 22.6, and 26.7; and tertiary peaks at 19.8, 21.4, and 24.4.

[00369] For Type A, TGA and DSC results (FIG. 117) show a weight loss of 0.6% up to 130 ºC and an endothermic peak at 199.0 ºC (onset temperature) before decomposition. For Type B, TGA and DSC data in FIG. 118 show a weight loss of 4.0% up to 100 ºC and two endothermic peaks at 102.2 ºC and 199.8 ºC (onset temperature) before decomposition. Also, the stoichiometry was speculated as 0.98 and 0.99 (acid/base) for Type A and B by ^{1}H NMR.

5.4.19 Nitrate

[00370] Two nitrate crystal forms were obtained via screening. Nitrate Type A (807919-07-D20) and Type B (807919-07-B20) were generated via solution crystallization (molar ratio of 1:1) in THF and EtOH at RT. The XRPD pattern for nitrate Type A is displayed in FIG. 119. XRPD data for nitrate Type A provide (peak shift within ±0.2°) primary peaks at 17.2, 20.5, and 21.6; secondary peaks at 9.1, 10.1, and 12.0; and tertiary peaks at 14.5, 16.2, and 25.0.

[00371] The XRPD pattern for nitrate Type B is shown in FIG. 120. XRPD data for nitrate Type B provide (peak shift within ±0.2°) primary peaks at 6.7, 9.1, and 25.5; secondary peaks at 9.7, 12.7, and 15.6; and tertiary peaks at 14.4, 20.1, and 26.8.

[00372] For Type A, TGA and DSC results in FIG. 121 show a weight loss of 1.6% up to 130 ºC and a sharp endothermic peak at 212.5 ºC (onset temperature) before decomposition. For Type B, TGA and DSC results (FIG. 122) show a weight loss of 0.6% up to 130 ºC and a sharp endothermic peak at 217.6 ºC (onset temperature) before decomposition. Also, the stoichiometric ratio was determined as 1.04 (acid/base) for both Type A and B by HPLC/IC.

5.5 Experiments of Polymorph Screening for Sulfate

5.5.1 Anti-solvent Addition

[00373] A total of 18 anti-solvent addition experiments were carried out. About 15 mg of starting sulfate (807919-21-A) was dissolved in 0.1-2.5 mL solvent to obtain a clear solution, and the solution was magnetically stirred followed by addition of 0.2 mL anti-solvent per step until precipitate appeared or the total amount of anti-solvent reached 15.0 mL. The obtained precipitate was isolated for XRPD analysis. Results in Table 5-23 show that no new form was obtained.

Table 5-23 Summary of anti-solvent addition experiments

Experiment ID	Solvent (v:v)	Anti-solvent	Solid Form
807919-24-A1	MeOH	MIBK	Sulfate Type A
807919-24-A2		EtOAc	Sulfate Type A
807919-24-A3		1,4-dioxane	Sulfate Type A
807919-24-A4**		$CHCl_3$	Sulfate Type A
807919-24-A5		Toluene	Sulfate Type A
807919-24-A6	EtOH	n-heptane	Sulfate Type A
807919-24-A7		MEK	Sulfate Type A
807919-24-A8		IPAc	Sulfate Type A
807919-24-A9	IPA/ACN (1:1)	MTBE	Sulfate Type A
807919-24-A10*		Toluene	Sulfate Type A
807919-24-A11	IPA/DCM (3:2)	n-heptane	Sulfate Type A
807919-24-A12*		Toluene	Sulfate Type A
807919-24-A13**	DMSO	Ethyl lactate	Clear
807919-24-A14		THF	Sulfate Type A
807919-24-A15	NMP	MIBK	Sulfate Type A
807919-24-A16		2-MeTHF	Sulfate Type A

Experiment ID	Solvent (v:v)	Anti-solvent	Solid Form
807919-24-A17	DMAc	Acetone	Sulfate Type A
807919-24-A18		MTBE	Sulfate Type A

*: solid was observed after stirring the clear solution from anti-solvent addition at 5 ºC for 2 days.

**: no solid was obtained via stirring the clear solution at 5 ºC and then evaporation was employed.

5.5.2 Solid Vapor Diffusion

[00374] Solid vapor diffusion experiments were conducted using 13 different solvents. Approximate 10 mg of starting sulfate (807919-21-A) was weighed into a 3-mL vial, which was placed into a 20-mL vial with 2 mL of volatile solvent. The 20-mL vial was sealed with a cap and kept at RT for 7 days allowing solvent vapor to interact with sample. The solids were tested by XRPD and the results summarized in Table 5-24 show that sulfate Type A and B were generated.

Table 5-24 Summary of solid vapor diffusion experiments

Experiment ID	Solvent	Solid Form
807919-25-A1	H_2O	Sulfate Type A
807919-25-A2	DCM	Sulfate Type A
807919-25-A3	EtOH	Sulfate Type A
807919-25-A4	MeOH	Sulfate Type A
807919-25-A5	ACN	Sulfate Type A
807919-25-A6	THF	Sulfate Type A
807919-25-A7	$CHCl_3$	Sulfate Type A
807919-25-A8	Acetone	Sulfate Type A
807919-25-A9	DMF	Sulfate Type A
807919-25-A10	EtOAc	Sulfate Type A
807919-25-A11	1,4-dioxane	Sulfate Type A
807919-25-A12	IPA	Sulfate Type A
807919-25-A13	DMSO	Sulfate Type B

5.5.3 Liquid Vapor Diffusion

[00375] Ten liquid vapor diffusion experiments were conducted. Approximate 15 mg of starting sulfate (807919-21-A) was dissolved in appropriate solvent to obtain a clear solution in a 3-mL vial. This solution was then placed into a 20-mL vial with 3 mL of volatile solvents.

The 20-mL vial was sealed with a cap and kept at RT allowing sufficient time for organic vapor to interact with the solution. The precipitates were isolated for XRPD analysis. After 7 days, solids were isolated for XRPD analysis. The results summarized in Table 5-25 show that only sulfate Type A was obtained.

Table 5-25 Summary of liquid vapor diffusion experiments

Experiment ID	Solvent (v:v)	Anti-solvent	Solid Form
807919-26-A1	MeOH	MEK	Sulfate Type A
807919-26-A2		IPAc	Sulfate Type A
807919-26-A3		2-MeTHF	Sulfate Type A
807919-26-A4	EtOH	Ethyl lactate	Sulfate Type A
807919-26-A5		1,4-dioxane	Sulfate Type A
807919-26-A6	IPA/ACN (1:1)	Acetone	Sulfate Type A
807919-26-A7	IPA/DCM (3:2)	MTBE	Sulfate Type A
807919-26-A8	NMP	THF	Sulfate Type A
807919-26-A9	DMSO	EtOAc	Sulfate Type A
807919-26-A10	DMAc	$CHCl_3$	Sulfate Type A

5.5.4 Slow Evaporation

[00376] Slow evaporation experiments were performed under eight conditions. Briefly, ~15 mg of starting sulfate (807919-21-A) was dissolved in 0.1-2.5 mL of solvent in a 3-mL glass vial. If not dissolved completely, suspensions were filtered using a nylon membrane (pore size of 0.45 μm) and the filtrates would be used instead for the follow-up steps. The visually clear solutions were subjected to evaporation at desired temperature with vials sealed by PARAFILM®. The solids were isolated for XRPD analysis, and the results summarized in Table 5-26 indicated that a mixture of sulfate Type A and hemi-sulfate Type A were generated.

Table 5-26 Summary of slow evaporation experiments

Experiment ID	Solvent (v:v)	Temperature	Solid Form
807919-27-A1	MeOH	RT	Sulfate Type A
807919-27-A2	EtOH		Sulfate Type A
807919-27-A3	IPA/ACN (1:1)		Sulfate Type A
807919-27-A4	IPA/DCM (3:2)		Sulfate Type A
807919-27-A5	H_2O		Sulfate Type A+Hemi-sulfate Type A
807919-27-A6	DMSO	50 °C	Sulfate Type A

Experiment ID	Solvent (v:v)	Temperature	Solid Form
807919-27-A7	NMP		Sulfate Type A
807919-27-A8	DMAc		Sulfate Type A

5.5.5 Polymer induced Crystallization

[00377] Polymer induced crystallization experiments were performed with two sets of polymer mixtures in three solvents. Approximate 15 mg of starting sulfate (807919-21-A) was dissolved in appropriate solvent to obtain a clear solution in a 3-mL vial. About 2 mg of polymer mixture was added into 3-mL glass vial. All the samples were subjected to evaporation at RT to induce precipitation. The solids were isolated for XRPD analysis. Results summarized in Table 5-27 show that only sulfate Type A was produced.

Table 5-27 Summary of polymer induced crystallization experiments

Experiment ID	Solvent (v:v)	Polymer	Solid Form
807919-28-A1	MeOH		Sulfate Type A
807919-28-A2	EtOH	Polymer mixture A	Sulfate Type A
807919-28-A3	IPA/ACN (1:1)		Sulfate Type A
807919-28-A4	MeOH		Sulfate Type A
807919-28-A5	EtOH	Polymer mixture B	Sulfate Type A
807919-28-A6	IPA/ACN (1:1)		Sulfate Type A

Polymer mixture A: polyvinyl pyrrolidone (PVP), polyvinyl alcohol (PVA), polyvinylchloride (PVC), polyvinyl acetate (PVAC), hypromellose (HPMC), methyl cellulose (MC) (mass ratio of 1:1:1:1:1:1)
Polymer mixture B: polycaprolactone (PCL), polyethylene glycol (PEG), poly(methyl methacrylate) (PMMA) sodium alginate (SA), and hydroxyethyl cellulose (HEC) (mass ratio of 1:1:1:1:1).

5.5.6 Slurry at RT

[00378] Slurry conversion experiments were conducted at RT in different solvent systems. About15 mg of starting sulfate (807919-21-A) was suspended in 0.5 mL of solvent in a 1.5-mL glass vial. After the suspension was stirred magnetically for 5 days at RT, the remaining solids were isolated for XRPD analysis. Results summarized in Table 5-28 indicated that hemi-sulfate Type A was generated besides sulfate Type A.

Table 5-28 Summary of slurry conversion experiments at RT

Experiment ID	Solvent (v:v)	Solid Form
807919-29-A1	IPA	Sulfate Type A
807919-29-A2	IBA	Sulfate Type A
807919-29-A3	MEK	Sulfate Type A

Experiment ID	Solvent (v:v)	Solid Form
807919-29-A4	MIBK	Sulfate Type A
807919-29-A5	EtOAc	Sulfate Type A
807919-29-A6	IPAc	Sulfate Type A
807919-29-A7	Ethyl lactate	Sulfate Type A
807919-29-A8	MTBE	Sulfate Type A
807919-29-A9	THF	Sulfate Type A
807919-29-A10	2-MeTHF	Sulfate Type A
807919-29-A11	1,4-dioxane	Sulfate Type A
807919-29-A12	Anisole	Sulfate Type A
807919-29-A13	ACN	Sulfate Type A
807919-29-A14	DCM	Sulfate Type A
807919-29-A15	MeOH/toluene (1:3)	Sulfate Type A
807919-29-A16	EtOH/n-heptane (1:3)	Sulfate Type A
807919-29-A17	Acetone	Sulfate Type A
807919-29-A18	Acetone/H_2O (a_w=0.2)	Sulfate Type A
807919-29-A19	Acetone/H_2O (a_w=0.4)	Sulfate Type A
807919-29-A20	Acetone/H_2O (a_w=0.6)	Sulfate Type A
807919-29-A21	Acetone/H_2O (a_w=0.8)	Hemi-sulfate Type A

5.5.7 Slurry at 50 °C

[00379] Slurry conversion experiments were also conducted at 50 °C in different solvent systems. About 15 mg of starting sulfate (807919-21-A) was suspended in 0.3 mL of solvent in a 1.5-mL glass vial. After the suspension was stirred for about 6 days at 50 °C, the remaining solids were isolated for XRPD analysis. Results summarized in Table 5-29 indicated that only sulfate Type A was obtained.

Table 5-29 Summary of slurry conversion experiments at 50 °C

Experiment ID	Solvent (v:v)	Solid Form
807919-30-A1	IPA	Sulfate Type A
807919-30-A2	IBA	Sulfate Type A
807919-30-A3	MEK	Sulfate Type A
807919-30-A4	MIBK	Sulfate Type A
807919-30-A5	EtOAc	Sulfate Type A
807919-30-A6	IPAc	Sulfate Type A

Experiment ID	Solvent (v:v)	Solid Form
807919-30-A7	Ethyl lactate	Sulfate Type A
807919-30-A8	MTBE	Sulfate Type A
807919-30-A9	THF	Sulfate Type A
807919-30-A10	2-MeTHF	Sulfate Type A
807919-30-A11	1,4-dioxane	Sulfate Type A
807919-30-A12	Anisole	Sulfate Type A
807919-30-A13	ACN	Sulfate Type A
807919-30-A14	$CHCl_3$	Sulfate Type A
807919-30-A15	MeOH/toluene (1:3)	Sulfate Type A
807919-30-A16	EtOH/n-heptane (1:3)	Sulfate Type A
807919-30-A17	Acetone	Sulfate Type A

5.5.8 Slow Cooling

[00380] Slow cooling experiments were conducted in seven solvent systems. About 20 mg of starting sulfate (807919-21-A) was suspended in 1.0 mL solvent in a 3-mL glass vial at RT. The suspension was then heated to 50 ºC, equilibrated for about two hours and filtered to a new vial using a nylon membrane (pore size of 0.45 μm). Filtrates were slowly cooled down to 5 ºC at a rate of 0.1 ºC/min. Clear solutions were transferred to cooling at -20 ºC for 2 days and the final clear solutions were subjected to evaporation at RT. Results summarized in Table 5-30 indicated sulfate Type A and B were generated.

Table 5-30 Summary of slow cooling experiments

Experiment ID	Solvent (v:v)	Solid Form
807919-31-A1*	MeOH/toluene (1:1)	Sulfate Type A
807919-31-A2	EtOH/n-heptane (1:1)	N/A
807919-31-A3	IPA/ACN (1:1)	Sulfate Type A
807919-31-A4	IPA/DCM (3:2)	Sulfate Type A
807919-31-A5	DMSO/EtOAc (1:3)	Sulfate Type A + B
807919-31-A6	NMP/MIBK (1:3)	Clear
807919-31-A7	DMAc/MTBE (1:3)	Sulfate Type A

N/A: limited solid for XRPD analysis.

*: solid was obtained at -20 ºC.

Example 2

1. Summary

[00381] Polymorph screening for resiquimod freebase was preformed and its polymorphism towards identifying a suitable crystal form for further pharmaceutical development was evaluated.

[00382] The starting material (Batch No.: 144875-48-9) as received was characterized by X-ray powder diffraction (XRPD), thermo-gravimetric analysis (TGA), and differential scanning calorimetry (DSC). The characterization results indicated the starting material conformed to freebase Type A - an anhydrate.

[00383] Using Type A as starting material, a polymorph screening was performed under 100 conditions through methods of anti-solvent addition, evaporation, slow cooling, slurry conversion, vapor diffusion and polymer-induced crystallization. Based on the XRPD comparison, a total of eight crystal forms were isolated, including one anhydrate (Type A), two metastable forms (Type C and F), four solvates (Type B, D, E, and G), and one acetate/acetic acid co-crystal (sample H). The characterization results were summarized in Table 2-1. As the inter-conversion illustration displayed in FIG. 144, all metastable forms and solvates converted to Type A after storage at ambient conditions or heating experiments, suggesting Type A was the thermodynamically stable form at room temperature (RT, 20 ± 3 ºC).

[00384] Type A was selected as a leading form and further evaluated on hygroscopicity and solid-state stability. Hygroscopicity was assessed using dynamic vapor sorption (DVS) at 25 ºC, and result indicated Type A was non-hygroscopic. Physicochemical stability was investigated under 25 ºC/60%RH and 40 ºC/75%RH for one week, and 80 ºC for 24 hours. No crystal form change or decrease of HPLC purity was observed, indicating good physical and chemical stability for Type A under tested conditions.

2. Characterization of Crystal Forms

[00385] Polymorph screening was performed under 100 experimental conditions, with eight crystal forms obtained, including one anhydrate (Type A), two metastable forms (Type C/F), four solvates (Type B/D/E/G), and one acetate/acetic acid co-crystal (sample H). The inter-conversion relationships among these forms were studied via storage and heating experiments, with the results illustrated in FIG. 144.

Table 2-1 Characterization summary of crystal forms from screening

Crystal Form (Sample ID)	Crystallization Conditions	Endotherm (peak, ºC)	Wt Loss (%)	Solvent Residual	Speculated Form
Type A (807920-05-A)	Not disclosed	194.1	2.5	N/A*	Anhydrate

Crystal Form (Sample ID)	Crystallization Conditions	Endotherm (peak, °C)	Wt Loss (%)	Solvent Residual	Speculated Form
Type C (807920-11-A11)	Solid vapor diffusion 1,4-dioxane	N/A	N/A	N/A	Metastable form
Type F (807920-09-A4)	Slow cooling MEK	N/A	N/A	N/A	Metastable form
Type B (807920-07-A13)	Evaporation IBA/Toluene	158.4, 192.9	10.8	Toluene 4.3%	Isomorphic forms
Type B (807920-08-A7)	Evaporation EtOAc	146.7, 191.9	9.3	EtOAc 5.2%	
Type B (807920-12-A2)	Solution vapor diffusion THF/H_2O	143.7, 194.4	6.5	THF 6.1%	
Type D (807920-12-A9)	Solution vapor diffusion DMAc/MTBE	94.1, 193.2	18.4	DMAc 18.3%	DMAc solvate
Type E (807920-16-A3)	Slurry NMP/MTBE	134.0, 187.4	25.5	NMP 22.9%	NMP solvate
Type G (807920-19-F)	Fast cooling Anisole	84.7, 193.9	14.6	Anisole 12.4%	Anisole solvate
Sample H (807920-22-A1)	Anti-solvent addition Ethyl lactate /n-heptane/Acetic acid	151.6, 156.9	12.1	Acetic acid 8.2%	Acetate/ acetic acid co-crystal

N/A: no data was collected due to the form transformation to Type A.

N/A*: no data was available.

[00386] Preparation procedures for crystal forms described below are described in Table 2-1a.

Table 2-3 Preparation procedures of salts

Crystal Form	Preparation Procedures
Isomorphism Type B (807920-12-A2) Method 1	1. Weigh 15.3 mg freebase Type A into 2.0 mL IBA to get a clear solution. 2. Add 15.0 mL toluene as anti-solvent to the system and clear solution was obtained. 3. Transfer the solution to stirring at 5 °C 2 days and clear solution was observed. 4. Transfer the solution to evaporation to dryness at RT. 5. Isolate the solids for analysis.
Isomorphism Type B	1. Weigh 8.5 mg freebase Type A into 2.0 mL EtOAc to get a clear

Crystal Form	Preparation Procedures
(807920-12-A2) Method 2	solution. 2. Transfer the solution to evaporation at RT 3. Isolate the solids for analysis.
Isomorphism Type B (807920-12-A2) Method 3	1. Weigh 60.1 mg freebase Type A into 4.0 mL THF to get a clear solution. 2. Pippte 1.0 mL freebase solution to a 3-mL glass vial. 3. Seal the vial into the 20-mL glass vial with 3-mL H_2O and keep the system at RT for 6 days. 4. Isolate the solids for analysis.
DMAc Solvate Type D (807920-12-A9)	1. Weigh 15.3 mg freebase Type A to 0.1 mL DMAc to get a clear solution in a 3-mL glass vial. 2. Seal the vial into the 20-mL glass vial with 3-mL MTBE and keep the system at RT for 6 days. 3. Isolate the solids for analysis.
NMP Solvate Type E (807920-16-A3)	1. Weigh 30.6 mg freebase Type A to 0.3 mL NMP to get a clear solution at RT. 2. Add 0.6 mL MTBE to induce precipitate. 3. Transfer the sample to stirring at 4 ºC overnight. 4. Isolate the solids for analysis.

Crystal Form	Preparation Procedures
Anisole Solvate Type G (807920-19-F)	1. Weigh 59.0 mg freebase Type A to 4.5 mL anisole and stir at 50 ºC for 1 hr to get a clear solution. 2. Keep the sample at 50 ºC for another 30 min and then transfer to -20 ºC. 3. Isolate the solids for analysis after 4 days.
Metastable Form Type C (807920-11-A11)	1. Weigh 10.1 mg freebase Type A into a 3-mL glass vial. 2. Seal the vial into the 20-mL glass vial with 2-mL 1,4-dioxane and keep the system at RT. 3. Isolate the solids for analysis after 7 days.
Metastable Form Type F (807920-09-A4)	1. Weigh 14.4 mg freebase Type A to 1.0 mL MEK and stir at 50 ºC for 2 hrs to get a suspension. 2. Filter the suspension and transfer the solution to slow cooling (50 ºC to 5 ºC, 0.1 ºC/min). 3. Isolate the solids for analysis after 14 days.

2.1 Anhydrate (Type A)

[00387] Starting material (Batch No.: 144875-48-9, with a CP ID 807920-05-A) was characterized by XRPD, TGA, DSC, and HPLC. The XRPD result in FIG. 124 conformed to the Type A reference (807919-05-A). XRPD patterns are displayed in FIG. 141 and provide (peak shift within ±0.2°) primary peaks at 8.9, 12.4, and 17.7; secondary peaks at 19.7, 21.5, and 23.4; and tertiary peaks at 16.5, 20.1, and 26.7.

[00388] TGA and DSC data for the anhydrate Type A crystal form show (FIG. 125) a weight loss of 2.5% up to 100 ºC and a sharp endothermic peak at 193.0 ºC (onset temperature) before decomposition. Also, a purity of 99.4 area% was detected by HPLC in Table 2-2. Considering all the results, Type A was deemed as an anhydrate.

Table 2-2 HPLC purity profile of Type A (807920-05-A)

#	RRT	Area%	#	RRT	Area%
1	0.75	0.08	4	1.00	**99.41**
2	0.83	0.24	5	1.07	0.10
3	0.87	0.05	6	1.61	0.13

2.2 Metastable Form

2.2.1 Type C

[00389] Type C was generated in 1,4-dioxane system. Type C sample (807920-11-A11) was obtained via solid vapor diffusion in 1,4-dioxane. As XRPD pattern displayed in FIG. 126, Type C converted to Type A after dried at ambient conditions overnight, suggesting metastable form for Type C at ambient conditions. XRPD patterns provide (peak shift within ±0.2°) primary peaks at 9.6, 18.7, and 19.8; secondary peaks at 12.1, 14.5, and 21.2; and tertiary peaks at 17.4, 20.7, and 28.5.

2.2.2 Type F

[00390] Type F sample (807920-09-A4) was obtained via slow cooling in MEK and the XRPD pattern was displayed in FIG. 127. XRPD patterns provide (peak shift within ±0.2°) primary peaks at 10.4, 16.5, and 21.2; secondary peaks at 8.3, 20.7, and 28.8; and tertiary peaks at 12.5, 17.7, and 24.8.

[00391] After storage at ambient conditions for 2 days, Type F converted to Type A, indicating Type F was metastable at ambient conditions.

2.3 Solvate

2.3.1 Type B

[00392] Isomorphism occurred to Type B. It can be prepared in several solvent systems, including IBA/toluene, EtOAc, THF/H_2O, and etc. XRPD patterns of Type B were displayed in FIG. 128. XRPD patterns provide (peak shift within ±0.2°) primary peaks at 6.2, 16.3, and 21.4; secondary peaks at 12.3, 22.3, and 24.7; and tertiary peaks at 20.4, 27.0, and 28.4.

[00393] Three batches of the isomorphism Type B crystal form were produced. Batch 1: TGA and DSC data (FIG. 129) show a weight loss of 10.8% up to 165 ºC and two endothermic peaks at 158.4 ºC and 192.9 ºC (peak temperature) before decomposition. Batch 2: TGA and DSC data (FIG. 130) show a weight loss of 9.3% up to 150 ºC and two endothermic peaks at 146.7 ºC and 191.9 ºC (peak temperature) before decomposition. Batch 3: TGA and DSC data (FIG. 131) show a weight loss of 6.5% up to 160 ºC and two endothermic peaks at 143.7 ºC and 194.4 ºC (peak temperature) before decomposition.

[00394] Also, ^{1}H NMR confirm a EtOAc content of 5.2% in Type B sample (807920-08-A7), which suggested EtOAc solvate for Type B (807920-08-A7). Also, ^{1}H NMR confirm a THF content of 6.1% in Type B sample (807920-12-A2), which suggested THF solvate for Type B (807920-12-A2).

Table 2-3 HPLC purity profiles of Type B (807920-07-A13) before and after heating

RRT	Area (%)

	Initial Type B	Type B heated to 160 ºC
0.69	0.09	--
0.75	0.13	0.09
0.83	0.38	0.29
0.87	0.09	0.06
1.00	99.09	99.51
1.04	0.10	--
1.07	0.12	0.05

2.3.2 Type D

[00395] Type D sample (807920-12-A9) was prepared via solution vapor diffusion in DMAc/MTBE. XRPD pattern was shown in FIG. 157. XRPD patterns are displayed in FIG. 132 and provide (peak shift within ±0.2°) primary peaks at 8.7, 17.6, and 23.9; secondary peaks at 11.2, 21.2, and 22.8; and tertiary peaks at 9.1, 15.5, and 16.9. TGA and DSC data (FIG. 133) show a weight loss of 18.4% up to 90 ºC and two endothermic peaks at 87.2 ºC and 190.2 ºC (onset temperature) before decomposition. Also, ^{1}H NMR confirm a DMAc content of 18.3% in Type D sample, indicating DMAc solvate for Type D.

2.3.3 Type E

[00396] Type E was generated in NMP/MTBE system. Type E sample was obtained via slurry in NMP/MTBE (1:2, v/v) at RT. The XRPD pattern is displayed in FIG. 134. XRPD patterns provide (peak shift within ±0.2°) primary peaks at 8.7, 17.9, and 23.9; secondary peaks at 16.9, 21.3, and 22.9; and tertiary peaks at 9.2, 11.2, and 12.5. TGA and DSC data (FIG. 135) show a weight loss of 25.5% up to 120 ºC and two endothermic peaks at 134.0 ºC and 187.4 ºC (peak temperature) before decomposition. Also, 1H NMR shows NMP content of 22.9% was detected, which was consistent with the TGA weight loss, indicating Type E was a NMP solvate.

2.3.4 Type G

[00397] Type G was generated in anisole system. Type G sample (807920-19-F) was obtained via fast cooling from 50 ºC to -20 ºC and the XRPD pattern displayed in FIG. 136. XRPD patterns provide (peak shift within ±0.2°) primary peaks at 9.7, 13.3, and 19.2; secondary peaks at 8.9, 13.8, 28.0; and tertiary peaks at 12.4, 20.6, and 23.4. TGA and DSC data (FIG. 137) show a weight loss of 14.6% up to 100 ºC and two endothermic peaks at 64.5 ºC and 193.0 ºC (onset temperature) before decomposition. ^{1}H NMR results indicate anisole of 12.4% was detected, which was consistent with the second weight loss in TGA, suggesting anisole solvate for Type G.

2.4 Salt/Co-crystal (Sample H)

[00398] Sample H (807920-22-A1) was obtained via anti-solvent addition in ethyl lactate/n-heptane with additional acetic acid (molar ratio 0.4:1, acid/base) and a mixture of Type A and sample H was generated via anti-solvent addition in ethyl lactate/n-heptane (with acetic acid content detected in ethyl lactate). The XRPD patterns shown in FIG. 138 provide (peak shift within ±0.2°) primary peaks at 9.7, 13.3, and 19.2; secondary peaks at 8.9, 13.8, 28.0; and tertiary peaks at 12.4, 20.6, and 23.4. TGA and DSC data (FIG. 139) show a weight loss of 14.6% up to 100 ºC and two endothermic peaks at 64.5 ºC and 193.0 ºC (onset temperature) before decomposition. Also, the acetic acid content of 0.47:1 (molar ratio, acid/base) was determined by ^{1}H NMR. Combined with the characterization data, sample H was speculated as an acetate/acetic acid co-crystal.

3. Evaluation of Leading Type A

[00399] Since all solvates and metastable forms converted to Type A after storage or heating experiments, anhydrate Type A was the thermodynamically stable form at RT and selected to be further evaluated on hygroscopicity and solid-state stability. Results show: 1) Type A was non-hygroscopic as evidenced by the limited water uptake in DVS; 2) Type A had good physicochemical properties under 25 ºC/60%RH and 40 ºC/75%RH for one week, and 80 ºC for 24 hours.

3.1 Hygroscopicity

[00400] DVS isotherm plot was collected at 25 ºC to investigate the solid form stability as a function of humidity for anhydrate Type A (807919-05-A). Solids were pre-dried at 0%RH to remove the unbounded solvent or water before started. As DVS plot shown in FIG. 140, a water uptake of 0.1% was observed up to 80%RH, suggesting Type A (807919-05-A) was non-hygroscopic. Also, no form change was observed after DVS test (FIG. 140).

3.2 Solid-state Stability

[00401] Physicochemical stability of Type A (807919-05-A) was evaluated under 25 ºC/60%RH and 40 ºC/75%RH for one week, and 80 ºC (closed) for 24 hours. Stability samples were characterized by XRPD and HPLC, with the results summarized in Table 3-1 and FIG. 142. No change was observed in HPLC purity or crystal form, suggesting good physical and chemical stability for Type A (807919-05-A) under tested conditions.

Table 3-1 Stability evaluation summary of Type A (807919-05-A)

Crystal Form (Sample ID)	HPLC Purity (Initial, area%)	Condition	HPLC Purity		Form Change
			Area%	% of Initial	
Freebase Type A	99.32	25 ºC/60%RH, 1 week	99.15	99.8	No

(807919-05-A)*		40 ºC/75%RH, 1 week	99.28	100.0	No
Freebase Type A (807919-05-A)	99.15	80 ºC, 24 hrs	99.23	100.1	No

*: Data was collected in salt screening section.

4. Conclusion

[00402] Using compound 001 freebase Type A as the starting material, a total of 100 polymorph screening experiments were set up, and XRPD analysis of the solids revealed that eight crystal forms were obtained. Form identification results show that there were one anhydrate (Type A), two metastable forms (Type C/F), four solvates (Type B/D/E/G), and one acetate/acetic acid co-crystal (sample H). The inter-conversion results show Type B~G all converted to Type A after heating or storage, indicating good physical stability for Type A. Type A was further evaluated by hygroscopicity and solid-state stability. The results show Type A was non-hygroscopic and possessed good physicochemical properties under 25 ºC/60%RH and 40 ºC/75%RH for one week, and 80 ºC for 24 hours. Combined with the characterization results, Type A was recommended for further pharmaceutical development.

5. Other

5.1 Sample Information

[00403] Starting materials as received were used directly in polymorph screening and evaluation experiments, with the detailed information provided in Table 5-1.

Table 5-1 Detailed information of starting materials

Compound	Batch No.	CP ID	Crystal Form
001	144875-48-9	807920-05-A	Type A
	NA	807919-05-A	Type A

NA: no information was available.

5.2 Abbreviation for Solvents Used

[00404] The solvent abbreviations are listed in Table 5-2.

Table 5-2 Abbreviations of solvents

Abbreviation	Solvent	Abbreviation	Solvent
MeOH	Methanol	THF	Tetrahydrofuran
EtOH	Ethanol	2-MeTHF	2-Methyltetrahydrofuran
IPA	Isopropyl alcohol	DCM	Dichloromethane
IBA	Isobutyl alcohol	$CHCl_3$	Trichloromethane

Abbreviation	Solvent	Abbreviation	Solvent
MEK	2-Butanone	ACN	Acetonitrile
MIBK	4-Methyl-2-pentanone	DMSO	Dimethylsulfoxide
EtOAc	Ethyl acetate	DMAc	N,N-Dimethylacetamide
IPAc	Isopropyl acetate	NMP	1-Methyl-2-pyrrolidone
MTBE	Methyl tert-butyl ether	--	--

5.3 Instruments and Methods

5.3.1 XRPD

[00405] For XRPD analysis, a PANalytical Empyrean X-ray powder diffract meter was used. The XRPD parameters used are listed in Table 5-3.

Table 5-3 Parameters for XRPD test

Parameters	XRPD (Reflection Mode)
X-Ray wavelength	Cu, kα, Kα1 (Å): 1.540598, Kα2 (Å): 1.544426 Kα2/Kα1 intensity ratio: 0.50
X-Ray tube setting	45 kV, 40 mA
Divergence slit	Automatic
Scan mode	Continuous
Scan range (°2TH)	3°-40°
Step size (°2TH)	0.0130
Scan speed (°/min)	About 7

5.3.2 TGA and DSC

[00406] TGA data were collected using a TA Q500/Q5000 TGA from TA Instruments. DSC was performed using a TA Q200/Q2000 DSC from TA Instruments. Detailed parameters used are listed in Table 5-4.

Table 5-4 Parameters for TGA and DSC test

Parameters	TGA	DSC
Method	Ramp	Ramp
Sample pan	Platinum, open	Aluminum, crimped
Temperature	RT - desired temperature	25 °C - desired temperature
Heating rate	10 °C/min	10 °C/min
Purge gas	N_2	N_2

5.3.3 HPLC

[00407] Agilent 1100 HPLC was utilized to analyze purity, with detailed method was listed in Table 5-5.

Table 0-1 HPLC method for purity test

HPLC	Agilent 1100 with DAD Detector	
Column	Alltima C18, 150×4.6 mm, 5μm	
Mobile phase	A: 0.1% TFA in H_2O	
	B: 0.1% TFA in Acetonitrile	
Gradient table	Time (min)	%B
	0.0	10
	10.0	40
	18.0	90
	20.0	90
	20.1	10
	23.0	10
Run time	23.0 min	
Post time	0.0 min	
Flow rate	1.0 mL/min	
Injection volume	5 μL	
Detector wavelength	UV at 228 nm, reference 500 nm	
Column temperature	40 ºC	
Sampler temperature	RT	
Diluent	Acetonitrile:H_2O=1:1	

5.3.4 DVS

[00408] DVS was measured via a SMS (Surface Measurement Systems) DVS Intrinsic. The relative humidity at 25 ºC were calibrated against deliquescence point of LiCl, $Mg(NO_3)_2$ and KCl. Actual parameters for DVS test were listed in Table 5-6.

Table 5-6 Parameters for DVS test

Parameters	DVS
Temperature	25 ºC
Sample size	10 ~ 20 mg
Gas and flow rate	N_2, 200 mL/min
dm/dt	0.002%/min
Min. dm/dt stability duration	10 min
Max. equilibrium time	180 min
RH range	0%RH to 95%RH
RH step size	10%RH from 0%RH to 90%RH 5%RH from 90%RH to 95%RH

5.3.5 Solution NMR

[00409] Solution NMR was collected on Bruker 400M NMR Spectrometer using DMSO-d6.

5.4 Polymorph Screening

[00410] The solubility of starting material (807920-05-A) was estimated at RT. Approximately 2 mg solids were added into a 3-mL glass vial. Solvents were then added step wise (100 µL per step) into the vials until the solids were dissolved or a total volume of 1 mL was reached. Results summarized in Table 5-7 were used to guide the solvent selection in polymorph screening.

[00411] Polymorph screening experiments were performed using different crystallization or solid transition methods. The methods utilized and crystal forms identified are summarized in Table 5-8.

Table 5-7 Approximate solubility of starting material (807920-05-A) at RT

Solvent	Solubility (mg/mL)	Solvent	Solubility (mg/mL)
n-heptane	S<2.0	2-MeTHF	7.0<S<21.0
H_2O	S<2.1	Acetone	7.1<S<25.0
MTBE	S<2.2	IPA	8.3<S<25.0
toluene	S<2.2	IBA	8.3<S<25.0
Anisole	S<2.3	THF	21.0<S<42.0
MEK	2.0<S<6.7	Ethyl lactate	22.0<S<44.0
IPAc	2.1<S<7.0	$CHCl_3$	22.0<S<44.0
MIBK	2.2<S<7.3	EtOH	23.0<S<46.0
EtOAc	2.3<S<7.7	NMP	S>40.0

Solvent	Solubility (mg/mL)	Solvent	Solubility (mg/mL)
ACN	2.5<S<8.3	DMSO	S>44.0
1,4-dioxane	6.7<S<20.0	MeOH	S>46.0
DCM	6.7<S<20.0	DMAc	S>48.0

Table 5-8 Summary of polymorph screening experiments

Method	No. of Experiments	Crystal Form
Anti-solvent Addition	20	Type A, B, G, sample H
Slow Evaporation	10	Type A, B
Slow Cooling	10	Type A, B, F, G
Polymer-induced Crystallization	6	Type A, B
Solid Vapor Diffusion	13	Type A, C
Solution Vapor Diffusion	10	Type A, B, D, E
Slurry at RT/50 ºC	31	Type A, C
Total	100	Type A~G, sample H

5.4.1 Anti-solvent Addition

[00412] A total of 20 anti-solvent addition experiments were carried out. About 15 mg of starting material (807920-05-A) was dissolved in 0.1-2.3 mL solvent to obtain a clear solution, and the solution was magnetically stirred followed by addition of 0.2 mL anti-solvent per step till precipitate appeared or the total amount of anti-solvent reached 15.0 mL. The obtained precipitate was isolated for XRPD analysis. Results in Table 5-9 show that Type B, G, and sample H were generated besides Type A.

Table 5-9 Summary of anti-solvent addition experiments

Experiment ID	Solvent	Anti-solvent	Solid Form
807920-07-A1	MeOH	H_2O	Type A
807920-07-A2**	IPA		Clear
807920-07-A3**	Acetone		Type A
807920-07-A4**	THF		Type A
807920-07-A5	DMSO		Type A
807920-07-A6	DMAc		Type A
807920-07-A7	NMP		Type A
807920-07-A8	EtOH	n-heptane	Type A
807920-07-A9	THF		Type A+B

Experiment ID	Solvent	Anti-solvent	Solid Form
807920-07-A10	2-MeTHF		Type A+B
807920-07-A11	Ethyl lactate		Type A+Sample H
807920-07-A12	$CHCl_3$		Type A+B
807920-07-A13**	IBA		Type B
807920-07-A14	DCM	Toluene	Type A
807920-07-A15*	1,4-dioxane		Type A
807920-07-A16*	MeOH		Type A
807920-07-A17**	Acetone	MTBE	Type B
807920-07-A18	$CHCl_3$		Type A
807920-07-A19**	EtOH	Anisole	Type G
807920-07-A20	DCM		Clear

*: solids were observed after stirring the clear solution from anti-solvent addition at 5 ºC for 2 days.

**: no solid was obtained via stirring the clear solution at 5 ºC and then evaporation was employed.

5.4.2 Slow Evaporation

[00413] Slow evaporation experiments were performed under ten conditions. Briefly, ~15 mg of starting material (807920-05-A) was dissolved in 1.0-2.0 mL of solvent in a 3-mL glass vial. If not dissolved completely, suspensions were filtered using a nylon membrane (pore size of 0.45 μm) and the filtrates would be used instead for the follow-up steps. The visually clear solutions were subjected to evaporation at RT with vials sealed by Parafilm®. The solids were isolated for XRPD analysis, and the results summarized in Table 5-10 indicated that Type A and B were obtained.

Table 5-10 Summary of slow evaporation experiments

Experiment ID	Solvent (v:v)	Solid Form
807920-08-A1	MeOH	Type A
807920-08-A2	IPA	Type A
807920-08-A3	Acetone	Type A
807920-08-A4	DCM	Type A
807920-08-A5	THF	Type A
807920-08-A6	ACN	Type A+B
807920-08-A7	EtOAc	Type B
807920-08-A8	EtOH/H_2O (1:1)	Type A
807920-08-A9	2-MeTHF/n-heptane (1:1)	Type B

Experiment ID	Solvent (v:v)	Solid Form
807920-08-A10	$CHCl_3$/n-heptane (1:1)	Type A+B

5.4.3 Slow Cooling

[00414] Slow cooling experiments were conducted in ten solvent systems. About 15 mg of starting material (807920-05-A) was suspended in 1.0 mL of solvent in a 3-mL glass vial at RT. The suspension was then heated to 50 ºC, equilibrated for about two hours and filtered using a nylon membrane (pore size of 0.45 μm). Filtrates were slowly cooled down to 5 ºC at a rate of 0.1 ºC/min. The obtained solids were kept isothermal at 5 ºC before isolated for XRPD analysis. Clear solutions were transferred to -20 ºC and if it was still clear, they were subjected to evaporation at RT. Results summarized in Table 5-11 indicated Type B, F, and G were generated besides Type A.

Table 5-11 Summary of slow cooling experiments

Experiment ID	Solvent (v:v)	Solid Form
807920-09-A1	ACN	Type A
807920-09-A2	EtOAc	Type A
807920-09-A3	IPAc	Type A
807920-09-A4	MEK	Type F
807920-09-A5	MIBK	Type A+B
807920-09-A6*	Anisole	Type G
807920-09-A7	Acetone/H_2O (1:3)	Type A
807920-09-A8	EtOH/n-heptane (1:3)	Type A
807920-09-A9	THF/toluene (1:3)	Type A+B
807920-09-A10	$CHCl_3$/MTBE (1:3)	Type B

No solids were obtained via slow cooling and all samples were transferred to -20 ºC.

*: limited solid was obtained and system was subjected to evaporation at RT.

5.4.4 Polymer induced Crystallization

[00415] Polymer induced crystallization experiments were performed with two sets of polymer mixtures in seven solvents. Approximate 15 mg of starting material (807920-05-A) was dissolved in appropriate solvent to obtain a clear solution in a 3-mL vial. About 2 mg of polymer mixture was added into 3-mL glass vial. All the samples were subjected to evaporation at RT to induce precipitation. The solids were isolated for XRPD analysis. Results summarized in Table 5-12 show that Type A and B were produced.

Table 5-12 Summary of polymer induced crystallization experiments

Experiment ID	Solvent	Polymer	Solid Form
807920-10-A1	MeOH		Type A
807920-10-A2	Acetone	Polymer mixture A	Type A
807920-10-A3	THF		Type A
807920-10-A4	MeOH		Type B
807920-10-A5	Acetone	Polymer mixture B	Type A
807920-10-A6	THF		Type A

Polymer mixture A: polyvinyl pyrrolidone (PVP), polyvinyl alcohol (PVA), polyvinylchloride (PVC), polyvinyl acetate (PVAC), hypromellose (HPMC), methyl cellulose (MC) (mass ratio of 1:1:1:1:1:1)
Polymer mixture B: polycaprolactone (PCL), polyethylene glycol (PEG), poly(methyl methacrylate) (PMMA) sodium alginate (SA), and hydroxyethyl cellulose (HEC) (mass ratio of 1:1:1:1:1).

5.4.5 Solid Vapor Diffusion

[00416] Solid vapor diffusion experiments were conducted using 13 different solvents. Approximate 10 mg of starting material (807920-05-A) was weighed into a 3-mL vial, which was placed into a 20-mL vial with 2 mL of volatile solvent. The 20-mL vial was sealed with a cap and kept at RT for 7 days allowing solvent vapor to interact with sample. The solids were tested by XRPD and the results summarized in Table 5-13 show that Type A and C were generated.

Table 5-13 Summary of solid vapor diffusion experiments

Experiment ID	Solvent	Solid Form
807920-11-A1	H_2O	Type A
807920-11-A2	DCM	Type A
807920-11-A3	EtOH	Type A
807920-11-A4	MeOH	Type A
807920-11-A5	ACN	Type A
807920-11-A6	THF	Type A
807920-11-A7	$CHCl_3$	Type A
807920-11-A8	Acetone	Type A
807920-11-A9	DMF	Type A
807920-11-A10	EtOAc	Type A
807920-11-A11	1,4-dioxane	Type C
807920-11-A12	IPA	Type A
807920-11-A13	DMSO	Type A

5.4.6 Liquid Vapor Diffusion

[00417] Ten liquid vapor diffusion experiments were conducted. Approximate 15 mg of starting material (807920-05-A) was dissolved in appropriate solvent to obtain a clear solution in a 3-mL vial. This solution was then placed into a 20-mL vial with 3 mL of volatile solvents. The 20-mL vial was sealed with a cap and kept at RT allowing sufficient time for organic vapor to interact with the solution. The precipitates were isolated for XRPD analysis. After 6 days, solids were isolated for XRPD analysis. The results summarized in Table 5-14 show that Type B, D, and E were generated besides Type A.

Table 5-14 Summary of liquid vapor diffusion experiments

Experiment ID	Solvent	Anti-solvent	Solid Form
807920-12-A1	EtOH	H_2O	Type A
807920-12-A2	THF		Type B
807920-12-A3	$CHCl_3$	Toluene	Type A+B
807920-12-A4	2-MeTHF		Type A
807920-12-A5	Acetone	n-heptane	Type A
807920-12-A6	IBA		Clear
807920-12-A7	DCM		Type A
807920-12-A8	Ethyl lactate	MTBE	Clear
807920-12-A9	DMAc		Type D
807920-12-A10	NMP		Type E

5.4.7 Slurry at RT

[00418] Slurry conversion experiments were conducted at RT in different solvent systems. About 15 mg of starting material (807920-05-A) was suspended in 0.5 mL of solvent in a 1.5-mL glass vial. After the suspension was stirred magnetically for 3 days at RT, the remaining solids were isolated for XRPD analysis. Results summarized in Table 5-15 indicated that only Type A was obtained.

Table 5-15 Summary of slurry conversion experiments at RT

Experiment ID	Solvent (v:v)	Solid Form
807920-13-A1	ACN	Type A
807920-13-A2	EtOAc	Type A
807920-13-A3	IPAc	Type A
807920-13-A4	MEK	Type A

Experiment ID	Solvent (v:v)	Solid Form
807920-13-A5	MIBK	Type A
807920-13-A6	Anisole	Type A
807920-13-A7	2-MeTHF	Type A
807920-13-A8	1,4-dioxane	Type A
807920-13-A9	IPA	Type A
807920-13-A10	IBA	Type A
807920-13-A11	MeOH/H_2O (1:3)	Type A
807920-13-A12	THF/n-heptane (1:3)	Type A
807920-13-A13	DCM/toluene (1:3)	Type A
807920-13-A14	acetone/H_2O (a_w=0.2)	Type A
807920-13-A15	acetone/H_2O (a_w =0.4)	Type A
807920-13-A16	acetone/H_2O (a_w =0.6)	Type A
807920-13-A17	acetone/H_2O (a_w =0.8)	Type A

5.4.8 Slurry at 50 °C

[00419] Slurry conversion experiments were also conducted at 50 °C in different solvent systems. About 15 mg of starting material (807920-05-A) was suspended in 0.3 mL of solvent in a 1.5-mL glass vial. After the suspension was stirred for about 3 days at 50 °C, the remaining solids were isolated for XRPD analysis. Results summarized in Table 5-16 indicated that Type A and C were obtained.

Table 5-16 Summary of slurry conversion experiments at 50 °C

Experiment ID	Solvent (v:v)	Solid Form
807920-14-A1	ACN	Type A
807920-14-A2	EtOAc	Type A
807920-14-A3	IPAc	Type A
807920-14-A4	MEK	Type A
807920-14-A5	MIBK	Type A
807920-14-A6	Anisole	Type A
807920-14-A7	2-MeTHF	Type A
807920-14-A8	1,4-dioxane	Type C
807920-14-A9	IPA	Type A
807920-14-A10	IBA	Type A
807920-14-A11	MeOH/H_2O (1:5)	Type A

Experiment ID	Solvent (v:v)	Solid Form
807920-14-A12	THF/n-heptane (1:5)	Type A
807920-14-A13	$CHCl_3$/toluene (1:5)	Type A
807920-14-A14	H_2O	Type A

[00420] The preceding disclosures are illustrative embodiments. It should be appreciated by those of skill in the art that the techniques disclosed herein elucidate representative techniques that function well in the practice of the present disclosure. However, those of skill in the art should, in light of the present disclosure, appreciate that many changes can be made in the specific embodiments that are disclosed and still obtain a like or similar result without departing from the spirit and scope of the invention.

[00421] Unless otherwise indicated, all numbers expressing quantities of ingredients, properties such as molecular weight, reaction conditions, and so forth used in the specification and claims are to be understood as being modified in all instances by the term "about." Accordingly, unless indicated to the contrary, the numerical parameters set forth in the specification and attached claims are approximations that may vary depending upon the desired properties sought to be obtained by the present invention. At the very least, and not as an attempt to limit the application of the doctrine of equivalents to the scope of the claims, each numerical parameter should at least be construed in light of the number of reported significant digits and by applying ordinary rounding techniques. Notwithstanding that the numerical ranges and parameters setting forth the broad scope of the invention are approximations, the numerical values set forth in the specific examples are reported as precisely as possible. Any numerical value, however, inherently contains certain errors necessarily resulting from the standard deviation found in their respective testing measurements.

[00422] The terms "a," "an," "the" and similar referents used in the context of describing the invention (especially in the context of the following claims) are to be construed to cover both the singular and the plural, unless otherwise indicated herein or clearly contradicted by context. Recitation of ranges of values herein is merely intended to serve as a shorthand method of referring individually to each separate value falling within the range. Unless otherwise indicated herein, each individual value is incorporated into the specification as if it were individually recited herein. All methods described herein can be performed in any suitable order unless otherwise indicated herein or otherwise clearly contradicted by context. The use of any and all examples, or exemplary language (e.g., "such as") provided herein is intended merely to better illuminate the invention and does not pose a limitation on the

scope of the invention otherwise claimed. No language in the specification should be construed as indicating any non-claimed element essential to the practice of the invention.

[00423] Groupings of alternative elements or embodiments of the invention disclosed herein are not to be construed as limitations. Each group member may be referred to and claimed individually or in any combination with other members of the group or other elements found herein. It is anticipated that one or more members of a group may be included in, or deleted from, a group for reasons of convenience and/or patentability. When any such inclusion or deletion occurs, the specification is deemed to contain the group as modified thus fulfilling the written description of all Markush groups used in the appended claims.

[00424] Certain embodiments of this invention are described herein, including the best mode known to the inventors for carrying out the invention. Of course, variations on these described embodiments will become apparent to those of ordinary skill in the art upon reading the foregoing description. The inventor expects skilled artisans to employ such variations as appropriate, and the inventors intend for the invention to be practiced otherwise than specifically described herein. Accordingly, this invention includes all modifications and equivalents of the subject matter recited in the claims appended hereto as permitted by applicable law. Moreover, any combination of the above-described elements in all possible variations thereof is encompassed by the invention unless otherwise indicated herein or otherwise clearly contradicted by context.

[00425] Furthermore, numerous references have been made to patents and printed publications throughout this specification. Each of the above-cited references and printed publications are individually incorporated herein by reference in their entirety.

[00426] Specific embodiments disclosed herein may be further limited in the claims using consisting of or and consisting essentially of language. When used in the claims, whether as filed or added per amendment, the transition term “consisting of” excludes any element, step, or ingredient not specified in the claims. The transition term “consisting essentially of” limits the scope of a claim to the specified materials or steps and those that do not materially affect the basic and novel characteristic(s). Embodiments of the invention so claimed are inherently or expressly described and enabled herein.

[00427] In closing, it is to be understood that the embodiments of the invention disclosed herein are illustrative of the principles of the present invention. Other modifications that may be employed are within the scope of the invention. Thus, by way of example, but not of limitation, alternative configurations of the present invention may be utilized in accordance

with the teachings herein. Accordingly, the present invention is not limited to that precisely as shown and described.

We claim:

1. A composition comprising resiquimod in the form of a sulfate salt in crystal form A, wherein crystal form A is characterized by x-ray powder diffraction spectrum that comprises peaks at 7 to 8 degrees 2θ, 13.5 to 14.5 degrees 2θ, 19 to 20 degrees 2θ, and/ or 19.5 to 20.5 degrees 2θ.

2. The composition of claim 1, wherein the sulfate salt is a monosulfate salt.

3. The composition of claim 1, wherein the sulfate salt is an anhydrate.

4. The composition of claim 1, wherein the crystal form A is thermodynamically stable at room temperature at least about 2 days.

5. The composition of claim 1, wherein the crystal form A is thermodynamically stable at room temperature at least about 1 week.

6. A dosage form comprising the composition of claim 1.

7. Use of a composition of claim 1 in the preparation of a medicament for the treatment of cancer in a subject in need thereof.

8. Use of a composition of claim 1 in the preparation of a medicament for the treatment of a tumor in a subject in need thereof.

9. The use of claim 8, wherein the tumor is a carcinoma, a sarcoma, or a blastoma.